Detecting Abnormalities in Aircraft Flight Data and Ranking their Impact on the Flight

Edward Smart

Institute of Industrial Research

University of Portsmouth

A thesis submitted for the degree of

Doctor of Philosophy

20th April 2011

Whilst registered as a candidate for the above degree, I have not been registered for any other research award. The results and conclusions embodied in this thesis are the work of the named candidate and have not been submitted for any other academic award.

I would like to dedicate this thesis to my family, Martin, Ruth,
Bryony, Adrian and also to my girlfriend, Kelly.

Acknowledgements

Completing this PhD has given me immense satisfaction. It is one of my greatest achievements in terms of difficulty and endurance and only my history A-level is comparable. Whilst it has sometimes been an immense source of frustration, the thrill of making a new discovery or finding a way to overcome a difficult problem always outshone the difficult times.

Firstly, I wish to thank my supervisor David Brown for his patience and encouragement. He always had an open door and made time for me to talk about my work. Furthermore he gave me the freedom to pursue my own research whilst asking the right questions so that I could achieve my full potential. Thank you very much for the many trips to Cafe Parisien!

I also wish to thank Flight Data Services Ltd for their eager participation in this project. Every time I have visited their offices I have always been made to feel welcome and part of the team. Biggest thanks goes to Dave Jesse, the CEO, who happily agreed to give me access to the flight data and the freedom of his offices to do my research. Warm thanks goes to Chris Jesse who was my mentor at Flight Data Services during the early part of the project. It was especially daunting for me as I had very little knowledge of flight data or the process of monitoring it but Chris was always happy to explain how to use the company systems and answer any questions I might have, especially the silly ones! Special thanks goes to members of the Engine Room. The banter was and remains first class and it was an absolute pleasure to be considered a part of that group. Particular thanks must

go to John Denman and Roger Rowlands who willingly and patiently explained to me the finer points of descending an aircraft.

Warmest thanks goes to members of the Institute of Industrial Research who were my companions for much of this thesis. Farshad, Xin, Medhi, Jiantao, and Zhaojie, thank you for making my time here enjoyable and for your helpful insights when the research appeared to stagnate.

The author would like to thank the EPSRC for funding this work which was supported by EPSRC Industrial CASE Voucher Number 06001600.

Abstract

To the best of the author's knowledge, this is one of the first times that a large quantity of flight data has been studied in order to improve safety.

A two phase novelty detection approach to locating abnormalities in the descent phase of aircraft flight data is presented. It has the ability to model normal time series data by analysing snapshots at chosen heights in the descent, weight individual abnormalities and quantitatively assess the overall level of abnormality of a flight during the descent. The approach expands on a recommendation by the UK Air Accident Investigation Branch to the UK Civil Aviation Authority. The first phase identifies and quantifies abnormalities at certain heights in a flight. The second phase ranks all flights to identify the most abnormal; each phase using a one class classifier. For both the first and second phases, the Support Vector Machine (SVM), the Mixture of Gaussians and the K-means one class classifiers are compared. The method is tested using a dataset containing manually labelled abnormal flights. The results show that the SVM provides the best detection rates and that the approach identifies unseen abnormalities with a high rate of accuracy. Furthermore, the method outperforms the event based approach currently in use. The feature selection tool F-score is used to identify differences between the abnormal and normal datasets. It identifies the heights where the discrimination between the two sets is largest and the aircraft parameters most responsible for these variations.

Contents

List of Figures

Glossary

AAIB	Air Accident and Investigations Branch	24, 27, 114, 116
AGL	Above Ground Level. Height above the arrival airport.	26
AIS	Artificial Immune System.	30
ALAR	Approach and Landing Accident Reduction (task force)	24, 27, 114
APMS	Aviation Performance Measuring System	13
AUC	Area Under the Receiver Operator Characteristic Curve	78, 96, 97
BER	Balanced Error Rate	78, 94, 96, 97
CAA	Civil Aviation Authority	8, 9, 24, 114
DAP	Descent Abnormality Profile	5, 72, 73, 78–80, 82–85, 87–92, 103–105, 116, 117
EVT	Extreme Value Theory.	29

FDM	Flight Data Monitoring	1, 2, 6, 8–10, 12, 16, 26
flap	A device on the aircraft wing to increase lift at low airspeeds.	11
FN	False Negatives	78, 94
FN	True Negatives	94
FN	True Positives	94
FP	False Positives	78, 94
fpm	feet per minute	25
ft	Feet	22, 23, 25, 26
Go Around	A procedure for making a second attempt at landing after the first was aborted, possibly for being unstable	97
GPWS	Ground Proximity Warning System	12, 97, 99, 104
HMM	Hidden Markov Models.	29, 30
IATA	International Air Transport Association.	68
ICAO	International Civil Aviation Organisation	7
ILS	Instrument Landing System	24, 25, 79, 80, 89
kts	Knots	22, 25, 26
MoG	Mixture of Gaussians.	41, 42, 58, 64, 76, 80, 83, 84, 87, 90, 95–97, 115

NATS	National Air Traffic Service.	68
NM	Nautical Miles	22, 25
PCA	Principle Component Analysis	15
QAR	Quick Access Recorder	8
RBF	Radial Basis Function	47, 48, 50, 52, 53, 109
SOP	Standard Operating Procedure	9–12, 25, 27, 86, 100, 115, 117, 118
SVDD	Support Vector Data Description	51, 53, 58
SVM	Support Vector Machine.	45, 47–50, 58, 61, 64, 74, 78, 80, 82–85, 87, 89, 95–97, 99, 111, 115, 116
Vref30	This is the reference speed used during the final approach. It is 1.3 times the minimum speed needed to keep the aircraft from stalling.	25, 26

Chapter 1

Introduction

1.1 Background

Flight safety is an important issue, ever since the first flights over a hundred years ago. Air accidents are almost always major headlines and can affect large numbers of people. Accidents can be particularly tragic due to a significant loss of life on the aircraft and possibly to civilians on the ground. Significant financial losses occur when the aircraft is damaged or written off, leading to the cost of replacement and the loss of revenue that the aircraft would have made had the accident not occurred.

The black box recorder is a very well protected device in the aircraft that records certain parameters and is designed to withstand a major crash. They are located as soon as possible after an accident so that investigators can try to identify the reasons behind it. Deducing why the aircraft crashed can take as long as 12 months due to the complexity of the aircraft's systems or if the accident occurred in a remote area that is mostly inaccessible. Once they have discovered the reasons behind the accident, they are then made known to the airlines and sometimes to the manufacturer so they can learn from it.

Given the fact that air accidents can be disastrous in terms of loss of life, property and revenue, research has been undertaken to try to identify any precursors to accidents or incidents. The first Flight Data Monitoring (FDM) programmes were created in order to routinely analyse data from all or most of the aircraft in a fleet. One of their aims is to identity any possible signs of damage to the aircraft or any instances where the aircraft is being flown outside of the airlines recommended procedures.

FDM programmes are an example of fault detection methodologies. If a recorded flight parameter exceeds a pre-specified threshold for a pre-specified time period then an exceedance or ’fault’ has occurred and flight safety officers can investigate it. Traditionally fault detection has been seen as a purely engineering discipline. However, in the past 10 years or so, it has become a multi-disciplinary approach, in particular utilising Artificial Intelligence (AI). AI techniques, combined with a robust understanding of the problem domain (in this case how aircraft are flown) have had success in not only detecting faults but also in predicting them. Fault detection approaches usually split into two areas.

- Online Fault Detection: This usually consists of sampling, preprocessing and analysing the data in real time or with a very minimal delay. This can be very valuable in alerting operators instantly to possible faults. Efficiencies must be made on the method of sampling and computation in order that the algorithm operates in real time.

- Offline Fault Detection: This usually consists of sampling, preprocessing and analysing the data sometime afterwards. For this approach, time is not as important, which can allow more computationally difficult algorithms to be utilised. However, it will not alert the operator to faults until after they have happened.

AI can be useful for both forms of fault detection, however this thesis is only concerned with offline fault detection. In simple terms, flight data is sent from aircraft, processed by software at Flight Data Services Ltd and can then be viewed in graphical or table form. The condition of the aircraft at a given height can be thought of as a function of ’useful’ recorded parameters at that height. By considering a large sample of flights that have been flown within the airlines Standard Operating Procedures, it is possible to create a profile of how the aircraft should be flown. Deviations from this profile can thus be regarded as abnormal and hopefully be detected and the airline alerted.

1.2 Problem Formulation

Fault detection is a very important part of modern civil and military systems. It is often such that fault detection is just as important as the system itself, particularly if a fault could be very dangerous. Whilst many fault detection systems are built into the system in question, some are retrofitted, perhaps in light of new information about possible faults or for reasons of cost.

Flight safety has been an important topic ever since the first aircraft flew. Accidents as far as possible were fully investigated and their lessons distributed to the relevant bodies. Modern aircraft have two backup systems for each of the main systems on board so that even if a main system and a backup fails, the remaining backup system should still be able to help fly the aircraft. Whilst these measures will help reduce the chance of mechanical failures, a lot of information on the state of the aircraft is available from the data recorded by the flight data recorders. Modern aircraft can record upwards of 600 parameters of frequencies between 0.25Hz and 8Hz. A 2 hour flight could therefore provide around 100Mbs worth of data. An event based system will utilise a small amount of these parameters and will notify the analyst if a parameter exceeds a given limit over a given time period. Furthermore, only events with the highest severity level (level 3) are looked at by analysts. and flight safety officers and so a large amount of data is not being inspected. A concern is that there may be unseen events or anomalies that the event based system has not detected. Using the raw values, it might be possible to identify any increasing trends; for example, airspeeds getting closer and closer to the level 3 limit on a particular phase of flight. This information could be passed onto the airline so that they can take remedial action before a problem actually happens. Furthermore, a system should be able to provide greater insight as to why level 3 events occur and provide a better understanding as to how their pilots are flying the aircraft.

The problem is therefore to explore ways to utilise more of the data, from all or part of a flight, in order to investigate if there are any unseen abnormalities and assess their relative impact on the flight. The data is in the form of a time series consisting of all recorded parameters over the period of the flight. To the best of the author's knowledge, this is one of the first times that a large quantity of flight data has been studied in order to improve safety.

1.3 Aims and Objectives

The dissertation intends to address the following aims.

1. To analyse individual flights and their parameters and identify which parameters are useful in understanding the state of the aircraft at a given point in time.

2. To identify what, if any, new information on trends or anomalies can be found from using more data than the event based system uses.

3. To create a system that is able to identify and assess the impact of anomalies of a flight and compare that flight to other such flights.

In order to achieve these aims, the followings objectives will be undertaken.

- Understand the existing event system, how limits are chosen and how events are triggered.

- Study which events are most common and why.

- Understand what parameters are available for analysis and their meaning relative to the state of the aircraft.

- Understand how an aircraft flies and the reasons for the standard operation procedures by which they are meant to be flown.

- Study the principles behind fault detection and one class classification.

- Investigate the available literature on flight safety.

- Investigate methods for ranking flights in terms of abnormalities and their impact.

1.4 Outline of Thesis

Chapter 2 contains a brief history of flight data recorders and flight safety in general. It looks at flight data monitoring programs and their key components. A literary review of research in the field of flight data analysis is conducted and in particular, the event based system is analysed to determine its advantages and disadvantages. Finally, the descent is analysed with reference to general descent principles and instructions from the airline in question.

Chapter 3 contains a study on one class classification methods. It explores the theory behind the methods, looks at each method and also identifies key papers that have used a given method successfully. It also identifies properties that a good classifier should have in order to potentially achieve good results. Finally, there is a review of ranking systems and some of their applications.

Chapter 4 explains the method used. It explains how the method was chosen, selection of the dataset, preprocessing, scaling, experimental methodology, parameter choice and the creation of the abnormal test set. Chapter 5 presents the results of the thesis and it has been split into two parts. The first part looks at a Descent Abnormality Profile (DAP) for each flight and how representative the DAPs are to the actual flight data and whether they highlight points of interest. The second section looks at how the overall effect of the abnormalities on a flight can be assessed and shows the results of ranking the abnormal test set against the normal data. The F-score algorithm is detailed and it highlights which heights are most useful in identifying the differences between the abnormal and normal data. Furthermore, it is also used to identify which parameters are responsible for this.

Chapter 6 presents the conclusions, the main contributions of the thesis and future work.

Chapter 2

Flight Safety

2.1 Introduction

When aircraft are involved in a major incident such as a mid air collision or loss of control resulting in a crash, the event almost always makes the front page of newspapers and is often the main story on national news. For these reasons, flight safety is of critical importance. An airline with a poor safety record will find it much harder to attract customers, hire the best crews and insure its operation.

In this chapter, a brief history of flight data recorders and their impact on flight safety can be found in section 2.2. Section 2.3.1 looks at the main features of a typical FDM program. Section 2.4 provides a literary review of methods of flight data analysis. Section 2.5 details the event based system and its advantages and disadvantages. Section 2.6 describes how to fly the descent and lists stablised approach criteria. Section 2.7 describes how the descent is flown by the airline whose data is used in this thesis. Section 2.8 concludes the chapter.

2.2 History of Flight Safety

2.2.1 History of Flight Data Recorders

In 1908, five years after the first flight, Orville Wright was demonstrating his flyer aircraft to the United States military in the hope of securing a contract with them to provide them with a military aeroplane [Howard, 1998; Prendergast, 2004;

Rosenberg, 2010]. The first two demonstration flights were successful. However, on the third, 'two big thumps' were heard and the machine started shaking. Despite desperate attempts to regain control, from a height of 75ft, the aircraft plunged into the ground, badly injuring Orville Wright and eventually killing his passenger. On analysis of the wreckage, Wright determined that the accident was caused by a stress crack in the propeller which caused it to fall off. The Wrights were able to make design changes to the aircraft using this analysis to try and reduce the chances of another such accident. Whilst in this case it was possible to discover the cause of the accident from the wreckage, there have been several accidents where either the wreckage is in a remote area or the wreckage provided no indication of the cause of the accident. Further knowledge could be obtained if a device was created that was attached to the aircraft and able to record data such as airspeed, rate of descent and altitude.

There is some doubt as to when the first flight data recorder was produced. In 1939, the first proven recorder was created by Francois Hussenot and Paul Beaudouin at the Marignane flight test centre in France [Fayer, 2001]. It was a photograph-based flight recorder. The image on the photographic film was made by a thin ray of light deviated by a tilted mirror according to the magnitude of the data to record.

In 1953, an Australian engineer, Dr David Warren created a device that would not only record the instrument readings but also any cockpit voices, providing further information as to the causes of any accident [Williamson, 2010]. A series of fatal accidents, for which there were neither witnesses or survivors led to growing interest in the device. Dr Warren was allocated an engineering team to help create a working design. The device was also placed in a fire proof and shock proof case. Australia then became the first country in the world to make cockpit voice recording compulsory.

Today, flight data recorders are governed by international standards. Recommended practices concerning flight data recorders are found in International Civil Aviation Organisation (ICAO) Annex 6 [ICAO, 2010]. It specifies that the recorder should be able to withstand high accelerations, extreme temperatures, high pressures and fluid immersions. They should also be able to record at least a minimum set of parameters, usually between 1 and 8Hz. Most recorders are capable of recording around 17-25 hours of continuous data.

2.2.2 History of Flight Data Monitoring

The development of 'black box' flight data recorders was a significant advance and allowed investigators to look at the raw data at the time of an accident to try and understand what happened. However, the device was only intended to be analysed at the time of an accident and so was little use for accident prevention. From the 1960's and 70's, some airlines found it beneficial to replay crash recorder data to assist with aircraft maintenance. However, multiple replays tended to reduce their lifespan and so the Quick Access Recorder (QAR) was introduced to record data in parallel with the crash recorder. Increases in the size of data storage devices made it became possible to store data from one or multiple flights.

The introduction of this technology led to the first FDM programs. The Civil Aviation Authority (CAA) defines FDM as "the systematic, pro-active and non-punitive use of digital flight data from routine operations to improve aviation safety." The success of such programs are such that ICAO recommend that all aircraft over 27 tonnes should be monitored by such a program. The UK, applying this recommendation, has made it a legal requirement since 1st January 2005 [CAA, 2003].

2.3 Flight Data Monitoring Programmes

There are a wide variety of aircraft in service with the world's airlines today. Some are very modern such as the Boeing 787 Dreamliner [Boeing, 2010] (first flight December 2009) and some are very old such as the Tupolev Tu-154 [Airliners, 2010] (first flight October 1968). Not all these aircraft were designed for the easy fitting of the QAR and furthermore there is a big difference as to what parameters the aircraft can record. Thus it is such that there is no standard FDM program but that one should be tailored to the aircraft in the fleet and the structure of the airline.

2.3.1 Features of a Typical Flight Data Monitoring Program

According to CAA recommendations as found in [CAA, 2003], a typical FDM program should include...

- The ability to identify areas of current risk and identify quantifiable safety margins - Flight data analysis could be used to identify deviations from the airlines Standard Operating Procedure (SOP) or other areas of risk. Examples might include the frequency of rejected take offs or hard landings.
- Identify and quantify changing operational risks by highlighting when non-standard, unusual or unsafe circumstances occur. - Flight data analysis can identify any deviations from the baseline but it should also be able to identify when any unusual or potentially unsafe changes occur. Examples could include an increase in the number of unstable approaches.
- To use the FDM information on the frequency of occurrence, combined with an estimation of the level of severity, to assess the risks and to determine which may become unacceptable if the discovered trend continues - By analysing the frequency of occurrence and by estimating the level of risk involved, it can be determined if it poses an unacceptable level of risk to either the aircraft or the fleet. It should also be able to identify if there is a trend towards unacceptable levels of risk.
- To put in place appropriate risk mitigation techniques to provide remedial action once an unacceptable risk, either actually present or predicted by trending, has been identified - Having identified the unacceptable level of risk, systems should be in place to undertake effective remedial action. For example, high rates of descent could be reduced by altering the SOP so that better control of the optimum rates of descent is possible.
- Confirm the effectiveness of any remedial action by continued monitoring - The FDM program should be able to identify that the trend in high rates of descent, for example, is reducing for the airfields in question.

Captain Holtom of British Airways [Holtom, 2006] states that from a flight operations perspective, an FDM program should identify

- Non-compliance and divergence from Standard Operating Procedures.
- An inadequate SOP and inadequate published procedures.
- Ineffective training and briefing, and inadequate handling and command skills from pilots and flight crew.
- Fuel inefficiencies and environmental un-friendliness.

From a maintenance perspective he states they should identify

- Aerodynamic inefficiency.
- Powerplant deterioration.
- System deficiencies.

Holtom highlights the value of FDM by including a quote from Flight International: "Knowledge of risk is the key to flight safety. Until recently that knowledge had been almost entirely confined to that gained retrospectively from the study of accident and serious incidents. A far better system, involving a diagnostic preventative approach, has been available since the mid-1970s."

2.3.2 Methodology of a Typical Flight Data Monitoring Program

1. Acquisition of Aircraft Data - Data is sent to the airline either wirelessly or by removing the tape/disk and uploading it via the Internet to the airline.
2. Validation of Aircraft Data - The binary data is processed into engineering units and validated to in order to ensure the data is reliable and that aircraft parameters are within ranges listed by the aircraft manufacturer.
3. Processing of the Data - The data is replayed against a set of events to look for exceedances and deviations from the SOP.

4. Interpretation of the Data - All events are analysed automatically and checked by analysts. Maintenance events are immediately sent to the maintenance department so that aircraft can be checked for any stresses or other damage. Operational events are then analysed and possible crew contacts initiated. Statistics of trends by time period, aircraft type, event type, etc can be created.

5. Remedial Action - Training procedures or SOPs can be modified to reduce the identified risk.

This thesis is concerned only with interpreting the data.

2.4 Literature Review of Flight Safety

A common analysis technique is one that is event driven [FDS, 2010]. Software such as Sagem's Analysis Ground Station [SAGEM, 2008] can process the raw data that the airlines have sent and then tabulate the parameters and display them on graphs. Airlines choose which events they would like detected and the limits that they should be triggered at. There are two main types of events: operational and maintenance. Operational events are concerned with the way in which the aircraft is flown and how that flying deviates (if at all) from the airline's SOP. Maintenance events are concerned with the physical condition of the aircraft, in particular the engines, hard landings and flying too fast on a certain flap setting. When maintenance events occur, the maintenance department of the airline in question is immediately notified so that if there is any damage, they can repair it. Events are created based on parameter exceedances and the greater the exceedance, the higher the severity level. Level 3 events are the most severe and are always reported to the airline's flight safety officer. From this, statistics can be produced to see which flights have the most events, which airline has the best event rate, which events are the most common, etc. Furthermore, each level 3 is validated by an analyst with experience in the field of flight safety to ensure that the airlines only see valid events and that any statistics produced contain valid events.

There are several providers of FDM in the current market. Whilst all use an event based approach, there are subtle differences in their implementation. This thesis is not interested in providing an overview of the market's solutions for FDM but an overview of how they use their event and snapshot data to identify abnormal flights. Aerobytes Ltd produced a fully automated solution in which events are validated automatically [Aerobytes, 2010a]. This will greatly reduce the workload for any analyst but it may prove difficult to configure the machine such that almost all of the events are valid. They use histograms to display information for a particular parameter from which the user can select thresholds and identify the percentage of flights for which that threshold was exceeded. Such an approach allows the user to gain a better understanding of how their aircraft are actually flying and whether the event limits are reasonable. They also utilise a risk matrix which consists of the state of the aircraft in the columns (air, ground, landing and approach, take off and climb) and event type (acceleration, configuration, height, etc) on the rows [Aerobytes, 2010b]. Each event is described by a number from 0 to 100 which rates the severity of the event with 100 being the most severe and 0 being normal. Severity appears to be based on the main event parameter so a Ground Proximity Warning System (GPWS) warning on the final approach at 400 feet radio altitude would be regarded as more severe than one at 800 feet radio altitude. A similar system is also used at British Airways [Holtom, 2006]. In this way, flight safety officers can focus on the events which have the higher severity ratings. The system has several advantages in that by attempting to measure event severity, flight safety officers can focus on the more abnormal flights. However, it is impossible to assess if the severity scale accurate reflects the impact of the event or if the automated system is able to display only valid events. The author has not had access to this system and this review is based on advertised capabilities.

In addition to event based analysis, British Airways uses histograms to show the distribution of the maximum value of a selected parameter during a given time period such as the maximum pitch during takeoff [Holtom, 2006]. These charts can help explain if certain types of events are occurring because crews are not adhering to the SOP. They can also identify if a problem is common to one or two individuals or if it is occurring across the whole fleet. This information can be passed on to the training department. Then the individual in question or all the pilots might benefit from extra training.

The airlines can see that an event has occurred but what they cannot see is why it occurred. Notification is very useful but it is just as important to identify any preliminary signs. Furthermore, the events are usually based on one or two parameters, describing only part of the situation at a single point in time.

Van Es and the work of the National Aerospace Laboratory [van Es, 2002] looks at the event based approach and extends it by making more use of the available data. Rather than just focussing on parameter exceedances, he considers data trends and looks at possible precursors to events. In other words, he analyses the 'normal' data and uses standard statistical significance testing to identify whether trends are significant or just part of normal data variability. A hard landing is one where the maximum recorded value of the acceleration due to gravity of the aircraft at touchdown is higher than usual. He provides examples such as the likelihood of a hard landing into certain airports and uses the Kolmogorov-Smirnoff test to show that the landings for two different airports are statistically different. This is deduced by comparing the cumulative frequency charts showing the maximum recorded acceleration due to gravity of each aircraft landing at these airfields and using the test to identify differences between the charts. This is of great use to the airline.

This approach is extended further in [Amidan and Ferryman, 2005]. Amidan and Ferryman have been involved in the creation of the analysis software Avionics Performance Measuring System (APMS) [NASA, 2007]. It analyses data using three phases. In the first phase, the individual flight is split into flight phases (such as take off) and then into sub-phases. For each sub-phase, a mathematical signature is created which stores the mean, the standard deviation, the minimum and the maximum of each variable, thus reducing the storage cost for each flight. The user then selects the characteristics of the flights to be studied and then K-means clustering is applied to it to locate atypical flights. The mathematical signatures are derived as follows. Each flight is split into the following flight phases;

1. Taxi Out

2. Take off
3. Low Speed Climb
4. High Speed Climb
5. Cruise
6. High Speed Descent
7. Low Speed Descent
8. Final Approach
9. Landing
10. Taxi In

Each of these phases is then split into subphases. The parameters are then summarised in different ways, depending on if they are continuous or discrete. For continuous parameters, the first second of a phase is taken as well as five seconds either side, creating an eleven second window. A centred quadratic least squares model

$$y = a + bt + ct^2 + e \tag{2.1}$$

is fitted where e is the error term. The error is the difference between the actual value and the predicted value. This is summarised by

$$d = \left[\sum \frac{e^2}{n-3}\right]^{1/2} \tag{2.2}$$

This is repeated for each second of the flight phase so if there were 10,000 seconds in the flight phase, a total of 10,000 sets of coefficients, a,b,c,d, would be computed. Then for each flight phase, the mean, standard deviation, maximum and minimum of each coefficient. Furthermore, the value of the parameter at the start and at the end of the phase is included. So if n flights are considered with p parameters then a data matrix can be formed with n rows and $18p$ columns.

The discrete parameters are calculated differently. A transition matrix shows the number of times the value of a parameter changes and how long it remains in that change. It also contains counts of time periods during the phase. This is converted into a related matrix by dividing the off diagonal counts by the total number of counts for the phase so that the off diagonal shows the percentage of time the parameter was recorded at each value. The diagonal of this matrix consists of the count of the number of times the parameter changed value. If there are q possible states for the parameter then the matrix is a q by q matrix. This is then vectorised into a vector with q^2 elements which is added to the signature matrix.

Phase 2 consists of clustering the signatures of the selected flights using K-means clustering and the computation of the atypicality score which is detailed below.

Each flight is given an atypicality score which is computed in the following way. Principal Component Analysis (PCA) is performed on the flight signatures keeping 90 percent of the variance. Using the formula below

$$A_i = \sum_{j=1}^{n} {PCA(j)_i^2}/{\lambda_i} \tag{2.3}$$

where i is the flight (row) from which the score is computed, A is the atypicality score, $PCA(j)$ is the jth PCA component vector of the ith flight and λ_j is the associated eigenvalue. A score close to zero indicates a high degree of normality. This is useful for comparing many flights to see which ones had a problem but it is not very useful if one wishes to compare a certain flight phase of multiple flights. To do this, they note that a gamma distribution is suitable for modelling the atypicalities. A cluster membership score using K-means is computed via

$$cms_i = \frac{n_i}{N} \tag{2.4}$$

where cms_i is the cluster membership score for flight phase I, n_i is the number of flights in flight phase I's cluster and N is the number of flights in that analysis. Then a global atypicality score is computed via

$$G_i = -\log(p_i) - \log(cms_i). \tag{2.5}$$

where G_i is the global atypicality score for flight/flight phase i, p_i is the p-value for flight/flight phase i and cms_i is the cluster membership score in equation 2.4. The negative values ensure the overall result is positive", with small values indicating a higher degree of normality. The atypicalities are all computed and the top 1% of the results are regarded as level 3 atypicalities, the next 4% level 3, the next 15% level 1 and the rest as typical flights.

The key benefits of this approach are that flights and flight phases can be compared for abnormality and a measure of the degree of abnormality can be computed. Parameters over eleven second periods in the flight phases are modelled by a quadratic. However, it may not have the flexibility to model the parameter accurately. For example, the parameter vertical g is computed every 8Hz and varies a large amount, too much for a quadratic curve to model accurately. Furthermore, the method requires a good selection of flights from which to make comparisons and also a lot of domain knowledge. For example, if an airline suddenly changes its procedure for an approach into a certain airport, those flights would be detected as abnormal initially even though they are regarded as normal. The atypicality computation depends on modelling the atypicality scores via a gamma distribution and on clustering. It is not known how suitable a gamma distribution is for such modelling, i.e. how many flights are needed to approximate the distribution to a certain degree of accuracy?

Furthermore there is no attempt to conduct experiments to identify how well the method is able to detect abnormal flights and there is no mention of how the authors define an abnormal flight. No figures are given for the numbers of flights used or whether for example the data came from different aircraft types. There appears to have been no attempt to compare their method to any other currently used to analyse flight data. These reasons make it nearly impossible to assess the validity of this method for identifying abnormal flights.

2.5 Event System

Events in FDM terminology are exceedances of one or more parameters at a specific height or between a specific height range. They are designed to identify typical threats to an aircraft and are separated into two groups; operation and

Table 2.1: A Sample of Flight Data Monitoring Events.

Event Type	Description	Level 1 Limit	Level 2 Limit	Level 3 Limit
Attitude	Pitch high at take off	10 deg	11 deg	12 deg
Attitude	Roll exceedance between 100ft and 20ft for 2 seconds	6 deg	10 deg	14 deg
Speed	Speed high during the approach from 1000ft to 500ft	Vref30 + 35 for 5 seconds	Vref30 + 45 for 5 seconds	Vref30 + 55 for 5 seconds
Speed	Speed low during the approach from 1000ft to 500ft	Vref30 + 5 for 5 seconds	Vref30 for 5 seconds	Vref30 - 5 for 5 seconds
Descent	High rate of descent during the approach from 1000ft to 500ft	-1200ft/min for 5 seconds	-1500ft/min for 5 seconds	-1800ft/min for 5 seconds
Configuration	Use of Speedbrakes in the final approach	n/a	n/a	above 50ft
Engine Handling	Low power on the approach under 500ft	50%	45%	40%

maintenance. Maintenance events concern threats to the structural integrity of the aircraft such as hard landings, flap over-speeds and engine temperature exceedances after take-off. These events are usually sent immediately to the airline so they can check the aircraft for any damage. Operations events look at how the pilots fly the aircraft and such events are triggered when the aircraft deviates substantially from parameter limits given in the aircraft's event specification.

Example events can be found in table 2.1.

Airlines are usually only interested in level 3 events, the most severe exceedance as these could be potentially hazardous to the aircraft, its crew and its passengers. Statistics can be generated to show which event occurs most often. Event rate is a common way of showing how often the events occur. See figure 2.1 for an example of some flight data with an event.

Figure 2.4 shows the number of events that occur in each flight phase. To assist the reader in understanding the figure, table 2.2 gives a description of each of the flight phases. The flight phases concerned with the take off and climb are 'take off', 'initial climb and 'climb' and they contribute 18.51% of the total events.

Figure 2.1: Example Flight Data with an Event.

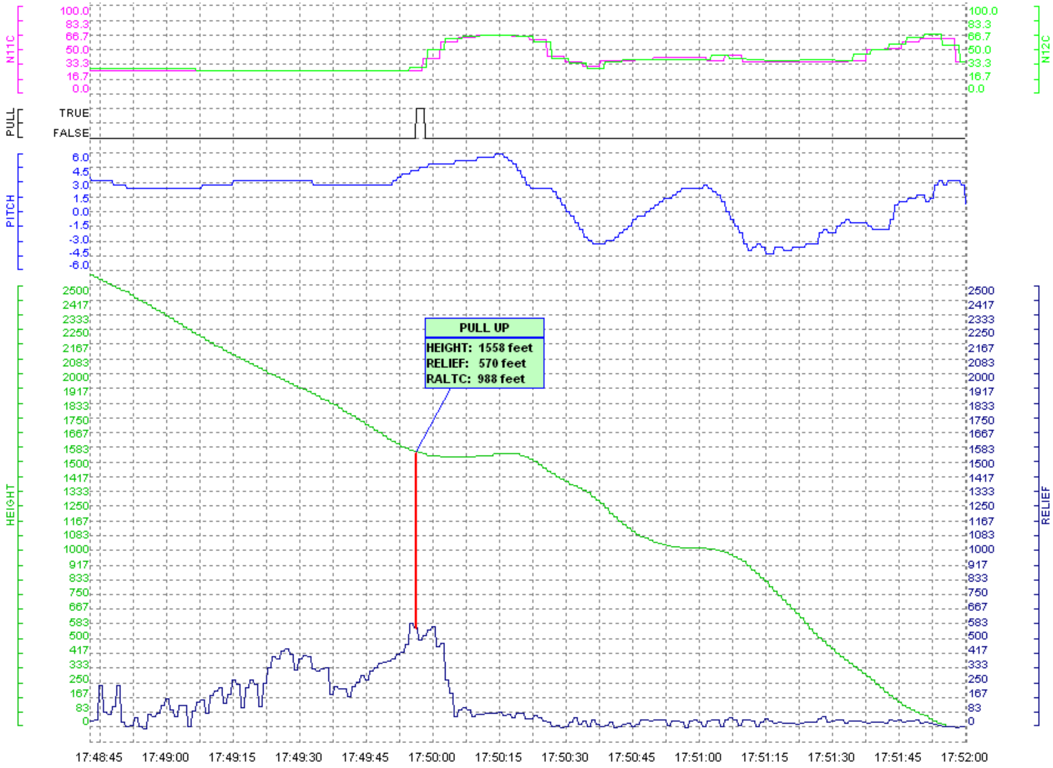

However, the flight phases 'descent', 'approach', 'final approach', 'go-around' and 'landing' encompass the act of 'descending' the aircraft from the cruise phase and these phases account for 72.17%, nearly three quarters of all events. It is likely that precursors to these events can also be found in these flight phases. Given that the majority of events are generated from the act of descending the aircraft, the research will focus on analysing flight data in the descent.

A further point to note is that while there are benefits for considering the flight as a whole, the vast majority of the level three events occur around the start and the end of a flight. In fact nearly 70% of level three events occur in the descent, approach, final approach and landing phases and 21% of events in the takeoff, initial climb and climb phases (see figure 2.4).

Figure 2.2: Example Flight Data - High Speed Approach with Events.

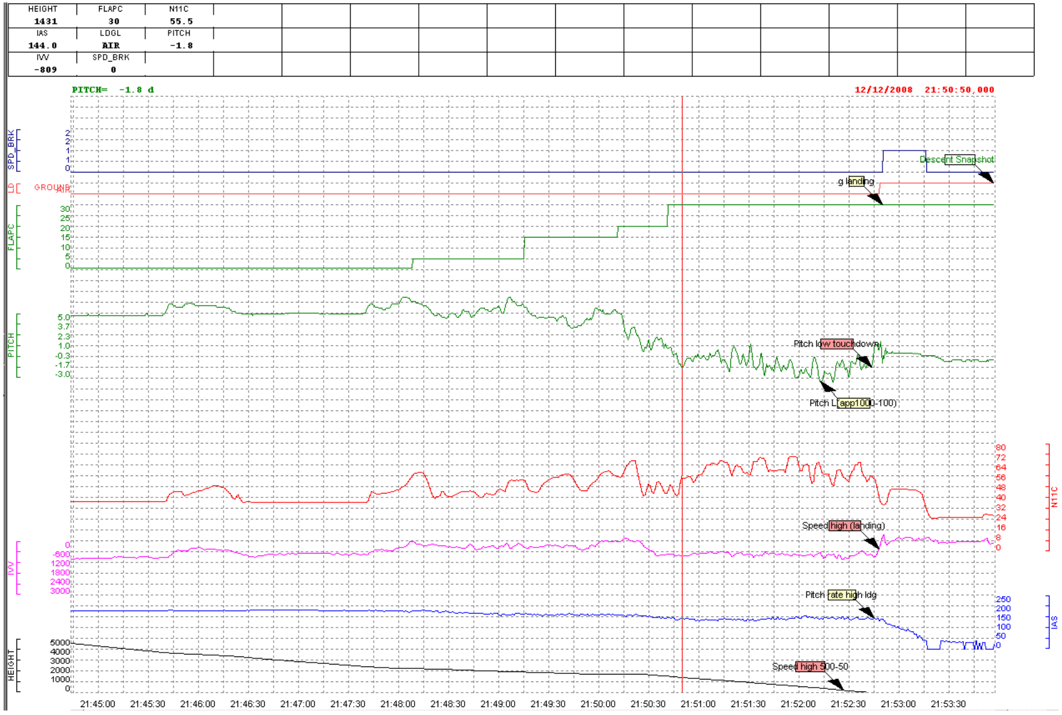

HEIGHT 1431	FLAPC 30	N11C 55.5
IAS 144.0	LDGL AIR	PITCH -1.8
IVV -809	SPD_BRK 0	

2.5.1 Advantages and Disadvantages of the Event Based System

The event based system is very popular because it allows comparisons with other airlines provided they have similar events and it provides a good overview of the airline's operation. Whilst there are many advantages to this approach (see section 2.5.1.1), there are several significant disadvantages (see section 2.5.1.2).

2.5.1.1 Advantages

- New events can be created as the need arises. Furthermore, they can be created to include as little or as many triggers as required.

- The airline chooses the event limits and they can be changed as required.

- Event occurrences lend themselves to a variety of useful statistics for an airline. A count of the number of events can show which events are causing the most problems. The event rate can show which events occur the most

Figure 2.3: Example Flight Data - Steep Descent.

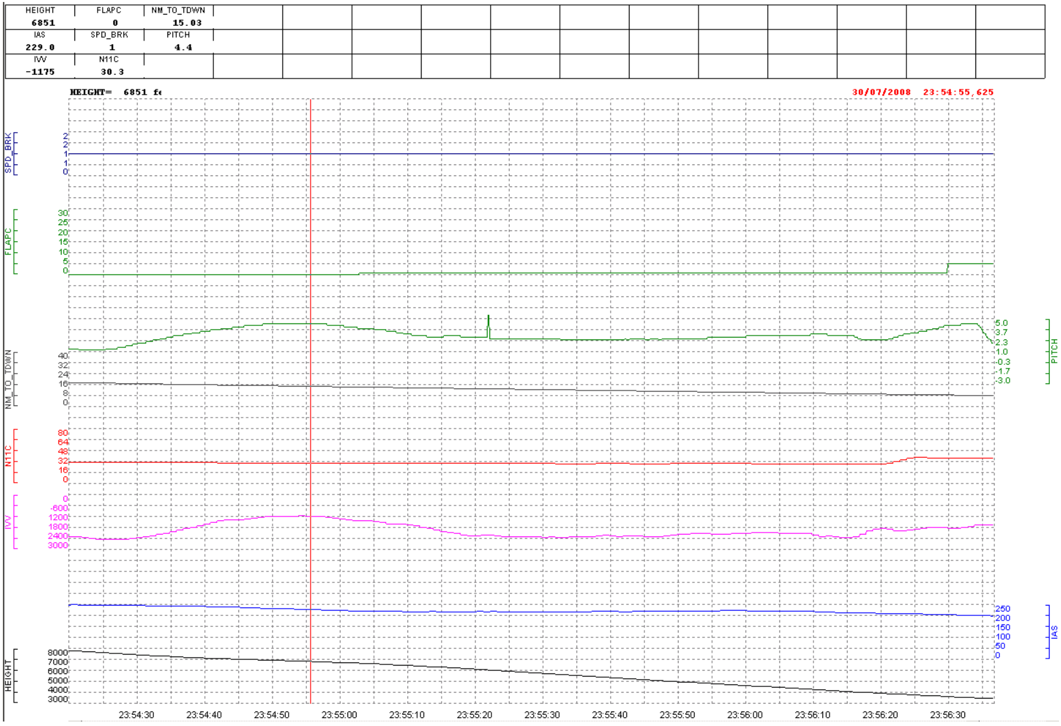

frequently. Furthermore, one can compute the event rate per arrival airfield, per month, per aircraft type, per dataframe, etc.

- The system is so widely adopted that airlines can be compared with each other to identify any generic problems.

2.5.1.2 Disadvantages

- If an airline changes the event limits often, it becomes increasingly difficult to identify any real changes in the parameter(s).
- If an event does not exist then a problem in a specific area may go unnoticed which could lead to a significant incident.
- Only level 3 events are validated by analysts to check if the event has triggered correctly in that instance. Whilst this is useful to the airline in that it only sees real events, it is also such that level 3 events occur on around 5% of flights so the vast majority of flights are unseen.

Figure 2.4: Event Percentages by Flight Phase.

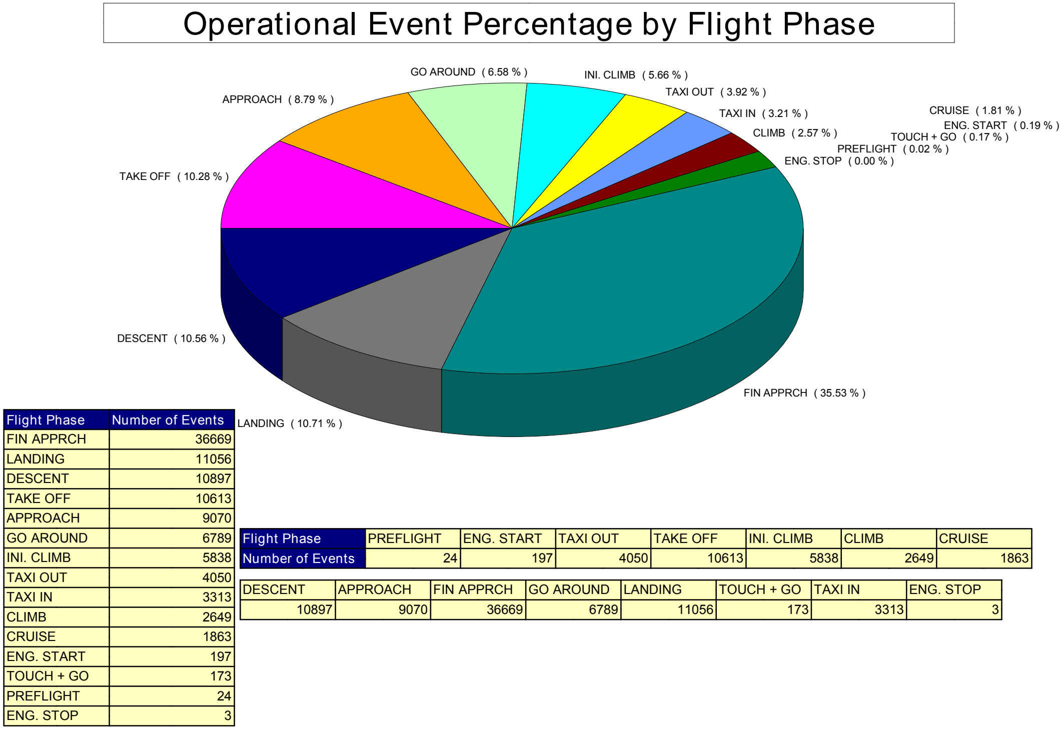

Flight Phase	Number of Events
FIN APPRCH	36669
LANDING	11056
DESCENT	10897
TAKE OFF	10613
APPROACH	9070
GO AROUND	6789
INI. CLIMB	5838
TAXI OUT	4050
TAXI IN	3313
CLIMB	2649
CRUISE	1863
ENG. START	197
TOUCH + GO	173
PREFLIGHT	24
ENG. STOP	3

Flight Phase	PREFLIGHT	ENG. START	TAXI OUT	TAKE OFF	INI. CLIMB	CLIMB	CRUISE
Number of Events	24	197	4050	10613	5838	2649	1863

DESCENT	APPROACH	FIN APPRCH	GO AROUND	LANDING	TOUCH + GO	TAXI IN	ENG. STOP
10897	9070	36669	6789	11056	173	3313	3

- The system implies that one level 3 event is more serious than any combination of level 1 or 2 events in that flights with just level 1 and 2 events will never be investigated. It is certainly feasible that a flight with 10 level 2 events in the descent is more concerning than a flight with just 1 level 3 event.

- The system has value in alerting airlines to events that have already happened, i.e. level 3 events. However it makes little attempt to identify precursors to these events. A key aspect of flight safety is to try and understand risks and their causes. Identifying precursors to events would be very useful in this regard.

2.6 Principles of the Descent

Whilst in the cruise and approaching the destination, the flight crew plan the descent based on information provided pre-flight, on updates received in flight,

Table 2.2: An explanation of flight phases.

Flight Phase	Description
Pre-flight	Fuel is flowing above a certain rate.
Engine Start	Pre-flight phase has occurred and an engine has started.
Taxi Out	Aircraft is moving and the heading changed are occurring.
Take Off	Indicated airspeed is greater than 50 knots for more than 2 seconds.
Initial Climb	Aircraft is climbing between 35 feet and 1500 feet.
Climb	Aircraft height is greater than 1500 feet and there is a positive rate of climb.
Cruise	Aircraft height is above 10000 feet and there are no large positive or negative rates of climb.
Descent	Aircraft rate of descent is negative and remains negative.
Approach	Height is less than 3000 feet or flaps are set greater than 0.
Final Approach	Height is less than 1000 feet or landing flaps selected.
Go-Around	Aircraft was in final approach or approach and initiated a climb.
Landing	Aircraft landing gear is on the ground.
Touch and Go	Aircraft lands momentarily and initiates climb.
Taxi In	Aircraft has landed, height remains constant and heading changes are occurring.
Engine Stop	Aircraft has landed and engine prop speed is below a certain value.

existing conditions and on the pilot's experience of a particular route, time of day, season etc. They aim for a continuous descent with the engines at idle power from the start of the descent until a predetermined point relative to the arrival runway. A continuous descent provides the best compromise between fuel consumption and time in the descent. It also minimises the noise footprint of the aircraft. Rules of thumb are used in the planning stage. For example if H is the altitude to be lost and D is the distance needed to descend and decelerate to 250kts then the following is used:

$$D = 3.5H + 3. \tag{2.6}$$

Different aircraft types will have different descent profiles detailed in the Flight Crew Manuals for that particular aircraft type based on manufacturers training notes. The Boeing 757 for example should be 40NM from the airport at 250kts as the aircraft passes 10000ft in the descent.

Traffic density, national Air Traffic requirements and weather can all be planned for. However, during the descent, these and many other factors can cause the pilots to revise their plan. For example when conflicting traffic leads to the pilot having to level the aircraft at an unplanned intermediate altitude. The pilot needs to compensate for the extra distance travelled whilst level once the descent resumes by either by descending faster in the remaining distance to the arrival runway or by maintaining the planned rate of descent but extending the distance over the ground or a combination of both.

All major airports have predetermined approach procedures - horizontal and vertical profiles- that should be followed to maximise traffic flow and minimise disruption to sensitive areas beneath the flight path. These can be viewed on approach plates, often called Jeppeson Plates. At times when traffic is light the restrictions detailed in these procedures can be removed, often at short notice; an aircraft cleared for a direct visual approach rather than an instrument approach.

Whether the disruption to the planned descent happens at an intermediate altitude or in the approach to the runway, the pilot has limited means to adjust his airspeed and/or height. Slowing down is often achieved by decreasing rate of descent and increasing rate of descent to meet a height restriction often causes an increase in airspeed. Devices such as speedbrakes are used to minimise the effects of speed/height changes but there are limits on their use e.g. speedbrakes cannot be used with flaps extended beyond 25. In some cases, the pilots may decide to extend the landing gear which increases the drag of the aircraft and therefore its rate of descent. However this method is usually only used during special circumstances.

Once in the approach phase the options available to slow down/lose height are more limited. The aircraft should be ”stabilized” at a set point in the approach. The airline in this thesis has an industry typical criteria for a stabilized approach where the aircraft should be stabilized at 1000ft and must be stabilized at 500ft above the runway. Stabilized is defined as: -

- On the correct flight path
- Only small changes in heading/pitch required to maintain the correct flight path

- Airspeed is +20/-0kts on the reference speed
- Flaps and landing gear are correctly configured
- Rate of descent is no greater than 1000 feet per minute
- Engine power should be appropriate for the aircraft configuration
- All briefings and checklists completed
- For an ILS approach the maximum deviation is 1 dot

Approaches that are not stabilized are frequently referred to as ”rushed” or unstablized approaches. The Approach and Landing Accident Reduction (ALAR) task force, set up by the Flight Safety Foundation, state that “Unstablized approaches cause ALAs (Approach and Landing Accidents)” [FSF, 2000]. Pilots are trained to recognise a rushed approach and are required to follow the airline's instructions which is to abandon the approach and make a second, more timely approach. The roots of a rushed approach can often be traced back to the planning stage of the descent, with disruption in the actual descent highlighting the planning deficiencies. Identifying the early signs of a rushed approach sooner rather than later in the descent, and giving the crew a clear warning of the danger ahead will be a positive step in accident prevention.

The Air Accident and Investigation Branch (AAIB) is a body in the UK that investigates and reports on air accidents in order to determine their causes. In 2004, they made a recommendation to the CAA [Foundation, 2004] that they should consider “methods for quantifying the severity of landings based on aircraft parameters recorded at touchdown” to help the flight crew determine if a hard landing inspection was required. This recommendation is significant because it understands that the state of the aircraft at touchdown can be better represented by several parameters rather than one or two. Limits for a typical hard landing event are thresholds on the parameter measuring the force exerted due to gravity by the aircraft at touchdown. Other parameters such as the rate of descent are useful in determining if a hard landing has taken place. However, to understand why it happened, it is useful to consider how the aircraft was flown in the final approach. Parameters such as airspeed, groundspeed, pitch and rate of descent can also be useful in determining the state of the aircraft at various points above the runway. By somehow quantifying how the state of the aircraft changes, it might be possible to identify the points in the descent which could make a hard landing more likely. Furthermore, it might be possible to apply this method to analysing the severity of the whole descent.

2.7 How the Airline fly the descent

Section 2.6 explains the general principles behind flying the descent. In this thesis, the data used in the experiments in chapter is taken from the approach into the same airport, the same runway and by the same airline. The SOP for this airline follows the general descent principles but includes some extra advice and conditions to reflect the capabilities of their aircraft.

The flight crew training manual advises that the aircraft should reach a point 40NM from the airfield at a height of 10000ft above the runway with a speed of 250kts. In terms of the descent, it also states that "The distance required for the descent is approximately 3.5NM/1000ft altitude for no wind conditions using ECON (economy) speed."Typical rates of descent for this aircraft at a speed of 250kts are 1500fpm or 2000fpmwith the speedbrakes deployed. Once the aircraft's speed reaches Vref30 + 80kts then typical rates of descent are 1200fpm rising to 1600fpm if the speedbrakes are open. It also advises that speedbrakes should not be used with flap settings higher than 5 and that they should not be used under 1000ft. It makes the point that if the rate of descent needs to be increased then the speedbrakes should normally be used. The landing gear can also have the same effect but it is not recommended as it reduces the life expectancy of the landing gear door. It also recommends that the aircraft should satisfy the stablised approach criteria as detailed in section 2.6. Furthermore, for a typical 3 degree ILS glidepath and flaps 30 in ideal landing conditions, the pitch angle of the aircraft should be about 2.2 degrees. For a 2.5 degree glidepath, the pitch angle should be around 2.7 degrees.

Whilst the use of speedbrakes in the descent below 10000ft is permitted, the flight crew training manual advises that speedbrakes should not be used with flaps greater than 5 selected. This is to avoid buffeting. However if circumstances dictate that such a course of action is necessary, high sink rates should be avoided. Furthermore, speedbrakes should be retracted before reaching 1000ft AGL.

When the aircraft reaches approximately 20ft above the runway, the flare should be initiated by increasing pitch altitude by around 2-3 degrees to slow the rate of descent. The thrust levers should be smoothly set to idle and small adjustments in pitch made to control the rate of descent. Ideally, the main gear should touch down on the runway as the thrust levers reach idle. Touchdown speed should be between Vref30 and Vref30 -5 kts. Pitch attitude should be monitored carefully as a tailstrike will occur if the pitch attitude is 12.3 degrees or greater. Touching down with thrust above idle should be avoided since this may establish an aircraft nose up pitch tendency and increased landing role.

2.8 Conclusion

This chapter has looked at a history of flight safety and flight data recorders, a typical FDM program, a literature review of flight data analysis methods and the principles used in descending an aircraft.

The brief study of the history of flight data recorders and how they led to the introduction of flight data monitoring programs illustrates the significant progress made in terms of being able to better recreate the state of the aircraft during flight. Furthermore, with the great increase in the number of parameters available and the frequency of which they are recorded, it is possible to perform a very thorough analysis of the condition of the aircraft. However, with the large number of parameters, the frequency of which they are recorded and the length of a typical flight, the quantity of flight data extracted from a single flight can be very large. Around 60,000 parameters can be recorded on a typical Boeing 777 and even if just 2,000 parameters are recorded then a single aircraft can produce as much as 50 Mb of data a day [Holtom, 2006]. Furthermore the engineering department at British Airways analyses 5 Gb of data each day! With so much data, it can be very hard to detect abnormalities in flights or instigate a comparison of many flights. Therefore the problem at hand should be simplified and reduced in complexity.

A typical flight data monitoring program was introduced and described briefly. A key feature of the program is its emphasis on interpretation of the data and remedial action. Whilst it is very valuable to produce charts and tables of events, the most important thing is to understand why these events took place. The events themselves tell the operator that deviances from the SOP have taken place but they rarely provide any information on precursors that might explain why the event(s) took place. If it is not clear to the airline why certain events have occurred then it makes it very difficult to instigate changes to their procedures to try and reduce the event rates.

Section 2.5 describes how the event based system works and in figure 2.4, the distribution of events by flight phase is shown. The most significant point is that nearly three quarters of events occur in the descent phases of flight, a level of threat clearly recognised by the ALAR task force [FSF, 2000] at the Flight Safety Foundation. By concentrating on understanding the descent, it is hoped that greater insight can be achieved into why certain events occur.

Section 2.6 describes the general principles behind the descent. It suggests that 1000ft above the runway on the approach is a good point to assess the state of the aircraft given that there are a set of recommended conditions for this height. Furthermore, recommendations made by the AAIB [Foundation, 2004] suggest that assessing the severity of hard landings would be useful in determining whether a full inspection of the aircraft is required. From their recommendation it was considered that it might be possible to assess the severity of not just the landing but the whole descent. In Chapter 3, methods for achieving are detailed and analysed.

Chapter 3

Novelty Detection

3.1 Introduction

A common problem in the area of machine learning is fault detection. In industry today, there are two types of maintenance; preventative and corrective. Corrective maintenance occurs when a machine, or part of a machine, is not working as designed. Often, the response is to shut the machine down and repair it, costing money for repair teams, replacement parts and loss of productivity. Preventative maintenance occurs when the machine is monitored and any abnormalities are spotted. Thus, potential problems can be corrected before they become dangerous.

A key challenge however is to define 'abnormality'. The Chambers dictionary defines it as "not normal" and more importantly "different from what is expected or usual" [Chambers, 2010]. This is imprecise and dependent on the situation in question. Abnormality for a jet engine might include a temperature exceedence, or a vibration exceedence. These might be events which have been seen before, or they may not. The complexity of the problem is increased as a classifier therefore has to detect possibly unseen errors.

A general multi-class classification problem can be reduced to a simpler two class classification problem [Fukunaga, 1990], for example using the 'one versus many' method. The problem is thus reduced to separating the two classes of data. A key point to note is that there are many examples of both classes and so a decision boundary can be drawn using information from both classes. However for novelty detection, this is not possible because one will have many examples of the 'normal' class but zero, or close to zero, of the abnormal class. Usually, there will be a lot of examples of the normal class and the aim is to describe the normal class so well that outliers can be identified as outliers [Tax, 2001]. In this chapter, the topics of general novelty detection and one class classification are introduced along with some general principles and an overview of some of the more popular methods. In section 3.2, novelty detection methods are reviewed and analysed. In section 3.3.1 one class classification is introduced and compared to the more common two class classification problem. In section 3.3.2 common classification terms are defined and the theory underpinning one class classification is analysed. In section 3.3.3 key points in section 3.3.2 are highlighted in order to introduce important considerations when selecting a one class classifier for a given problem. The main types of one class classification methods are reviewed in sections 3.3.4, 3.3.5 and 3.3.6. Section 3.3.4 reviews density methods, section 3.3.5 reviews boundary methods and section 3.3.6 reviews reconstruction methods. A literary review is in these three sections on methods to highlight how they have been used for novelty detection problems. Section 3.3.7 looks at all the methods listed and assesses their properties with reference to section 3.3.3. Section 3.3.8 states which classifiers were chosen for the experiments in this thesis. Section 3.4 looks at a literature review of ranking systems.

3.2 Novelty Detection Methods

Novelty detection has been an important part of the topic of classification for at least the last 20 years. Markou and Singh [Markou and Singh, 2003a,b] present a thorough review of novelty detection methods by analysing the main methods.

Extreme Value Theory (EVT) [Roberts, 2002] studies abnormally high or low values in the tails of a distribution and has been used with some success to identify tremors in the hands of patients and also the detection of epileptic fits. They use a Gaussian Mixture Model to train the data. However, this method can be affected by the presence of abnormalities in the dataset.

Hidden Markov Models (HMM) [Duda and Hart, 1973] are stochastic models for sequential data. A HMM contains a finite number of hidden states and transitions between such states take place using a stochastic process to form Markov chains. State dependant events can occur for each state. The probability of these events occurring is determined by a specific probability distribution for each state. Usually an expectation-maximisation (EM) algorithm is used to determine the parameters of the HMM. Thresholds can be applied for novelty detection. [Yeung and Ding, 2003] use HMMs to detect intrusions in computer networks and they show that dynamic model HMMs outperform static models. However, they require that the dataset only contains normal data which could be difficult for other applications where there are unknown faults.

Artificial Immune Systems (AIS) have inspired new methods for novelty detection. An overview of their development since the 1990s can be found in [Stepney et al., 2004] and [Dasgupta, 2007]. In humans, novelty detection (detecting unknown proteins) is carried out by T-cells. Should such an object be found, it can be destroyed by the T-cells. [Dasgupta et al., 2004] use a negative selection algorithm to analyse aircraft behaviour using a flight simulator and achieves a high detection rate for minimal false positives. [Bradley and Tyrrell, 2000] use artificial immune systems to detect hardware faults in machines and demonstrate its ability to recognise invalid transitions as well error detection and recovery.

Section 3.3 is about one class classification, its principles and methods and why it is useful for novelty detection.

3.3 One Class Classification

3.3.1 Definition and Description

In a typical two class classification problem, well sampled data is available for both classes and the classification algorithm attempts to separate the two classes accordingly and assigns a new object to either class. The success of the classifier depends on many factors, such as the degree of representation of each class in the training set and also the features used to differentiate between objects of both classes. The classifier's decision making process is thus aided by the fact that well sampled data is available from BOTH classes [Tax, 2001].

The term 'one class classification' appears to have originated from [Moya et al., 1993]. One class classification differs in one essential regard to the two classification problem. It assumes that data from only one class, the target class is available. This means that the training set only consists of objects from the target class and a decision boundary must be estimated without the benefit of a well sampled outlier class or in fact any outlier objects at all. Such a situation could arise when outlier objects are hard to obtain; either because of the rarity of the event or the costs involved in generating such data.

In the literature, one class classification can be referred to as 'outlier detection'[Aggarwal and Yu, 2001; Hodge and Austin, 2004], 'abnormality detection' [Davy et al., 2006; Duong et al., 2005] and 'novelty detection' [Japkowicz et al., 1995; Ma and Perkins, 2003]. These terms refer to the different applications that one class classification can be applied to.

Several reviews of novelty detection methods have been carried out, for example [Juszczak, 2006; Markou and Singh, 2003a,b; Tax, 2001]. This chapter will not contain an exhaustive review of each and every such method but it will highlight the principle methods and explain the author's choice of classifiers used in Chapter 4.

3.3.2 Theory

Let $X = \{\mathbf{x}_i\}$ denote the dataset where each object x is represented in d dimensional space by the feature vector $\mathbf{x}_i = (x_{i1}, x_{i2}, x_{i3}, ..., x_{ip})$. For each object $\mathbf{x}_i$ a label y_i is attached where $y_i \in \{-1, 1\}$. In order to the perform the classification, a function f must be derived from the training set and should be such that

$$\begin{aligned} &f : \mathbb{R}^d \rightarrow \{-1, 1\} \\ &f(\mathbf{x}) = \mathbf{y} \end{aligned} \tag{3.1}$$

Usually the class of functions and the associated parameters are determined beforehand, denoted by $f(\mathbf{x}; \mathbf{w})$ where $\mathbf{w}$ denotes the parameters. To find the optimal parameters $\mathbf{w}$ for f on the training set X_{tr}, an error function must be defined. Assuming that the objects in the training set are independently distributed, the total error function is given as

$$\varepsilon(f, \mathbf{w}, X_{tr}) = \frac{1}{N}\sum_{i} \varepsilon(f(\mathbf{x}_i; \mathbf{w}), y_i) \tag{3.2}$$

The error function is the 0-1 loss function, given by

$$\varepsilon_{0-1}(f(\mathbf{x}_i; \mathbf{w}), y_i) = \begin{array}{ll} 0 & \text{if } f(\mathbf{x}_i; \mathbf{w}) = y_i \\ 1 & \text{otherwise.} \end{array}$$

Thus by minimising the error ε on the training set, it is hoped that a good classification can be achieved. However, this is unlikely if the training set is unrepresentative of real data or it contains too few data points. Furthermore, there can sometimes be no way of knowing if the distribution of points in the training set is even representative of real life data. In this case, it is often such that the larger the training set, the more representative it is of real life because the characteristics of the data can be determined with greater clarity. However, even if a training set which characterises real life data and is of a good size is available, the number of possible functions that approximate the data can be very large, even infinite. The main aim therefore is to choose a classification function that has a good generalisation ability, in that it is able to classify new and unseen data points successfully.

The 'true' error is defined by

$$\varepsilon_{true}(f, \mathbf{w}, X) = \int \varepsilon(f(\mathbf{x}; \mathbf{w}), y)p(\mathbf{x}, y)dxdy \tag{3.3}$$

where the integration is carried out over the whole of the 'true' distribution $p(\mathbf{x}, y)$.

A good classification function is not only one that has very low classification error on the training set but also one with low error on an unseen independent testing set. The best such function is the Bayes rule ([Duda and Hart, 1973]), given by

$$f_{Bayes}(\mathbf{x}) = \left\{ \begin{array}{rl} 1 & \text{if } p(w_a|\mathbf{x}) \geq p(w_b|\mathbf{x}) \\ -1 & \text{if } p(w_a|\mathbf{x}) < p(w_b|\mathbf{x}) \end{array} \right. \tag{3.4}$$

where $p(w_a|\mathbf{x}$ is the posterior probability of class w_a and $p(w_b|\mathbf{x}$ is the posterior probability of class w_b for a given $\mathbf{x}$. The Bayes rule is the theoretical optimum rule and assuming all erroneously classified objects are weighted equally, it has the best classification performance over all classifiers [Bishop, 1995a]. It is very difficult to apply this rule in practise because it requires the true posterior probabilities of all classes for all data points. Similarly, it is almost impossible to be able to compute the true error (see equation 3.3). It is approximated by an error term known as the empirical error, given by

$$\varepsilon_{emp}(f, \mathbf{w}, X_{tr}) = \frac{1}{N} \sum_{i} \varepsilon(f(\mathbf{x}_i; \mathbf{w}), y_i). \tag{3.5}$$

When the sample size is large and the training data is distributed like the real life data, ε_{emp} is a close approximation to ε_{true}. However, a low value for ε_{emp} on the training set can still lead to a large true error (see equation 3.3) on an independent testing set and this situation is referred to as overfitting. This is possible when a sufficiently flexible function $f(\mathbf{x}; \mathbf{w})$ fits all the data perfectly including any noise. A function that is sufficiently flexible can always be found to fit the training data perfectly and thus give zero empirical error. The overfitting problem can become much worse as the number of features used increases. This is because the volume needed to be described increases exponentially. This is known as the curse of dimensionality [Duda and Hart, 1973]. Equally if the function is not complex enough to describe all the characteristics of the data, the phenomenon known as underfitting occurs. As the complexity of the model increases, the bias component of the error decreases but the variance component increases as see in figure 3.1. The best model is therefore one which minimises the total error, that is, one that represents a tradeoff between the bias and variance contributions [Geman et al., 1992].

Fortunately the bias-variance problem can be reduced by adding prior knowledge into the design of the function $f(\mathbf{x}|\mathbf{w})$. An example of this is the number of clusters in the K-means method. However, if no such prior knowledge is available, an extra error term $\varepsilon_{struct}(f, \mathbf{w})$ is added to the empirical error 3.5 to make the total error ε_{tot}, given by

$$\varepsilon_{tot}(f, \mathbf{w}, X_{tr}) = \varepsilon_{emp}(f, \mathbf{w}, X_{tr}) + \lambda \varepsilon_{struct}(f, \mathbf{w}) \tag{3.6}$$

Figure 3.1: The tradeoff between the bias and variance contributions.

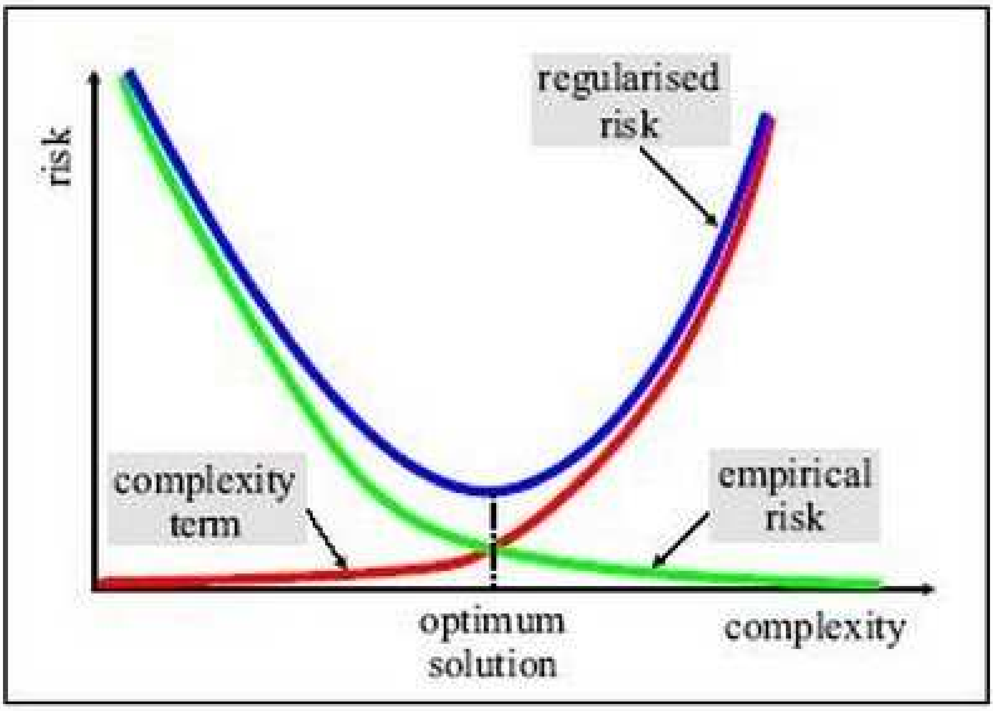

The error term ε_{struct} adds extra complexity to the total error and λ is the regularisation parameter, the size of which measures the impact of the structural term. To simplify the problem the structural error term is modelled on the continuity assumption, that two objects close to each other in the feature space closely resemble the other in real life, imposing a degree of smoothness on the function. Thus the smoother the function the lower the complexity. The main point is that that the minimisation of the structural error should suppress high complexity solutions for $f(\mathbf{x}, \mathbf{w})$. It has been shown that if the complexity constraints are enforced, then the true error closely approaches the empirical error and it is more likely that $f(\mathbf{x}, \mathbf{w})$ can classify new objects with greater accuracy [Smolensky et al., 1996].

One way to try and design smoother functions f is to minimise the curvature of the function. Therefore large fluctuations are discouraged. Regularisation theory [Girosi et al., 1995] is suited to designing such functions; for example the

Table 3.1: Classification possibilities in one class classification

	Target Object	Outlier Object
Classified as a Target Object	True Positive, $f_{(T+)}$	False Positive (ε_{II}), $f_{(O-)}$
Classified as a Outlier Object	False Negative (ε_I), $f_{(T-)}$	True Negative, $f_{(O+)}$

Tikhonov stabilizer:

$$\varepsilon_{struct} = \sum_{k=0}^{K} \int_{x_0}^{x_1} \left\| \frac{\partial^k}{\partial x^k} f(\mathbf{x}; \mathbf{w}) \right\|^2 \mu_k dx \tag{3.7}$$

where μ_k is a weighting function which is non-negative for $0 \leq k \leq K-1$ and strictly positive for $k = K$ which indicates how smooth the kth derivative is of $f(\mathbf{x}, \mathbf{w})$ ([Bishop, 1995a]).

When applying this theory to the one class classification problem, the immediate issue is that there is only data from the target class which makes finding the best separation between the target and outlier classes much harder. In order to compute $\varepsilon_t rue$, the complete probability density $p(\mathbf{x}, y)$ should be known. However for one class classification, only $p(\mathbf{x}|w_T)$ is known where w_T is the probability density of the target class. Thus only those target objects not accepted, the false negatives, can be minimised. This is referred to as an error of the first kind ε_I. Unfortunately this can be easily satisfied by including all target objects in the description. If there are no outlier objects available, or it is impossible to estimate their probability density $p(\mathbf{x}|w_O)$, then it is clearly impossible to estimate the number of outlier objects accepted by the classifier. The number of outlier objects accepted, or the false positives, is an error of the second kind $\varepsilon_I I$

Table 3.1 shows the classification space, the space of all possible outcomes. Note that $f_{(T+)} + f_{(T-)} = 1$ and $f_{(O+)} + f_{(O-)} = 1$. The main difficulty thus is that whilst $f_{(T+)}$ and $f_{(T-)}$ can be estimated, nothing at all is known about $f_{(O-)}$ or $f_{(O+)}$. Furthermore without example outliers, ε_{emp} can only be defined on the target data. There should also be extra constraints on the structural error ε_{struct} so that smoothness can be enforced and conditions set in order to enclose the target data in all directions.

Several different models have been proposed for one class classification. The simplest models involve the generation of artificial outlier data around a target set. A classifier is then trained on such data to separate target and outlier data [Roberts et al., 1994]. However, the method scales very poorly in high dimensions.

Another possible approach is to use density methods. They directly estimate the density of the target objects $p(\mathbf{x}|w_O)$ [Barnett and Lewis, 1994]. These methods assume a uniform outlier distribution and by application of the Bayes rule (see equation 3.4), they are able to model the target distribution. Such methods work best when they are able to produce a density estimate in the complete feature space. However, this often requires a large amount of data. In fact, if the feature space is high dimensional, it can require an extremely large amount of data. Furthermore, it also requires the data to be a typical sample from the true data distribution and if the true data distribution is not known beforehand, this can affect the performance of the model. However, it is often such that when a large amount of typical data is available the method should work well. Examples of density models include a Parzen windows estimator [Bishop, 1994] and a Gaussian estimator [Parra et al., 1996].

If prior knowledge is available, it is possible to take advantage of it by using reconstruction methods. In these methods, an object $\mathbf{x}$ is encoded in the model and measurements can be reconstructed from this encoded object. The reconstruction error is a measure of how well the object fits the model. It is assumed that the lower the error, the better the fit. The advantages of such methods include their incorporation of prior knowledge into the model and also that they can work well with a low sample size. However, if the model does not fit the data well, then biases can severely weaken its ability to classify.

In cases where only small amounts of data are available, it can prove very difficult to obtain an accurate density model. Boundary methods avoid estimating the complete density of the data and seek to identify a boundary between the target and outlier data samples. Therefore in training such methods, they are only interested in data near the boundary so the data need not be completely representative of the feature space. However, it is not immediately obvious how to choose the boundary around the target class. Such methods generally depend on distances, usually Euclidean, between objects $\mathbf{x}$ and the training set X_tr. The feature space must therefore permit well defined distances and the data should also be scaled so one feature does not dominate the others.

3.3.3 Choosing a Suitable Classifier

There are many considerations to take into account when designing a one class classifier. There are two key elements that all methods contain. The first element is a measure of distance $d(z)$ or probability $p(z)$ of an object z to the training class X. The second element is a threshold θ on this distance or probability. Thus new objects are accepted when the distance to the training set is less than θ_d:

$$f(z) = I(d(z) < \theta_d) \tag{3.8}$$

or when the probability is larger than θ_p:

$$f(z) = I(p(z) > \theta_p) \tag{3.9}$$

where I is an indicator function. The difference between the classification methods is in how $d(z)$ and $p(z)$ are defined, how these variables are optimised and also how the thresholds are chosen.

Another important feature is the trade off between the fraction of the training set that is accepted,$f_{(T+)}$, and the fraction of outliers that is rejected, $f_{(O-)}$; in other words, a trade off between an error of the first kind, ε_I, and an error of the second kind, ε_{II}. The $f_{(T+)}$ can easily be measured on an independent test set drawn from the same distribution as the training class. The $f_{(O-)}$ are more difficult to measure. It is usually assumed that outliers are drawn from a bounded normal distribution.

There are several good characteristics that a one class classifier should exhibit.

Outlier Robustness: It is assumed that the training set is representative of the modelled class and that it contains no outliers. However sometimes this is not the case. A good classifier will be able to interpret these objects as outliers; otherwise they are assumed to be normal objects and their inclusion will skew the supposed distribution of the training data.

Outlier Incorporation: If there are labelled outliers in the training set then a good method will be able to use them to make a better definition of the training data distribution. There should be a parameter that can manage the balance between test set acceptance and outlier rejection.

Magic Parameters: Magic parameters are parameters that have a large impact in the classifier performance but there are no clear methods of how to choose them. A good method will be intuitive and there will be details of the impact certain parameter settings will have. If there are many parameters to be set, it can be very hard to find the optimum configuration for the problem at hand.

Computation Time/Storage: Such requirements of course depend on the problem. If the training class changes often, for example, aircraft have different operating abilities in different environments, then it would be desirable if the training time was relatively fast.

There are four main approaches, yielding a variety of methods, for creating a one class classifier and they are detailed below.

3.3.4 Density Methods

The most straightforward approach is to estimate the density of the training data and then set a threshold on this density to determine outliers [Tarassenko et al., 1995]. The simplest method is the Gaussian model.

3.3.4.1 Gaussian Model

The Central Limit Theorem [Ullman, 1978] says that when it is assumed that objects from one class originate from one prototype and are additively disturbed by a large number of small independent disturbances, then the model is valid. The probability distribution for a d-dimensional object x is given by

$$P\left(\mathbf{z};\mu,\Sigma\right)=\frac{1}{(2\pi)^{d/2}\left|\Sigma\right|^{1/2}}\exp\left\{-\frac{1}{2}(\mathbf{z}-\mu)^{T}\Sigma^{-1}(\mathbf{z}-\mu)\right\} \tag{3.10}$$

where μ is the mean and Σ is the covariance matrix. This method imposes a strict uni-modal and convex density model on the data. The number of free parameters in the model is given by

$$N=d+\frac{1}{2}d(d-1). \tag{3.11}$$

The main computational effort is on the computation of the inverse of Σ. Problems may arise if the data is badly scaled as the inverse may not exist. In such cases the pseudo inverse should be used, $\sum^{+} = \sum^{T}\left(\sum\sum^{T}\right)^{-1}$ [Strang, 1980] or the matrix should be modified using a regularisation parameter $\sum^{*} = \sum + \lambda I$.

If the data is truly normally distributed, it is possible to compute the optimum threshold depending on the percentage of true positives desired. If there are d independent normally distributed random variables x_i, the new variable $x\sum_i (x_i - \mu_i)^2/\sigma_i$ is distributed with a X^2_d distribution. Using the squared Mahanalobis distance, the variable

$$\Delta^2 = (\mathbf{x} - \mu)^T \Sigma^{-1} (\mathbf{x} - \mu) \tag{3.12}$$

should also be distributed like X^2_d. The threshold θ on Δ^2 should be set at

$$\theta : \int_0^{F_{T+}} \mathrm{X}^2_d(\Delta^2) d(\Delta^2) = F_{(T+)} \tag{3.13}$$

where F_{T+} is the required true positive rate. In practice however, the data is rarely perfectly normally distributed and so it is not used.

In general, the distribution will not be known; that is, μ, Σ^2 will need to be estimated. A method for doing this is the maximum likelihood method. Given a normal distribution $N(\mu, \sigma^2)$ with probability distribution function (pdf)

$$f(x|\mu, \sigma^2) = \frac{1}{\sqrt{2\pi}\sigma} \exp\left(-\frac{(x-\mu)^2}{2\sigma^2}\right), \tag{3.14}$$

the likelihood function is defined as

$$\begin{aligned} f(x_1, x_2, ..., x_n|\mu, \sigma^2) &= \prod_{i=1}^{n} f(x_i|\mu, \sigma^2) & (3.15)\\ &= \left(\frac{1}{2\pi\sigma^2}\right)^{n/2} \exp\left(-\frac{\sum_{i=1}^{n}(x_i-\mu)^2}{2\sigma^2}\right) & (3.16)\\ &= \left(\frac{1}{2\pi\sigma^2}\right)^{n/2} \exp\left(-\frac{\sum_{i=1}^{n}(x_i-\overline{x})^2 + n(\overline{x}-\mu)^2}{2\sigma^2}\right) & (3.17)\\ & & (3.18) \end{aligned}$$

Let the likelihood function for this distribution be defined as $L(\mu, \sigma^2)$. This is maximised over both parameters. Thus we have

$$0 = \frac{\partial}{\partial \mu} \log \left(\left(\frac{1}{2\pi\sigma^2} \right)^{n/2} \exp \left(-\frac{\sum_{i=1}^{n} (x_i - \overline{x})^2 + n(\overline{x} - \mu)^2}{2\sigma^2} \right) \right) \tag{3.19}$$

$$= \frac{\partial}{\partial \mu} \left(\log \left(\frac{1}{2\pi\sigma^2} \right)^{n/2} - \frac{\sum_{i=1}^{n} (x_i - \overline{x})^2 + n(\overline{x} - \mu)^2}{2\sigma^2} \right) \tag{3.20}$$

$$= \frac{2n(\overline{x} - \mu)}{2\sigma^2} \tag{3.21}$$

$$= \frac{n(\overline{x} - \mu)}{\sigma^2}. \tag{3.22}$$

$$\tag{3.23}$$

Therefore

$$\overset{\wedge}{\mu} = \overline{x} = \frac{1}{n} \sum_{i=1}^{n} x_i. \tag{3.24}$$

The expectation value is $E\left[\overset{\wedge}{\mu}\right] = \mu$. This is a maximum as it is a unique solution and the second derivative is negative. Also, it follows that

$$0 = \frac{\partial}{\partial \sigma} \log \left(\left(\frac{1}{2\pi\sigma^2} \right)^{n/2} \exp \left(-\frac{\sum\limits_{i=1}^{n} (x_i - \overline{x})^2 + n(\overline{x} - \mu)^2}{2\sigma^2} \right) \right) \tag{3.25}$$

$$= \frac{\partial}{\partial \sigma} \left(\frac{n}{2} \log \left(\frac{1}{2\pi\sigma^2} \right) - \frac{\sum\limits_{i=1}^{n} (x_i - \overline{x})^2 + n(\overline{x} - \mu)^2}{2\sigma^2} \right) \tag{3.26}$$

$$= \frac{n(\overline{x} - \mu)}{\sigma^2}. \tag{3.27}$$

$$\tag{3.28}$$

Therefore

$$\overset{\wedge}{\sigma}^2 = \frac{\sum_{i=1}^{n} (x_i - \overset{\wedge}{\mu}^2)}{n}. \tag{3.29}$$

Thus the maximum likelihood estimator is given by $\left(\overset{\wedge}{\mu}, \overset{\wedge}{\sigma}^2\right)$. This provides an estimator for the distribution and so one can locate abnormalities by defining outlier percentages.

This method is very useful if it is known beforehand that the data is normally distributed. The main computational burden is in computing Σ^{-1}. If the data is badly scaled then the inverse might be impossible to compute. To overcome this difficulty a regularization parameter is needed which must be chosen by the user. Furthermore, the estimators for the mean and the covariance matrix are not robust against outliers. To overcome this, a common approach is to use the Minimum Covariance Determinant method [Rousseeuw and Van Driessen, 1999]. The user specifies a fraction of training data to be fitted with a Gaussian. The subset that results in the smallest determinant of the covariance matrix is used for training. This ensures robustness even if there are a high fraction of outliers in the training data.

The difficulty in using this method is that there are very few situations where a univariate Gaussian model will accurately represent the target distribution, except in artificial cases.

3.3.4.2 Mixture of Gaussians Standard

The assumption that the data is uni-modal and convex is rarely true for most data sets. To overcome this problem, a Mixture of Gaussians MoG can be used. The method uses a linear combination of normal distributions [Bishop, 1995b]. The model looks like:

$$f(\mathbf{x}) = \sum_{i=1}^{K} P_i \exp\left(-(\mathbf{x}-\mu_i)^T \sum_i^{-1} (\mathbf{x}-\mu_i)\right). \tag{3.30}$$

The classifier is defined as:

$$h(\mathbf{x}) = \begin{cases} \text{target} & \text{if } f(\mathbf{x}) \geq \theta \\ \text{outlier} & \text{otherwise } f(\mathbf{x}) < \theta \end{cases}$$

The parameters P_i, μ_i and Σ_i are optimised using the expectation minimisation algorithm.

The MoG classifier has been used on a number of occasions for novelty detection. [Hansen et al., 2002] used it to identify education related documents from the CMU WebKB repository with a good degree of success. They also used the classifier to identify a “miscellaneous” set drawn from the same repository as novel, of which 40% were identified as novel. There is no mention of error rates on this set so it is difficult to judge how successful the classifier was. The MoG method has been used before to detect motor faults [Parra et al., 1996] by transforming the data via symplectic mappings to take the form of a Gaussian distribution. The resulting classification error is comparable or better to multi-layered Perceptrons, hyperspherical clustering and nearest neighbour. [Morgan et al., 2010] compares a Gaussian and a MoG classifier against an existing fixed limit method for detecting faults in marine engines. The sensitivity for all engines was at least 65% and the resulting ROC curve was superior to that of the fixed limit method.

3.3.4.3 Mixture of Gaussians

The MoG classifier has not been designed to handle the presence of outliers in the training set and as such, any abnormal descents could negatively affect performance. The classifier can be modified [Tax, 2009] to use outlier objects for training. Individual mixtures of Gaussians are fitted to both target and outlier data (having K_t and K_o Gaussians respectively). Objects are then assigned to the class with the highest probability. Since this method allows outlier objects in training, the decision boundary around the target class is not closed. This is achieved by adding one extra outlier cluster with a very wide covariance matrix. This cluster is fixed and although it is not adapted by the expectation minimisation algorithm ([Bishop, 1995b]) in training, it is used in the computation of probability density, resulting in the following model

$$
\begin{aligned}
f(\mathbf{x}) = \sum_{i=1}^{K\_t} P_i \exp\left(-(\mathbf{x}-\mu_i)^T \Sigma_i^{-1} (\mathbf{x}-\mu_i)\right) && (3.31)\\
- P_* \exp\left(-(\mathbf{x}-\mu_i)^T \Sigma_*^{-1} (\mathbf{x}-\mu_i)\right) && (3.32)\\
- \sum_{j=1}^{K\_o} P_j \exp\left(-(\mathbf{x}-\mu_j)^T \Sigma_i^{-1} (\mathbf{x}-\mu_j)\right). && (3.33)
\end{aligned}
$$

In this model, μ is the mean of the complete dataset and Σ_* is taken as 10Σ, where Σ is the covariance matrix of the complete dataset. The P_* is optimised in the expectation minimisation procedure such that $P_* + \Sigma_j P_j = 1$.

Furthermore, to ensure that the covariance matrix is invertible, Principal Component Analysis is performed on each of the training sets, retaining 90% of the variance.

3.3.4.4 Parzen Windows Density Estimation

A probability density function (pdf) $p(\mathbf{x})$ is a continuous real valued function such that

1. $$P(a < \mathbf{x} < b) = \int\limits_a^b p(\mathbf{x})dx$$

2. $$p(\mathbf{x}) \geq 0 \qquad \text{for all real } \mathbf{x}$$

3. $$\int\limits_{-\infty}^{\infty} p(\mathbf{x})dx = 1.$$

Given n data samples $\mathbf{x}_1, \mathbf{x}_2, ...\mathbf{x}_n$, an estimate to $p(\mathbf{x})$ is sought. Two formulae are derived. The probability that a vector $\mathbf{x}$ lies in region R is given by $P = \int\limits_R p(\mathbf{x})dx$. Assume that R is small enough such that $p(\mathbf{x})$ varies a tiny amount. Then the following holds

$$P = \int\limits_R p(\mathbf{x})dx \approx p(\mathbf{x}) \int\limits_R d\mathbf{x} \approx p(\mathbf{x})V_R \tag{3.34}$$

where V_R is the volume of R. Now suppose that n data samples $\mathbf{x}_1, \mathbf{x}_2, ...\mathbf{x}_n$ are independently drawn according to $p(x)$ and that k out of n samples lie in region R. Thus $P = \frac{k}{n}$ and so $p(x) = \frac{k}{nV_R}$. Let R be an d-dimensional hypercube and let h be the length of its edge so that $V_R = h^d$. Position the hypercube so that it is centred on the vector x. Define ϕ such that

$$\phi\left(\frac{\mathbf{x}_i - \mathbf{x}}{h}\right) = \begin{cases} 1 & \text{if } \frac{|x_{ik} - x_k|}{h} \leq \frac{1}{2} \text{ k = 1, 2, ..., d} \\ 0 & \text{otherwise.} \end{cases}$$

In other words, the function is non-zero if x_i is in the hypercube. Thus when k samples fall in the hypercube, k can be written as

$$k = \sum_{i=1}^{n} \phi\left(\frac{\mathbf{x}_i - \mathbf{x}}{h}\right). \tag{3.35}$$

Thus the Parzen window density estimator [Parzen, 1962] can be written as

$$p(\mathbf{x}) = \frac{k}{nV_R} = \frac{1}{n}\sum_{i=1}^{n} \frac{1}{h^d}\phi\left(\frac{\mathbf{x}_i - \mathbf{x}}{h}\right). \tag{3.36}$$

A common choice for ϕ is the Gaussian function and so the estimator becomes

$$p(x) = \frac{k}{nV_R} = \frac{1}{n}\sum \frac{1}{\sqrt{(2\pi)^n \,||\, \Sigma}} \exp\left(-\frac{1}{2}(\mathbf{x}-\mu)^T \Sigma^{-1} (\mathbf{x}-\mu)\right). \tag{3.37}$$

This method is an extension on the mixture of Gaussians model. The density estimated is a mixture of usually Gaussian kernels centred on the individual training objects with (often) diagonal covariance matrices $\sum_i = hI$. It takes the form

$$p_p(\mathbf{x}) = \frac{1}{N}\sum_i p_N(\mathbf{x}; \mathbf{x}_i, hI). \tag{3.38}$$

The equal width h in each feature direction means that the Parzen density estimator assumes equally weighted features and so will be sensitive to scaling. The free parameter h is optimised using the maximum likelihood solution. Since there is just one parameter, the data model is very weak and so success depends entirely on a representative training set. The training time is very small but the testing time is rather expensive, especially with large feature sets in high dimensional spaces. This is because all the training objects have to be stored and during testing, distances to all the training objects must be computed and then sorted.

[Yeung and Chow, 2002] uses Parzen windows to detect network intrusion attacks. They compare their method to the method with the best results in the KDD cup for 1999 [ACM, 2010]. The results are comparable to the method used by the winners which is an ensemble of decision trees with bagged boosting. However the Parzen windows has more success in detecting some of the rarer attacks such as U2R (user to root) with a success rate of around 93% compared to only 26%. [Stibor et al., 2005] use it in experiments on the same dataset used by Yeung. Although the focus of their paper was introducing a real valued positive selection algorithm based on artificial immune systems, they also compare their method to parzen windows and the one class SVM. Whilst their method has the best results, it is only marginally superior in performance to the parzen windows and the one class SVM. [Tarassenko et al., 1995] used it to identify abnormalities in mammograms and has a good degree of success though the method is not available to discriminate between benign and cancerous tumours.

3.3.5 Boundary Methods

[Vapnik, 2000] argued that when there is just a limited amount of data, one should avoid solving a more general problem as an intermediate step to solving the original simpler problem. This is because more data might be needed to solve the general problem than the intermediate problem so any answer produced might be rather weak. In this case, the general problem is estimating a complete data density for the one class classifier. Furthermore, it is only necessary to find the optimised data boundary for the training set. Such methods rely on distances from objects and thus are sensitive to scaling. Furthermore it should not be assumed that the output of boundary methods can be interpreted as a probability; in fact it cannot. Suppose that a method is trained such that a fraction r of the data is rejected. There is now a threshold T_f for this rejection rate based on the choice for d (which is a replacement for $p(x)$). Changing r might require the retraining of the method as decreasing T_f does not guarantee that the high density areas are captured.

3.3.5.1 One Class Support Vector Machine

The one class SVM [Schölkopf et al., 2000] is a useful novelty detection method based on the support vector machine. To formalise the problem, a dataset is drawn from a probability distribution P and a small subset S of the input space is estimated such that the probability of a test point from P lying outside of S equals some pre-specified $v \in (0, 1)$. In other words, a function f that is positive on S but negative on its complement is to be estimated.

As before, consider training data $x_1, x_2, ..., x_l \in X \subseteq \mathbb{R}^n$. Let ϕ be the mapping $\phi : X \to F$ into some feature dot product space F with a kernel given by $k(x,y) = (\phi(x), \phi(y))$. The data is separated from the origin using the maximum margin method.

The following quadratic programming problem is solved;

$$\begin{array}{cl} \min\limits_{w \in F, \xi \in \mathbb{R}^l, \rho \in \mathbb{R}} & \frac{1}{2}\|w\|^2 + \frac{1}{vl}\sum\limits_{i=1}^{l} \xi_i - \rho, \\ \text{subject to} & (w \cdot \phi(x_i)) \geq \rho - \xi_i, \\ & \xi_i \geq 0. \end{array} \tag{3.39}$$

Using Lagrangian multipliers, it is such that

$$L(w, \rho, \xi, \alpha_i, \beta_i) = \frac{1}{2}\|w\|^2 + \frac{1}{vl}\sum_{i=1}^{l} \xi_i - \rho - \sum_{i=1}^{l} \alpha_i(\xi_i - \rho - (w \cdot \phi(x_i))) - \sum_{i=1}^{l} \beta_i \xi_i. \tag{3.40}$$

The derivatives of L w.r.t. the primal variables are zero so it follows that

$$\frac{\partial L}{\partial w} = 0 \Rightarrow w = \sum_{i=1}^{l} \alpha_i \phi(x_i), \tag{3.41}$$

$$\frac{\partial L}{\partial \rho} = 0 \Rightarrow \sum_{i=1}^{l} \alpha_i = 1, \tag{3.42}$$

$$\frac{\partial L}{\partial \xi_i} = 0 \Rightarrow \alpha_i + \beta_i = \frac{1}{vl}. \tag{3.43}$$

The dual problem is formulated to give

$$\begin{array}{cl} \min\limits_{\alpha \in \mathbb{R}^l} & \sum\limits_{i,j=1}^{l} \alpha_i \alpha_j k(x_i, x_j), \\ \text{subject to} & \sum\limits_{i=1}^{l} \alpha_i = 1, \\ & 0 \leq \alpha_i \leq \frac{1}{vl}. \end{array} \tag{3.44}$$

The support vectors are $w = \sum\limits_{i=1}^{l} \alpha_i \phi(x_i)$ when $0 \leq \alpha_i \leq \frac{1}{vl}$. Solutions for the dual problem yield parameters w_0, ρ_0 where

$$w_0 = \sum_{i=1}^{N_s} \alpha_i \phi(s_i), \tag{3.45}$$

$$\rho_0 = \frac{1}{N_s} \sum_{j=1}^{N_s} \sum_{i=1}^{N_s} \alpha_i k(s_i, x). \tag{3.46}$$

Here, N_s is the number of support vectors and s_i denotes a support vector. The decision function is given by

$$f(x) = \operatorname{sgn}(w \cdot \phi(x) - \rho_0) = \operatorname{sgn}\left(\sum_{i=1}^{N_s} \alpha_i k(s_i, x) - \rho_0 \right). \tag{3.47}$$

The 'abnormality' detection function is then given by

$$g(x) = \rho_0 - \sum_{i=1}^{N_s} \alpha_i k(s_i, x). \tag{3.48}$$

The user has to choose the appropriate kernel, with its associated parameters, for the problem. However, rather than choosing an error penalty C as via the classical SVM method, one chooses a value for ν which is the fraction of outliers to be misclassified.

In training an SVM, there are several parameters to consider and they are as follows;

- Choice of Kernel - The choice of kernel for the SVM is limited to Mercer kernels. Common choices are the linear kernel $K(\mathbf{x}, \mathbf{y}) = \mathbf{x}^T \cdot \mathbf{y}$, RBF kernel $K(\mathbf{x}, \mathbf{y}) = e^{-\|\mathbf{x}-\mathbf{y}\|^2/2\sigma^2}$, the polynomial kernel $K(\mathbf{x}, \mathbf{y}) = (\gamma \mathbf{x} \cdot \mathbf{y} + r)^p$ and the sigmoid kernel $K(\mathbf{x}, \mathbf{y}) = \tanh(\kappa \mathbf{x} \cdot \mathbf{y} - \delta)$.

  The choice of kernel is an active research topic and there is no method for choosing a kernel given a specific dataset. It has been proven by [Keerthi and Lin, 2003] that under certain conditions, the linear kernel is essentially a special case of the RBF kernel. The polynomial kernel has more parameters than the RBF kernel and so increases the complexity of the model by increasing the number of parameters that need to be optimised. Furthermore, the RBF kernel has fewer numerical issues. To illustrate this, it is noted that $0 \leq K_{i,j} \leq 1$ for RBF kernels. However for polynomial kernels, if the degree is large, values may approach infinity when $\gamma \mathbf{x} \cdot \mathbf{y} + r > 1$ or zero when $\gamma \mathbf{x} \cdot \mathbf{y} + r < 1$. Furthermore, the RBF kernel is able to suppress growing distances in larger feature spaces [Tax and Duin, 1999a]. The sigmoid kernel is in general not the best choice as it is not positive definite for all choices of κ and δ [Lin and Lin, 2003]. [Lin and Lin, 2003] also show that for certain values of κ and δ the sigmoid kernel behaves in a similar fashion to the RBF kernel, in part due to the fact that the tanh function can be written in terms of exponentials. They conclude that in general the RBF kernel is the better choice. Therefore for the research contained in this thesis, the RBF kernel is used.

- RBF Kernel Parameters - The RBF kernel parameters are the kernel width σ and the fraction of the training set to be rejected ν. In addition, [Keerthi and Lin, 2003] studied the asymptotic behaviour of the parameters σ and C for the two class SVM and deduced several relations regarding σ and C.
    - Severe Underfitting - This occurs if σ^2 is fixed and $C \rightarrow 0$, $\sigma^2 \rightarrow 0$ and C is fixed sufficiently small and if $\sigma^2 \rightarrow \infty$ and C is fixed.
    - Severe Overfitting - This occurs when $\sigma^2 \rightarrow 0$ and C is fixed sufficiently large.

  [Chen et al., 2005] showed that there is a connection between ν-SVM and C-SVM and suggests that for admissible ν, where ν is increasing, C decreases. This suggests that the problems of overfitting and underfitting could be avoided if σ^2 is not extremely large or small and ν is not extremely close to 0 or 1.

[Clifton et al., 2006] use the one class SVM to detect combustion instability. Combustion occurs in 3 channels and a one class SVM is trained on each channel to identify any instability. They identify the first sign of combustion instability and note the data index where it occurred. The mean, maximum, minimum and product of these data indices are computed in order to assess which rule is best at detecting the first sign of combustion instability based on information from all three combustion channels.

The maximum combination rule is given by

$$\hat{g}(\mathbf{x}) = \max_{i=1}^{R} g_i(\mathbf{x}) \tag{3.49}$$

The minimum combination rule is given by

$$\hat{g}(\mathbf{x}) = \min_{i=1}^{R} g_i(\mathbf{x}) \tag{3.50}$$

The mean combination rule is given by

$$\hat{g}(\mathbf{x}) = \frac{1}{R}\sum_{i=1}^{R} g_i(\mathbf{x}) \tag{3.51}$$

The product combination rule is given by

$$\hat{g}(\mathbf{x}) = \frac{\prod_{i=1}^{R} g_i(\mathbf{x})}{\prod_{i=1}^{R} g_i(\mathbf{x}) + \prod_{i=1}^{R}(1 - g_i(\mathbf{x}))} \tag{3.52}$$

where $g_i(\mathbf{x})$ is the novelty score generated from the ith classifier and R is the total number of classifiers.

They note that

$$\min_{i=1}^{R} g_i(\mathbf{x}) \leq \frac{1}{R}\sum_{\substack{i=1\\i=1}}^{\substack{R\\R}} g_i(\mathbf{x}) \leq \max_{i=1}^{R} g_i(\mathbf{x}) \tag{3.53}$$

and so the maximum and the minimum serve as upper and lower bounds for the mean rule.

They conclude that pre-cursors to combustion instability are detected via the mean rule whereas the product rule gives little variability in novelty scores during stable combustion, thus allowing a more sensitive novelty threshold to be applied. The minimum rule provides little early warning whereas the maximum rule gives optimum results. Their method therefore shows some success in detecting pre-cursors for a defined abnormal event.

[Cohen et al., 2004] use the one class SVM to detect nosocomial infections. Data consisted of 688 patient records (of which 11% had infections) and 83 variables. They sought the advice of experts in nosocomial infections to reduce the number of variables and whilst they could detect around 92% of infections, just over 1 in 4 patients with no infection were classified wrongly. However, some of this imbalance could result from an apparent lack of scaling.

[Gardner et al., 2006] use the one class SVM for seizure analysis in intercranial EEGs. Their results outperform the benchmark results which were also produced from the same dataset. The low false positive rate is attributed to the fact that the non-parametric one class SVM is better at modelling the data than the benchmark detector. Whilst results are a little worse than others reported in the field, the key benefits of Gardner's method are that it does not need to be trained on seizures and nor is it patient specific.

[Hayton et al., 2000] use the one class SVM for novelty detection in jet engine vibration spectra. The results show a clear difference between the cumulative novelty scores of the training data (all normal engines) and the scores of the test data (the abnormal engines).

[Manevitz and Yousef, 2002] uses the one class SVM for document classification. They also compare the one class SVM with a modified version and also with a compression neural network, prototype algorithm, naive Bayes and the nearest neighbour classifier. The results for the one class SVM and the compression neural network are comparable and the modified one class SVM is slightly worse. The results for the other classifiers are much worse.

[Shin et al., 2005] use the one class SVM for machine fault detection. They compare the one class SVM (using the four main kernels) and a multi-layered perceptron. The results for each of the kernels and the neural network are comparable though when the training set is increased in size, the RBF kernel consistently produces the best results.

[Spinosa and de Carvalho, 2005] use the one class SVM for novel class detection in bioinformatics. Results are presented for rates of Leukemia and Lymphoma detection and whilst the accuracy rates for these novel data sets are high, the percentage of false positives is between 30 and 60% which is rather high.

[Wang et al., 2005] use the one class SVM with different kernels for intrusion detection. They compare the polynomial kernel, the RBF kernel, the STIDE kernel and the Markov kernel. The STIDE and Markov kernels provided the best results, although the RBF kernel was close behind. A disadvantage of the STIDE and Markov kernels is that they can only be trained on normal data.

3.3.5.2 Support Vector Data Description (SVDD)

Support Vector Data Description (SVDD) [Tax and Duin, 1999b] is based on support vector machines [Vapnik, 2000]. It seeks to enclose the data in the smallest possible hypersphere, so that outliers are outside this hypersphere. Furthermore, it utilizes kernels for difficult problems.

SVDD seeks to describe a class of objects, to be able to distinguish it from all the others. A common approach is to estimate the probability density function of the data distribution but if the data is not bountiful, this can be difficult and often inaccurate.

The data set consists of N data objects $\{x_i | i = 1, ...N\}$. A sphere of centre a and radius R is to be computed so that it encloses all or almost all of the data objects. Because of the difficulty in deciding which objects are outliers, discrepancies are allowed for by introducing slack variables and constraints are obtained below

$$(x_i - a)(x_i - a)^T \leq R^2 + \xi_i, \tag{3.54}$$

$$\xi_i \geq 0. \tag{3.55}$$

R is minimised and the size of the slack variables

$$F(R, a, \xi_i) = R^2 + C \sum_{i=1}^{N} \xi_i \tag{3.56}$$

for a given constant C which balances the volume of the sphere against the size of the slack variables. To solve this problem with the above constraints, the following Lagrangian is constructed

$$L(R, a, \xi_i, \alpha_i, \beta_i) = R^2 + C \sum_{i=1}^{N} \xi_i - \sum_{i=1}^{N} \alpha_i (R^2 + \xi_i - x_i^2 + 2ax_i - a^2) - \sum_{i=1}^{N} \beta_i \xi_i. \tag{3.57}$$

It is such that

$$\frac{\partial L}{\partial R} = 0 \Rightarrow 2R - 2R\sum_{i=1}^{N} \alpha_i = 0 \tag{3.58}$$

$$\Rightarrow \sum_{i=1}^{N} \alpha_i = 1 \tag{3.59}$$

$$\frac{\partial L}{\partial a} = 0 \Rightarrow 2a\sum_{i=1}^{N} \alpha_i - 2\sum_{i=1}^{N} \alpha_i x_i = 0 \tag{3.60}$$

$$\Rightarrow a = \sum_{i=1}^{N} \alpha_i x_i \tag{3.61}$$

$$\frac{\partial L}{\partial \xi_i} = 0 \Rightarrow C - \alpha_i - \beta_i = 0 \tag{3.62}$$

$$\Rightarrow 0 \leq \alpha_i \leq C. \tag{3.63}$$

Thus L is maximised w.r.t. α_i where L is given by

$$L = \sum_{i=1}^{N} \alpha_i (x_i \cdot x_i) - \sum_{i,j=1}^{N} \alpha_i \alpha_j (x_i \cdot x_j) \tag{3.64}$$

with constraints

$$\sum_{i=1}^{N} \alpha_i = 1, \tag{3.65}$$

$$a = \sum_{i=1}^{N} \alpha_i x_i, \tag{3.66}$$

$$0 \leq \alpha_i \leq C. \tag{3.67}$$

If there is an unknown data object z then z is accepted if it is such that

$$(z-a)(z-a)^T = (z \cdot z) - 2\sum_{i=1}^{N} \alpha_i K(z \cdot x_i) + \sum_{i,j=1}^{N} \alpha_i \alpha_j K(x_i \cdot x_j) \leq R^2 \tag{3.68}$$

for some Mercer kernel K. As with support vector machines, popular kernel choices are the polynomial and the radial basis function kernel. The RBF kernel is given by

$$K(x_i, x_j) = \exp(-(x_i - x_j)^2/\sigma^2). \tag{3.69}$$

Since $K(x_i, x_i) = 1$, the acceptance rule becomes

$$(z-a)(z-a)^T = 1 - 2\sum_{i=1}^{N} \alpha_i K(z \cdot x_i) + \sum_{i,j=1, i \neq j}^{N} \alpha_i \alpha_j K(x_i \cdot x_j) \leq R^2. \tag{3.70}$$

A number of observations about the RBF kernel in this formulation can be made. When σ is very small, $K(x_i, x_j) \approx 0, i \neq j$ and L is maximised when $\alpha_i = 1/N$. This is similar to the Parzen density estimation where each object supports a kernel. For very large σ, $K(x_i, x_j) \approx 1$ and L is maximised when exactly one and all the others are zero. We note that

$$\frac{1}{N} \leq C \leq 1. \tag{3.71}$$

This is so because if $\frac{1}{N} \geq C$ then $\sum_{i=1}^{N} \alpha_i = 1$ cannot be satisfied.

To use this method, one only needs to supply F_{T-}, the fraction of training examples that should lie outside the hypersphere.

[Lai et al., 2002] uses this method to identify images. The images used are texture images and the features extracted from a bank of filters applied to the database of images. Weighting is applied so that no one feature is able to dominate the others. Images are represented either by feature vectors (the average of the filter response over the whole image), or by a cloud of points consisting of multiple feature vectors representing different patches of the image. The SVDD is fitted around the cloud of points and images are regarded as very similar if the number of outliers is small. They also experiment with multiple classifiers because performance could suffer from a large overlap between individual clouds of points. The query image Q of a classifier profile is defined as

$$\mathbf{S}(Q) = [S_1(Q), S_2(Q), ..., S_N(Q)] \tag{3.72}$$

They propose to compare the query profile with those of the images in the database. To make this comparison, different dissimilarity measures are proposed such as the Euclidean distance

$$D_E(Q, I_i) = \|\mathbf{S}(Q) - \mathbf{S}(I_i)\|, i = 1, ..., N \tag{3.73}$$

or the cosine distance

$$D_{\cos} = \frac{1}{2}\left(1 - Sim(\mathbf{S}(Q), \mathbf{S}(I_i))\right) \tag{3.74}$$

where Sim is defined by

$$Sim(Q, I_i) = \frac{\mathbf{x}_Q^T \mathbf{x}_{I_i}}{\left\|\mathbf{x}_Q^T\right\| \left\|\mathbf{x}_{I_i}\right\|} \tag{3.75}$$

where $\mathbf{x}_Q^T$ and $\mathbf{x}_{I_i}$ are vector representations of the query and image respectively using the L2 norm. The larger the value the more similar the images. The images most similar to the query image are found by ranking $D_E(Q, I_i)$, similar to a method used by [Kuncheva and Jain, 2000].

The experiments consist of comparing each image against those in the training set. The best results are obtained by combining the classifiers using the Euclidean distance and the cosine distance. The ranking method was less promising, in part because the outcome is only based on pairs of clouds which can suffer from large cloud overlap.

The experiment does suggest that combinations of classifiers can help improve performance.

3.3.6 Reconstruction Methods

These methods are not usually used for one-class classification problems but for data modelling. By using prior knowledge about the data and making certain assumptions, one can generate a model to fit the data. New objects can then be described in terms of the model. Many of these methods make assumptions about the clustering characteristics of the data or their distribution in subspaces. A set of prototypes or subspaces is defined and a reconstruction error is minimised. It is assumed that outliers are objects that do not satisfy assumptions about the target distribution. The outliers should be represented worse than the true objects and their reconstruction error should be high. The reconstruction error of a test object by these data compression methods is used as a distance to the target set. The empirical threshold has to be obtained using the training set.

3.3.6.1 K-means

The simplest method is the k-means clustering technique [Bishop, 1995b]. Target objects are represented by the nearest prototype vector measured by the Euclidean distance. The placing of prototypes is optimised by minimising the following error:

$$\varepsilon = \sum_i \left(\min_k \|x_i - \mu_k\|^2 \right). \tag{3.76}$$

In the k-means method, the distances to the prototypes of all objects are averaged. This means that the method is more robust against remote outliers, more so than the k-centers method. The distance d of an object z to the target set is defined as the squared distance of that object to the nearest prototype:

$$d(z) = \min_k \|z - \mu_k\|^2 . \tag{3.77}$$

3.3.6.2 Learning Vector Quantisation (LVQ)

The LVQ algorithm [Carpenter et al., 1991] is a supervised version of the k-means clustering method. For each training object x_i, a label y_i indicates which cluster it belongs to. The LVQ is trained as a conventional neural network, with the exception that each hidden unit is a prototype, where for each prototype μ_k, a class label y_k is defined. The training algorithm is such that it only updates the prototype nearest to the training object x_i.

$$\Delta\mu_k = \begin{cases} +\eta(x_i - \mu_k) & \text{if } y_i = y_k \\ -\eta(x_i - \mu_k) & \text{otherwise.} \end{cases} \tag{3.78}$$

where η is the learning rate. This update rule is iterated over all training objects until convergence is reached. In this algorithm, the μ have to be estimated so we have kd free parameters. Also, the user needs to supply the learning rate.

3.3.6.3 Principal Component Analysis (PCA)

This method is useful for data distributed in a linear subspace. The PCA mapping [Bishop, 1995b] finds the orthonormal subspace which captures the variance in the data as best as possible (using the squared error). The simplest procedure uses eigenvalue decomposition to compute the eigenvectors of the target covariance matrix. The eigenvectors with the largest eigenvalues are the principal axis of the d-dimensional data and point in the direction of the largest variance. These vectors are basis vectors for the mapped data. The number of basis vectors M is optimised to explain a certain user defined fraction of the variance of the data. The basis vectors W become a $d \times M$ matrix. Since these form an orthonormal basis, the number of free parameters is $\begin{pmatrix} d-1 \\ M \end{pmatrix}$. It is often assumed that the data has a mean of zero. The reconstruction error of an object z is now defined as the squared distance from the original object and its mapped version:

$$\begin{aligned} d(z) &= \left\| z - (W(W^T W)^{-1} W^T) z \right\|^2 && (3.79) \\ &= \left\| z - (WW^T) z \right\|^2 . && (3.80) \end{aligned}$$

3.3.6.4 Auto-encoders and Diablo Networks

Auto-encoders [Bregler and Omohundro, 1994] and diablo networks [Schwenk, 1998] use neural networks in order to learn a representation of the data. They are such that if trained successfully, the input patterns should be reproduced at the output layer.

The main difference between auto-encoders and diablo networks is the number and size of the hidden layers. Often, auto-encoders have very few hidden layers but many units in these layers. Diablo networks have more hidden layers but fewer units. The middle such layer is referred to as the bottle neck layer on account of it having fewer units. In this section, the auto-encoder will have one hidden layer and the diablo network will have three, with the middle layer being the bottleneck layer.

They are both trained by minimising the mean square error

$$\varepsilon_{\mathrm{MSE}}(f(\mathbf{x}_i;\mathbf{w}), y_i) = (f(\mathbf{x}_i;\mathbf{w}) - y_i)^2 \tag{3.81}$$

using terminology from section 3.3.2. It is intended that the target data is reconstructed with a smaller error than the outlier data.

Given an object $\mathbf{z}$, its distance to the training set is given by

$$\begin{aligned} d_{autoen}(\mathbf{z}) &= \|f(\mathbf{z};\mathbf{w}) - \mathbf{z}\|^2 \\ d_{diablo}(\mathbf{z}) &= \|f(\mathbf{z};\mathbf{w}) - \mathbf{z}\|^2 \end{aligned} \tag{3.82}$$

If just one hidden layer is used in the auto-encoder then the data description is similar to a PCA data description. A small number of neurons in the bottleneck layer of a diablo network compresses information. Best results are obtained (the smallest reconstruction error) when the subspace coded by these neurons matches the subspace of the original data. In fact, outliers can be perfectly rejected. However, results can be very poor when the this subspace is as large as the original feature space.

Both neural networks have a large number of parameters to be optimised. The number of input and output neurons for both networks is given by the dimensionality of the data (d). Let h_{auto} denote the number of hidden units in the auto-encoder. Then the total number of weights in the network including bias terms is

$$n_{auto} = d \times h_{auto} + h_{auto} + h_{auto} \times d + d = (2d+1)h_{auto} + d \tag{3.83}$$

For the diablo network, let there be h_{diab} units in the bottleneck layer and $2h_{diab}$ in the other hidden layers. Then the number of parameters to be optimised is

$$\begin{aligned} n_{diab} &= d \times 2h_{diab} + 2h_{diab}(h_{diab}+1) + h_{diab}(h_{diab}+1) + 2h_{diab}(d+1) + d \qquad (3.84) \\ &= h_{diab}(4d + 4h_{diab} + 5) + d \qquad (3.85) \end{aligned}$$

Whilst the networks in principle can be very effective, the number of parameters to be optimised is very large. Furthermore they require the use to supply the stopping criterion and the learning rates. Although they can be very powerful when implemented correctly, this can be difficult for a non-expert user.

3.3.7 Method Analysis

In this chapter, many one class classification methods have been introduced and their advantages and disadvantages have been mentioned. Robustness is an important factor in choosing a classifier. For extremely large amounts of target data it can be very difficult to identify any outliers in the training set, particularly if they have been mislabelled or the outlier represents an unknown fault. Table 3.2 lists the classifiers compared in this chapter and whether they are resistant or vulnerable to unlabelled or labelled outliers. For the full version of this table, see section 3.6 of [Tax, 2001]. Whilst all methods are set to reject a certain fraction of the training set, some methods are still vulnerable to outliers in the training set. For example the estimation of the Gaussian covariance matrix will be impaired if outliers are in the training set. The K-means and the Parzen windows can model the density around the outlier and it will not have too much effect on the classifier. The SVDD and the one class SVM are largely insensitive to outliers.

The classifiers used in the experiments in Chapter 4 will be training in principle on normal data however, given the large amount of data and the possibility of unidentified abnormalities in the training set, the classifiers will possibly encounter unlabelled outliers in training.

Another important consideration when choosing a classifier is the number of parameters to optimise in order to achieve the best classification. Table 3.3 shows the number of free parameters and the number of user defined parameters. It is adapted from a table in section 3.7 of [Tax, 2001]. Methods such as the auto-encoder and the diabolo networks have a large number of parameters to optimise which, if successful, can lead to very good results but a non-expert may struggle. Classifiers such as Parzen windows have no free parameters to optimise and so require little expert input. However, they are totally dependent on a representative training set which may be hard to obtain or indeed verify that it is representative.

3.3.8 Classifier Choices

The classifiers presented all have a variety of strengths and weaknesses. The classifiers chosen for the experiments of Chapter 4 are the MoG classifier, the K-means classifier and the one class SVM classifier. The Mixture of Gaussians method has been adapted in order to model the presence of outliers in the training set. This is considered to be a very valuable property, given the dataset contains outliers, some of which are difficult to identify by experts. The K-means classifier

Table 3.2: This table compares the robustness of one class classification methods. The '+' indicates the method is resistant to outliers and the '-' indicates the method is vulnerable to outliers.

Method		Unlabelled Outliers in Training		Labelled Outliers in Training
Gaussian	-	Estimation of the covariance matrix is impaired	-	Outlier density should be modelled on a few examples.
Mixture of Gaussians Standard	-	Estimation of the covariance matrix is impaired	-	Outlier density should be modelled on a few examples.
Mixture of Gaussians with Outliers	-	Estimation of the covariance matrix is impaired	+	Outlier density can be modelled.
Parzen Windows	+	Density is estimated locally	+	Outlier density should be modelled.
One Class SVM	+	User can reject a given fraction	+	Outliers can be forced outside the hyperplane
SVDD	+	User can reject a given fraction	+	Outliers can be forced outside the sphere
K-Means	-	Outliers will influence prototype position	-	Cannot repel from outliers
LVQ	-	Outliers influence prototype position	+	Outliers are repelled

Table 3.3: This table compares the robustness of one class classification methods. The '+' indicates the method is sensitive to scaling. In this table d denotes the dimensionality of the data, N denotes the number of training objects, k denotes the number of clusters, M denotes the dimensionality of the subspaces and h denotes the number of hidden units.

Method	Scaling Sensitivity	Number of Free Parameters	Number of User Defined Parameters
Gaussian	-	$d + d(d+1)/2$	Regularisation λ
Mixture of Gaussians Standard	+	$(d+2)N_{MoG}$	N_{MoG}, number of iterations
Mixture of Gaussians	+	$(d+2)N_{MoG}$	N_{MoG}, number of iterations
Parzen Windows	+/-	1	0
SVDD	+	N	kernel parameters
OCSVM	+	N	kernel parameters
K-means	+	kd	K, number of iterations
PCA	-	$\begin{pmatrix} d-1 \\ M \end{pmatrix}$	Fraction of preserved variance
Auto-encoder	-	$(2d+1)h_{auto} + d$	Number of hidden units
Diabolo network	-	$h_{diab}(4d + 4h_{diab} + 5) + d$	Number of hidden units and dimension subspace size

can be improved by scaling the data and with a suitable number of clusters can be very powerful. The one class SVM is insensitive to outliers and it is guaranteed to find the global minimum. Whilst there is no general method for choosing the kernel, plenty of research has been done in this area.

3.4 Ranking Systems

There has been very little research into ranking systems. Often for a mechanical system such as a machine, the focus is on accurately detecting faults rather than assessing the severity of the faults. For many systems, the means to rank the fault is not as important because all or many of the faults are regarded with equal importance in the sense that the presence of such a fault can cause mechanical failure [Nandi and Toliyat, 1999, 2002].

In many cases the faults are well defined and although they may be poorly sampled due to the cost of obtaining them. For many mechanical systems, there exists methods that have a high degree of success in detecting faults. However, for some systems, the impact of a fault occurring can be disastrous and the safety systems seek to measure how close the current state of the system is to an unsafe state.

When driving along motorways and roads, it is quite likely that one will see a sign on the back of a heavy goods vehicle with words similar to "How am I driving?" and then an invitation to call a given number if the driving appears poor (or good for that matter). Such an action is dependant on subjective opinion and the person's ability to correctly identify good or bad driving.

For a haulage firm, the knowledge of how its drivers are performing could be very valuable. Drivers that were driving outside normal ranges often could be interviewed about it or perhaps asked to take some more training and practise to improve their skills. The firm may be able to identify a particular route that causes even experienced drivers problems. They could then decide to choose another route or look to provide extra training and advice about the difficulties the current route poses. For a haulage firm, an accident can result in the loss of the vehicle, the driver, nearby civilians and the loss of the goods being carried. It leads to bad publicity for the firm and may make customers more reluctant to let the firm transport their goods. All of this assumes of course that accurate and reliable information can be provided about the state of the vehicle and the current level of driving.

A lot of the research done in this area is aimed at assessing the risks and their severities for a given application or field. Coding errors in computer programs are an important area of research. It is very important for software development teams to deliver software to customers that is on time and which satisfies the agreed specification. Pieces of software can contains millions of lines of code and numerous classes and so it can be very difficult to spot errors in the design and testing stages of development. To this end, fault prediction models based on object orientated design metrics have been developed [Gyimothy et al., 2005; Subramanyam and Krishnan, 2003; Thwin and Quah, 2005; Zhou and Leung, 2006]. Software faults vary in their degree of severity, ranging from low severity (a cosmetic fault for example) to high severity faults which could have potentially catastrophic consequences. [Zhou and Leung, 2006] compares various object orientated design metrics. The research is important because whilst previous studies had looked at predicting classes that were more fault-prone than others, no research had been undertaken to study what type of faults occurred (high or low severity) and the impact they had on a piece of software. The research concluded that the object orientated design metrics considered were better able to predict low severity faults than high severity faults in fault-prone classes.

[Gomes et al., 2002] looks at fault simulation in large mixed signal circuits. A novel feature of this work is their attempt to rank the faults according to their severity. They study the effect of a parameter deviation at a local level on the system level specification for the general circuit. They show a strong linear correlation between the true rank and expected rank for gain specification faults and total harmonic distortion faults. An advantage of their study is that the true rank of the faults is known already and it is clearly defined.

Ranking systems play an important role in sport. [Huang et al., 2006] considers ranking methods for identifying the best performing partnerships in the game of bridge. They make the point that sometimes it can be difficult to assess the performance of an individual in a team sport because a rating often does not take into account the abilities of his or her opponents. They consider two convex minimisation formulas with efficient solutions in order to rank individual performance. They minimise a regularised least squares formula and a log-likelihood method. Results are assessed by computing the correlation between the ranking methods but mainly by considering an order relation on partnerships. Let $r = (r_1, r_2)$ be the ranks of two bridge partnerships. They define an order relationship on two groups $r = (r_1, r_2)$ and $\overline{r} = (\overline{r_1}, \overline{r_2})$ by

$$r \text{ better than } \overline{r} \text{ if } \max(r_1, r_2) < \min(\overline{r_1}, \overline{r_2}). \tag{3.86}$$

That is, if the weakest partnership from r is better than the strongest partnership from $\overline{r}$ then the group r should be superior to $\overline{r}$. From this, in order to assess the performance, they use the ratio

$$\frac{\text{number of violations}}{\text{number of hits}} \tag{3.87}$$

where a violation occurs if r is better than $\overline{r}$ but $\overline{r}$ beats r and a hit occurs if r is better than $\overline{r}$ and r beats $\overline{r}$. The maximum likelihood method provides the best results. This situation is not very similar to detecting abnormalities in aircraft flight data because the relations between partnership performance (the match results) are known beforehand whereas whether one flight is 'safer' than another is a matter of opinion. However, the methods in this paper show that good rankings can be obtained using models that are convex (and so have a guaranteed global minimum).

Wang et al. [Wang and Li, 2004] use rough set theory to rank faults occurring on a bump machine which is used for energy transformation. Accelerometers measure vibration signals which are then the attributes used to create the rule base. The system is only capable of detecting the four known faults that can affect the machine. An order on the faults is created and whilst this is not a measure of severity, it is a measure on the likelihood of each fault. Thus in the event of a machine breakdown, the maintenance engineer can reduce downtime for that machine by checking for the most likely faults first.

Ranking systems and fault severity are topics that appear in aviation. [Zakrajsek and Bissonette, 2005] use information about bird strikes on aircraft to create a ranking system in order to identify which bird poses the greatest threat to the aircraft. Bird strikes can potentially be very dangerous as they can break the windscreen in the cockpit or damage the engines if they are ingested inside. Bird strikes are rated by the level of damage they cause to the aircraft. A class A strike is most serious which usually involves loss of multiple lives and/or loss of the aircraft. Class B strikes cause major damage to the aircraft and/or permanent disability to a passenger or crew and a class C strike leads to minor damage to the aircraft and passengers. The ranking system is based on the mean numbers of strikes per class each year and weighting constants for each class reflecting the mean value of damage caused. Whilst the proposed method utilised low dimension inputs to create the ranking, it does show that there is good value in assessing threats to aircraft. The ranking of blackbirds and starlings at number 4 was considered unusual given their relatively small size so ranking systems can help identify threats that appear to be minor but on closer inspection are in fact much more significant.

3.5 Conclusion

In this chapter, the field of novelty detection and one class classification has been reviewed and analysed for their abilities to detect abnormalities. When constructing the dataset and analysing flight data, it was clear that whilst events provided information about a specific point or interval in the flight, there was no clear method for identifying whether a descent was abnormal or not. This meant that a training set could contain abnormal data and therefore it was important to choose classifiers that would be able handle abnormal data in the training phase. The classifiers chosen (SVM, MoG and K-means) were all able to accommodate abnormal data in the training set. Furthermore, given the vastly differing numerical ranges of some of the parameters (see table 4.3), scaling the data was necessary and the classifiers chosen benefit from scaling.

Ranking systems were reviewed in this chapter and it was found that there is very little research on ranking datasets with large numbers of features. However Clifton et al [Clifton et al., 2006] has success in detecting precursors for combustion instability. The ability to combine several channels of information via the combination rules to make a conclusion about the combined state could be very valuable for a flight data monitoring approach. By extracting information from different heights, it might be possible to say something about the whole descent. This idea is explored more thoroughly in chapter 4.

Chapter 4

Method

4.1 Introduction

In this chapter a two phase method is proposed for detecting abnormalities and ranking flights based on these abnormalities. Section 4.2 details how the dataset was chosen, the heights and features used, how it was pre-processed and also some example data. Section 4.3.1 details the proposed method and how the parameter ranges for the classifiers were selected so that the valid results could be achieved. Section 4.4 details the abnormal test set and how it was constructed.

The first section details the proposed method and gives explanations for the design. The next section introduces an abnormal test set. As stated before, whilst events provide a good analysis of the state of a flight at a given point in time, there is no formal system for assessing a larger section of the flight. The abnormal test set therefore represents the opinions of experts at Flight Data Services who analysed flights based on the principles with which the pilots descend the aircraft.

4.2 Data Preparation and Dataset Creation

4.2.1 Dataset Selection

The dataset consists of 1,518 flights into the same airport in the United Kingdom. The flights are all by Boeing 757-200 aircraft. This is important as whilst the approach into an airport is the same for large jet aircraft, airlines may have

Table 4.1: Heights used in the training and testing sets.

10000	9000	8000	7000
6000	5000	4000	3500
3000	2500	2000	1500
1000	750	500	400
300	200	150	100
75	50	25	0

variations in their operating procedures for different aircraft types which could confuse the model of normality. The time period was from May 2007 to June 2008. This time period covers both summer and winter flying variations and so allows a better model of normality to be created.

4.2.2 Heights Chosen

When trying to analyse time series data for anomalies, it is useful to have some idea about which anomalies are likely to be encountered for they can help determine how often the data should be sampled. On the descent, height is very important as the higher the aircraft, the more time it has to correct any possible problems. Therefore anomalies affecting aircraft closer to the ground are likely to be more serious than those higher up.

The events used for the 757-200 aircraft focus on heights mostly below 2000ft. The purpose of these events in general is to detect a possible unstable approach by monitoring parameters such as airspeed, rate of descent and flap setting. However, as stated before, there are few events analysing heights higher up. Therefore, the proposed system, whilst looking at heights below 2000ft, will also analyse heights up to 10000ft. The upper height of 10000ft was chosen as it is the height at which the pilots are not meant to engage in non-essential communication. Snapshot data was extracted from the descent at the heights found in table 4.1.

Of these 24 heights, 14 are at or below 2000ft and the remaining 10 are between 10000ft and 2500ft. The benefit of having more heights at lower altitudes is that a detailed analysis can be made of any abnormalities and the impact they have on the flights. For example, it would be possible to identify if the same event on one flight has a greater or lesser impact than the same event on another flight.

Having extra heights above 2000ft should allow the system to spot abnormalities or unusual behaviour that could help to explain events at lower altitudes.

4.2.3 Feature Choice

Feature selection is an active research topic [Polat and Guenes, 2009; Weston et al., 2001] and has been shown to improve classifier performance [Chen and Lin, 2006]. However for the purposes of creating this dataset, features were selected on the advice of former pilots, navigators, aeronautical engineers and air traffic controllers. In order to create an accurate model of the descent, these experts were interviewed in order to understand how pilots of jet aircraft control the aircraft and which parameters are important at which heights.

The features selected were chosen after extensive consultation with former pilots, navigators, flight engineers and air traffic controllers with a combined experience of over 150 years. Their experience includes time spent in the Royal Air Force, the International Air Traffic Association (IATA), National Air Traffic Control(NATS) and several UK airlines. The features can be found in table 4.2. Features included at a given height are marked with **Y** and those which are not are marked by N.

4.2.4 Pre-processing

Pre-processing is an important step in preparing a dataset for classification. Erroneous values can reduce the accuracy of the classification and distort the model of normality which is trying to describe the data. From an operational perspective, aircraft parameters are usually within a pre-defined range and so meaningless values can be filtered out. For the dataset, only flights that had snapshot data for all the 24 heights were used. Typical ranges for the parameters used can be found in table 4.3.

4.2.5 Scaling

When a dataset contains features whose values occur in very different ranges, scaling is used so that one feature does not dominate the others. In this thesis,

Table 4.2: Features chosen (see table 4.3 for parameter meanings)

Height	CASC	V-Vref	IVV	Pitch	GS	Loc	Flap	LDG	SPD	N1	DIST	ROD
									BRK		RAT	DIFF
10000	**Y**	N	**Y**	N	N	N	**Y**	**Y**	N	N	**Y**	N
9000	**Y**	N	**Y**	N	N	N	**Y**	**Y**	N	N	**Y**	N
8000	**Y**	N	**Y**	N	N	N	**Y**	**Y**	N	N	**Y**	N
7000	**Y**	N	**Y**	N	N	N	**Y**	**Y**	N	N	**Y**	N
6000	**Y**	N	**Y**	N	N	N	**Y**	**Y**	N	N	**Y**	N
5000	**Y**	N	**Y**	N	N	N	**Y**	**Y**	N	N	**Y**	N
4000	**Y**	N	**Y**	N	N	N	**Y**	**Y**	N	N	**Y**	N
3500	**Y**	N	**Y**	N	N	N	**Y**	**Y**	N	N	**Y**	N
3000	**Y**	N	**Y**	N	N	N	**Y**	**Y**	N	N	**Y**	N
2500	**Y**	N	**Y**	N	N	N	**Y**	**Y**	**Y**	N	**Y**	N
2000	**Y**	N	**Y**	N	**Y**	**Y**	**Y**	**Y**	**Y**	**Y**	**Y**	N
1500	**Y**	N	**Y**	N	**Y**	**Y**	**Y**	**Y**	**Y**	**Y**	N	N
1000	N	**Y**	**Y**	**Y**	**Y**	**Y**	**Y**	**Y**	**Y**	**Y**	N	**Y**
750	N	**Y**	**Y**	**Y**	**Y**	**Y**	**Y**	**Y**	**Y**	**Y**	N	**Y**
500	N	**Y**	**Y**	**Y**	**Y**	**Y**	**Y**	**Y**	**Y**	**Y**	N	**Y**
400	N	**Y**	**Y**	**Y**	**Y**	**Y**	**Y**	**Y**	**Y**	**Y**	N	**Y**
300	N	**Y**	**Y**	**Y**	**Y**	**Y**	**Y**	**Y**	**Y**	**Y**	N	**Y**
200	N	**Y**	**Y**	**Y**	**Y**	**Y**	**Y**	**Y**	**Y**	**Y**	N	**Y**
150	N	**Y**	**Y**	**Y**	**Y**	**Y**	**Y**	**Y**	**Y**	**Y**	N	**Y**
100	N	**Y**	**Y**	**Y**	**Y**	**Y**	**Y**	**Y**	**Y**	**Y**	N	N
75	N	**Y**	**Y**	**Y**	N	N	**Y**	**Y**	**Y**	**Y**	N	N
50	N	**Y**	**Y**	**Y**	N	N	**Y**	**Y**	**Y**	**Y**	N	N
25	N	**Y**	**Y**	**Y**	N	N	**Y**	**Y**	**Y**	**Y**	N	N
0	N	**Y**	**Y**	**Y**	N	N	**Y**	**Y**	**Y**	**Y**	N	N

Table 4.3: Typical Ranges for Dataset Parameters (all heights).

Parameter	Description	Units	Typical Range
Ratio of height to distance to landing	Height divided by track miles to landing	Feet/NM	200 to 400
Flap	Flap setting	No Units	0 to 30
Glideslope Deviation	Deviation in the vertical from optimum landing path	Dots	-3 to 3
IAS	Indicated Airspeed	Knots	110 to 300
IVV	Rate of Descent	Feet/Min	-4000 to 0
Landing Gear	Landing gear deployment	No Units	0 or 1
Localiser Deviation	Deviation in the horizontal from optimum landing path	Dots	-3 to 3
Engine Speed	Percentage of nominal maximum speed	No Units	30 to 70
Pitch	Angle of aircraft relative to the horizon	Degrees	-2 to 5
Difference between IVV and Recommended Rate of Descent (ROD)	Difference between actual descent rate and recommended descent rate	Feet/Min	-300 to 300
Speedbrake	Speedbrake deployment	No Units	0 or 1
V-Vref	Difference between indicated airspeed and reference landing speed	Knots	-5 to 50

Table 4.4: Example Data from the Training and Testing Set at 1000ft

Data Set	V-Vref	IVV	Pitch	GS	Loc	Flap	LDG	SPD BRK	N1	ROD DIFF
Train	5.85	-728	2.3	0.031	0.003	30	1	0	56.3	21.0
Train	15.20	-622	0.7	0.009	-0.030	30	1	0	41.4	6.0
Train	10.52	-699	0.9	0.027	0.023	30	1	0	39.4	55.5
Train	13.77	-724	1.2	-0.031	-0.008	30	1	0	46.0	8.5
Train	12.40	-608	1.8	0.076	-0.043	30	1	0	62.0	25.5
Test	42.84	-1067	-0.2	1.295	0.320	20	1	0	38.1	-81.5
Test	48.88	-1202	-3.5	0.134	0.023	20	0	0	30.6	-370.5
Test	20.29	-896	-1.6	0.027	-0.010	30	1	0	38.1	-42.5
Test	5.65	-682	2.6	0.027	0.013	30	1	0	52.3	-21.0
Test	64.60	-1210	0.4	-0.063	-0.038	20	1	1	38.3	-296.0

range scaling and normalisation are compared. Range scaling linearly maps the data onto a chosen range, commonly [0 1]. Range scaling preserves the distance between features of different data points.

Let $X = \{x_i | i = 1, ..., n\}$ denote the training set and $Y = \{y_i | i = 1, ..., m\}$ denote the testing set. Then the range scaled training and testing sets X_R and Y_R are given by

$$X_R = \left\{ \frac{x_i - x_{\min}}{x_{\max} - x_{\min}} | i = 1, ..., n \right\} \tag{4.1}$$

$$Y_R = \left\{ \frac{y_i - x_{\min}}{x_{\max} - x_{\min}} | i = 1, ..., m \right\} \tag{4.2}$$

respectively where x_{min} and x_{max} are the smallest and largest elements of X.

4.2.6 Example Snapshot Data

Table 4.4 contains an example of some of the snapshot data from the dataset used in this thesis. It is taken from 1000ft and shows the values of each of the features that are most useful at this height (see table 4.2).

4.3 Framework

4.3.1 Framework

In this section, the 2 phase method framework is introduced. Steps 1 to 3 consist of selecting the data and partitioning it into the appropriate steps. Steps 4 to 5 represent Phase 1 of the method from which a DAP can be produced from. Steps 6 to 9 detail Phase 2 of the method.

1. Select flights to form training and testing sets in an 80%:20% ratio.
2. Extract snapshot data from training and testing flights at heights given in table 4.1. The features used for each height can be found in table 4.2.
3. Form training and testing sets containing snapshot data at each of the given heights.
4. Train a classifier on each of the training sets and test on the testing set containing data at the same height.
5. For each data point at each height, compute the distance between the data point and the threshold chosen by the classifier.
6. For each flight, form a feature vector containing distances to the thresholds at each height.
7. Train a classifier on feature vectors from flights in the original training set and test on those from the testing set.
8. Compute the distance of the data point to the threshold for each data point.
9. Sort the values in ascending order.

4.3.2 1st Phase Method

This subsection details the 1st Phase Method and how they produce the DAP.

Figure 4.1: Block Diagram illustrating proposed method.

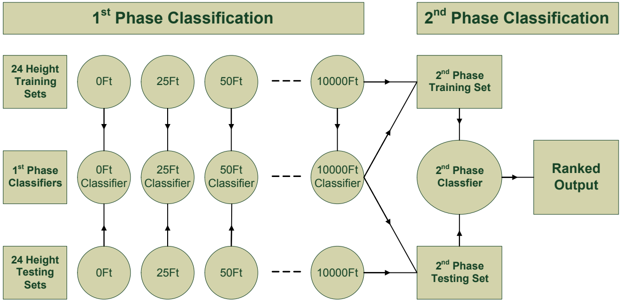

4.3.2.1 Method Details

For the 1st phase, snapshot data from the dataset is extracted from the 24 heights and then split into training and testing sets for each height such that for a given descent, its snapshots are either all in the training set or the testing set. The classifiers will be trained on the training set over their parameter space and then tested on the testing set. Training is done by snapshot height so for example the snapshot training set containing data from 50ft is trained upon and then tested on the snapshot testing set also containing data from 50ft.

A block diagram of the method can be found in figure 4.1. For a given descent, the distance from the classifier threshold is taken for each of the heights which is then plotted against height. Such a chart is known as a DAP.

4.3.2.2 DAP Comments

A key point to note is that at each height, different numbers of features are used (see section 4.2) to create the classifier model. If the number of features used varies widely (by orders of magnitude) then it will become very difficult to compare distances to thresholds at different heights (though abnormalities can still be detected). This is because the volume of region enclosed by the classifier threshold in the feature space increases if the numbers of features increase [Duda and Hart, 1973]. However, because the numbers of features used for each height varies between 5 and 10, the impact of this will be negligible.

4.3.3 Parameter Selection

As already stated, the number of possible modes of abnormality for an aircraft is large and ill defined. This makes the task of identifying the optimum parameter set much harder because a framework needs to be established. As indicated, the method for identifying abnormalities consists of two phases. The first tries to identify abnormalities on individual flights and the second compares individual flights to identify the most abnormal flights overall (given the abnormalities scores computed for each of the heights).

To this end, in consultation with experts at Flight Data Services, an abnormal test set was created which contains flights that would be of interest to the safety departments of most airlines. The engine room at Flight Data Services has over 150 years combined experience in flight safety so the test set is based on expert opinion. However, some airlines may have differing requirements regarding flight safety so whilst the abnormal test set cannot be regarded as comprehensive, it should be regarded as a solid basis by which the proposed method can be judged. Details of the abnormal test set, which contains 63 flights, are found in section 4.4.

The parameters selected for each classifier are those which rank the highest number of flights in the abnormal test set in the top 63 positions, such that parameter choices conform as far as possible to best practise in current research.

For each of the three classifiers used, the following subsections explain how the parameters were chosen.

4.3.3.1 Support Vector Machine Parameter choice

The SVM has the following parameters:

- 1st Phase Kernel Width σ_{P1}
- 1st Phase Fraction Rejected ν_{P1}
- 2nd Phase Kernel Width σ_{P2}
- 2nd Phase Fraction Rejected ν_{P2}

Whilst there is no known method for choosing the optimum values for a given training set, many studies have analysed the parameter space to see what impact it has on generic classification. It is known that too large or too small values for σ can result in under or over-fitting of the training set. If the training set is under-fitted, the decision function may not be complex enough to describe the data adequately whilst if over-fitting occurs, data points in the training set can be given too much importance leading to a loss of generalization on the testing set. A more detailed explanation can be found in Chapter 3. It has also been shown that choosing σ as the reciprocal of the number of features in the dataset can lead to good results. Thus a solution that contains too few or too many support vectors should be rejected. Given that training sets in the 1st phase contain between 5 and 13 features, $\sigma = 0.1$ would seem a good choice. The parameter ν is an upper bound on the proportion of outliers and also a lower bound on the number of support vectors. Common values for ν are 1%, 5% and 10%.

The ranges for the parameters are given below:

$$\sigma_{P1}, \sigma_{P2} \in \left\{10^i | i = -4, -3, -2, -1, 0, 1, 2\right\} \tag{4.3}$$

$$\nu_1, \nu_2 \in \{0.01, 0.05, 0.1, 0.15, 0.2, 0.3, 0.4, 0.5, 0.6, 0.7, 0.8, 0.9, 1\}. \tag{4.4}$$

4.3.3.2 K-Means Data Description Parameter choice

The K-Means has the following parameters:

- 1st Phase Number of Clusters C_{P1}
- 1st Phase Fraction Rejected ν_{P1}
- 2nd Phase Number of Clusters C_{P2}
- 2nd Phase Fraction Rejected ν_{P2}

For this classifier, there is no optimum method for selecting suitable parameters for a given training set. Therefore all possible parameter combinations will be analysed and averaged over 10 runs. The parameters are chosen from the following ranges:

$$C_{P1}, C_{P2} \in \{1, 2, ..., 20\} \tag{4.5}$$

$$\nu_{P1}, \nu_{P2} \in \{0.01, 0.05, 0.1, 0.15, 0.2, 0.3, 0.4, 0.5, 0.6, 0.7, 0.8, 0.9, 1\}. \tag{4.6}$$

4.3.3.3 Mixture of Gaussians Parameter choice

The MoG has the following parameters:

- 1st Phase Fraction Rejected ν_{P1}
- 1st Phase Number of Training Gaussians T_{P1}
- 1st Phase Number of Outlier Gaussians O_{P1}
- 2nd Phase Fraction Rejected ν_{P2}
- 2nd Phase Number of Training Gaussians T_{P2}
- 2nd Phase Number of Outlier Gaussians O_{P2}

A brute force approach was used based on parameters chosen from these ranges

$$\nu_{P1}, \nu_{P2} \in \{0.01, 0.05, 0.1, 0.15, 0.2, 0.3, 0.4, 0.5, 0.6, 0.7, 0.8, 0.9, 1\} \tag{4.7}$$

$$T_{P1}, O_{P1}, T_{P2}, O_{P2} \in \{1, 2, ..., 20\}\,. \tag{4.8}$$

Table 4.5: Severity level distribution in the Abnormal Test Set

Maximum Severity Level	Quantity
3	20
2	15
1	21
0	7

4.4 Abnormal Test Set

The abnormal test set contains 63 flights. Whilst there are several flights with level 3 events in this set, there are also many flights with events whose maximum severity level is 1 or 2. Furthermore there are also a few flights with no events whatsoever. Table 4.5 shows the numbers of flights in the abnormal test that have events where the maximum severity level is between 0 and 3. Note that a flight with a maximum severity level of 0 indicates the flight has no events at all.

On investigation, it was found that the number of events and their severity level bore little relation to the ranked position of the flight after 2nd Phase classification. This is not particularly surprising given that events mostly focus on the state of the aircraft below 2,000ft whereas the method considers the descent from 10,000ft. Furthermore, an event is noted as having happened and the numerical exceedance is not used for compiling airline statistics. Another key point to note is that an event is representative of the state of one or perhaps two parameters whereas the method in question looks at all relevant parameters for that height. In order to compare how accurate the ranking was, the data was inspected by hand and, after consultation with experts at Flight Data Services, a special test set was created which contains flights that most flight safety departments would like to know about. This set will be called the Abnormal Test Set throughout the rest of the thesis.

Chapter 5

Results

5.1 Introduction

This chapter presents the main results of the thesis. The results split into 2 phases, contained in sections 5.2 and 5.3. Section 5.2 contains DAPs of some flights in the test and training sets and shows that flights that have no level 3 events in the descent can have large negative regions on their DAPs. It also shows how negative regions on the DAPs compare with the actual parameter values at those heights. Section 5.3 presents the raw-value and combination rule methods for phase 2. Section 5.4 explains the performance metrics used to evaluate the results and also introduces the feature selection tool F-score. Section 5.4.2 details a simple method which is used in comparison with the 2nd phase methods to validate them. Section 5.4.3 shows the results of the 2nd phase rankings for all classifiers and compares the Balanced Error Rate (BER), Area Under the Curve (AUC), False Positives (FP), False Negatives (FN), number of abnormal flights in the top 63 and the average ranking of flights with level 3 events. Section 5.4.4 contains an analysis of the false positives for the SVM via the raw-value and combination rule methods. Section 5.4.6 presents the details of the F-score algorithm. It also details how F-score was used to analyse which heights were most significant in identifying differences between the training set and the abnormal test set. Section 5.5 introduces the concept of visualisation and demonstrates how it can provide added value to flight safety officers and how it can identify unusual flights in the training set.

Figure 5.1: Training Flight DAP using SVM.

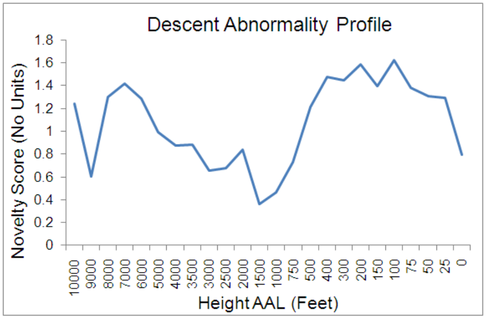

5.2 1st Phase Results

5.2.1 Descent Abnormality Profiles

Results of the first phase of classification are represented by Descent Abnormality Profiles (DAPs). These are charts with the height on the x-axis and the abnormality value produced by the classifier on the y-axis. In this thesis, negative abnormality values indicate a deviation from normal parameter configurations and positive values indicate normal parameter configurations. They provide a clear visual representation of the behaviour of a particular flight during the descent and allows the flight safety officer to quickly identify which heights, if any, are of interest.

Figure 5.1 shows an example DAP. The line is always above the x-axis, indicating that the vast majority of parameters for all heights are within the expected ranges.

Note: The DAPs are created using the optimum settings that produce the highest average number of abnormal flights in the top 63, whether from the raw-value method or the combination rule method. More details can be found in section 5.4.

In this subsection, a selection of flights are presented and their DAPs are analysed. For each flight, the resulting DAPs from the 3 classifiers are looked at and their similarities and differences studied. The flights presented are as follows.

- Flight 329601: Late capture of ILS
- Flight 418404: Early deployment of landing gear and flaps

- Flight 421357: Unstable Approach. No events but the data shows otherwise
- Flight 524055: Very steep descent
- Flight 619605: High speed event
- Flight 312013: Normal descent

5.2.1.1 Flight 329601 - Late capture of the ILS.

The main point of interest is the failure to capture the localiser until around 500ft. Usually capture occurs from around 2000ft to 1500ft but it is almost always captured by 1000ft. The events for this flight are found in table 5.2.

Table 5.1 shows various parameters at various heights on this descent and compares them to the averages for those parameters at those heights in the training set. On the SVM and the K-means DAP (see figures 5.2 and 5.3), the data points at 2000ft and 1500ft are close to zero. However, at 1000ft and 750ft, there are large negative values indicating strong abnormalities. This is because almost every flight is established on the ILS at these heights so it is very unusual to see one that is not. However, because this flight has no level 3 events, it has not been seen by a flight safety officer; thus highlighting the value of this method in detecting abnormal flights over the event based system. The MoG DAP (see figure 5.4) is very different to the others and it indicates regions of abnormalities where the line is a little below or on the x-axis. Furthermore, regions from 7000ft to 5000ft and 2500ft to 2000ft have similarly low values from which one could draw the conclusion that such regions had a similar level of abnormality, which is not the case.

5.2.1.2 Flight 418404 - Early deployment of landing gear and flaps.

This flight is notable more for the unusual descent rather than any safety issues. The descent is rather late, 26.4NM at 10000ft and 20.5NM at 8000ft, a rate of descent of nearly 400ft per NM, steeper than the 1 in 3 rule. At 8000ft, the aircraft deployed the landing gear in order to increase the rate of descent. Flap 1 is selected which is very unusual. Flap 5 is selected around 5000ft and flap 20 at around 4000ft. The aircraft is stable at 1000ft and the final approach is

Table 5.1: Points of Interest Flight 329601.

Height	Parameter	Parameter Value	Parameter Percentile	Average Value	Parameter
6000	IAS	199	2	235	
2000	LOC	3.997	96	0.223	
2000	GS	0.893	99	-0.412	
1500	LOC	3.763	99	0.261	
1500	GS	0.987	99	0.024	
1000	LOC	4.688	100	-0.003	
1000	GS	0.277	98	0.021	
750	LOC	1.820	100	-0.067	
750	GS	-0.161	6	-0.001	

Table 5.2: Event List Flight 329601.

Event Name	Severity Level	Height
Late Heading Change	2	42
Localiser Deviation Below 1000ft	2	990
Speed Low during Approach 1000-500ft	1	763
Speed Low during Approach 500-50ft	1	495

Figure 5.2: Flight 329601 DAP using SVM.

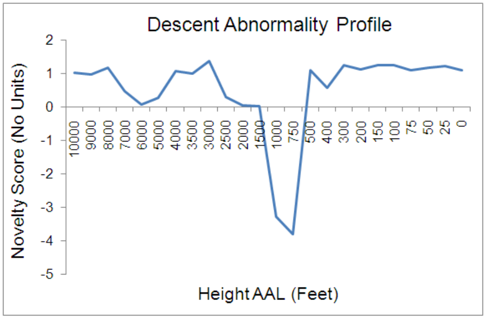

Figure 5.3: Flight 329601 DAP using K-means.

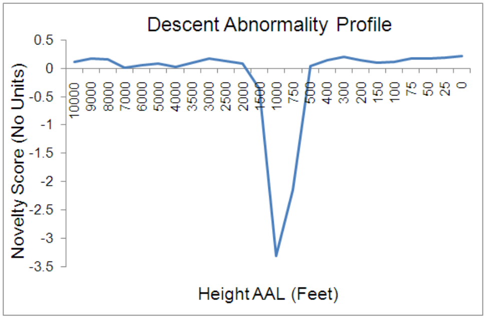

Figure 5.4: Flight 329601 DAP using MoG.

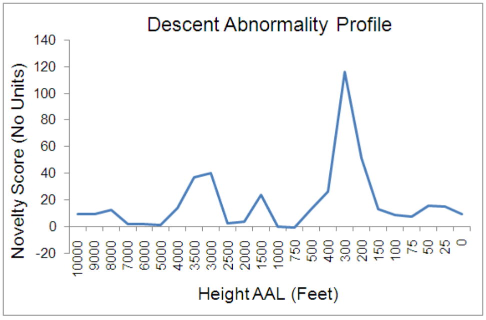

normal, hence the lack of events. However, since this flight has no level 3 events, a flight safety officer would not have seen it. Whilst the aircraft managed the steep descent well, it is not recommended practise and the airline would be interested to see if this type of descent happens often. See table 5.4 for a list of events.

Table 5.3 shows some of the heights and parameters of interest for this flight. The SVM and the K-means DAPs (see figures 5.5 and 5.6) show a large region of abnormality from around 9000ft to 3000-2500ft, resulting from the steep descent,

Table 5.3: A Sample of Points of Interest Flight 418404.

Height	Parameter	Parameter Value	Parameter Percentile	Average Value	Parameter
9000	IAS	225	3	260	
9000	DISTRAT	23.58	99	36.07	
8000	IAS	192	0	252	
8000	Flap	1	99	0.01	
8000	LDG	1	99	0	
8000	DISTRAT	20.49	1	32.22	
5000	Flap	5	99	0.08	
4000	Flap	20	100	0.63	

Table 5.4: Event List Flight 418404.

Event Name	Severity Level	Height
No Events	n/a	n/a

Figure 5.5: Flight 418404 DAP using SVM.

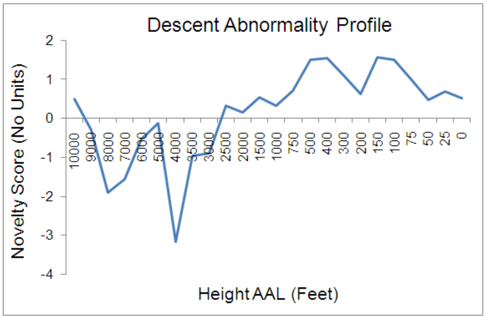

the low airspeeds and the high flap settings. At 8000ft and 4000ft there is a clear ’spike’ on both charts, resulting from flap 1 and the landing gear being selected at around 8000ft and from flap 20 being selected at around 4000ft. The MoG DAP (see figure 5.7) positions the line approximately on the x-axis from 10000ft to 1500ft and also from 300-200ft and 75-0ft. The SVM and the K-means DAPs show slight dips in the line at these heights. This is due to slightly lower than average power settings at these heights and a slightly higher than recommended rate of descent; neither of which are significant.

Figure 5.6: Flight 418404 DAP using K-means.

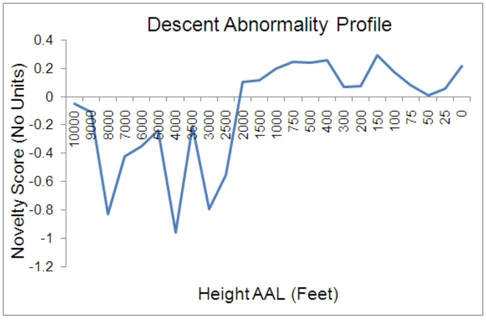

Figure 5.7: Flight 418404 DAP using MoG.

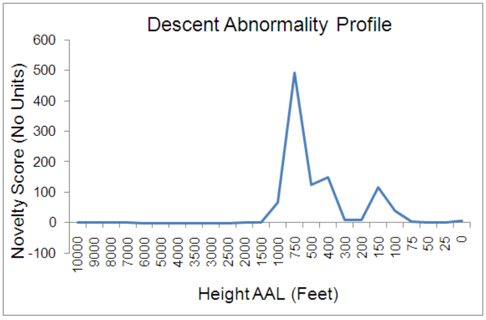

5.2.1.3 Flight 421357 - Unstable Approach. No events but the data shows otherwise.

On the surface it might seem that the DAPs for this flight should contain mostly positive regions due to the fact it apparently contains no events. However, after around 2000ft, there is a large negative region and upon closer inspection of the data, this flight should contain several events and does. The flight had been incorrectly labelled and table 5.6 shows the events that were detected. This was spotted during initial experimentation and it highlights the ability of the method to detect abnormal flights however they are labelled.

Table 5.5 shows some of the heights of interest for this flight. The K-means and the SVM DAP (see figures 5.8 and 5.9) both show a large region of negativity extending from around 1500ft down to around 25ft with the largest trough at 750ft and 500ft. The unstable approach is clearly highlighted and it provides an immediate visual indication to the flight safety officer that this unstable approach continued all the way to the ground. The MoG DAP (see figure 5.10) also

Table 5.5: A Sample of Points of Interest Flight 421357.

Height	Parameter	Parameter Value	Parameter Percentile	Average Value	Parameter
2000	GS	1.174	99	-0.419	
2000	LOC	1.754	93	0.223	
1500	GS	1.326	99	0.024	
1500	LOC	1.719	99	0.026	
1000	GS	1.295	100	0.021	
1000	LOC	0.32	99	-0.003	
1000	V-Vref	43.84	99	12.46	
1000	Flap	20	0	29.22	
750	GS	2.402	100	-0.001	
750	Flap	25	1	29.87	
750	ROD	-339.4	0	5.4	
750	V-Vref	29.08	99	8.69	
500	GS	1.915	100	0.001	

Figure 5.8: Flight 421357 DAP using SVM.

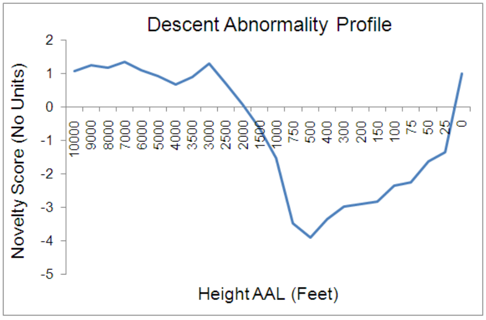

illustrates this fact also via a line approximately on the x-axis. However, it gives no indication of differing abnormalities during this phase, unlike the SVM and the K-means DAPs.

5.2.1.4 Flight 524055 - Very steep descent.

Although the DAPs for flight 524055 show a large negative region, the flight has no level 3 events and so therefore will not have been seen by a flight safety officer. The large negative region is caused by the very steep descent of the aircraft. At 10000ft, the aircraft has just 24NM track miles to go compared to the average value of 40NM. This leads to high rates of descent, high airspeeds

Table 5.6: Event List Flight 421357.

Event Name	Severity Level	Height
Low Power on Approach below 500ft	3	199
Glideslope Deviation Below 1000ft	3	855
Glideslope Deviation Below 500ft	2	430
High Speed 500-50ft	2	494
Pitch Low on Final Approach	1	679
Late Flap on Approach	1	560

Figure 5.9: Flight 421357 DAP using K-means.

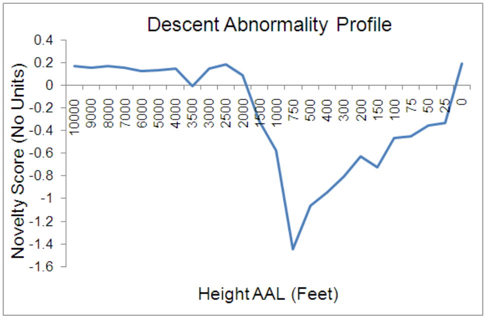

Figure 5.10: Flight 421357 DAP using MoG.

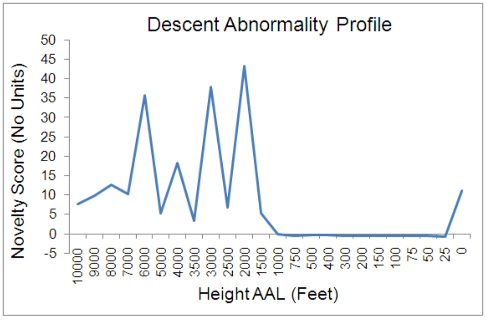

and heavy speedbrake usage. Furthermore, at 2500ft and 2000ft, the aircraft has the speedbrakes deployed but with more than 10 degrees of flap set, which is prohibited in the airline's SOP. However, the aircraft manages the descent well as seen by the largely positive region of flight after 1000ft. This is an example where a potentially unsafe approach has been corrected and the lack of high severity

Table 5.7: A Sample of Points of Interest Flight 524055.

Height	Parameter	Parameter	Parameter	Average	Parameter
		Value	Percentile	Value	
10000	DISTRAT	23.75	0	40.05	
9000	DISTRAT	20.36	0	36.07	
8000	DISTRAT	18.03	0	32.22	
7000	DISTRAT	15.54	0	27.22	
6000	DISTRAT	13.03	0	22.71	
3000	IVV	-3002	0	-973.36	
2500	IVV	-2368	1	-875.33	
2000	IVV	-1926	1	-798.40	
1500	IVV	-1507	1	-823.33	

Table 5.8: Event List Flight 524055.

Event Name	Severity Level	Height
High Descent Rate >2000ft	1	2935
High Speed 500-50ft	1	286

Figure 5.11: Flight 524055 DAP using SVM.

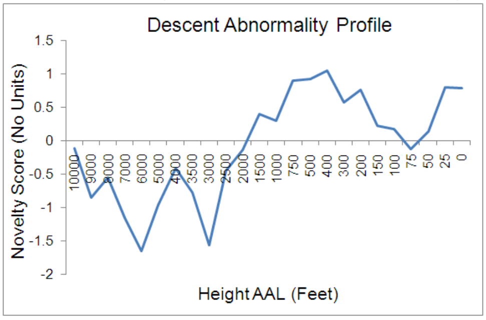

level events shows this. Nonetheless a flight safety officer would be interested in this descent as it may indicate a wider problem. See table 5.8 for a list of events.

Table 5.7 shows some of the heights of interest for this flight. The SVM and the K-means DAPs (see figures 5.11 and 5.12) are fairly similar from 10000ft down to around 3000ft. However the K-means DAP is almost always negative throughout the whole flight as is the MoG DAP (see figure 5.13) bar the region 1000ft to 750ft.

Figure 5.12: Flight 524055 DAP using K-means.

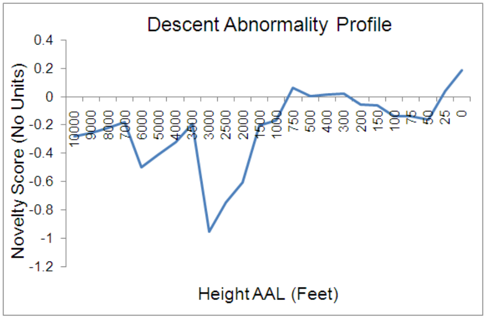

Figure 5.13: Flight 524055 DAP using MoG.

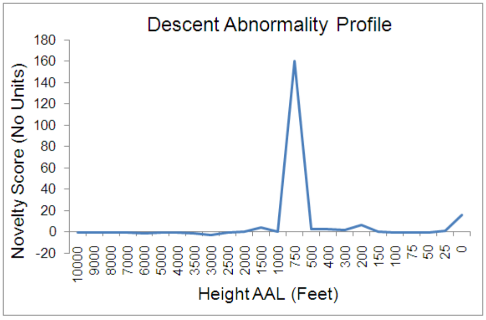

5.2.1.5 Flight 619605 - High speed event

At 10000ft the aircraft is 60NM from the runway at an airspeed of 207kts. The average track miles to landing is 40NM and the average indicated airspeed is 275kts. From the available evidence the aircraft chose a shallow descent, because of high winds. Once the aircraft reaches a height of around 750ft, the airspeed begins to increase and the pitch angle becomes negative. See table 5.10 for a list of events.

Table 5.9 shows some of the heights of interest for this flight. The slightly negative region shown on all DAPs (see figures 5.14, 5.15 and 5.16) resulted from the aircraft descending earlier than usual and at a slower than average indicated airspeed. Whilst this is not unsafe, it is unusual. However, the main point of interest is after 500ft. At 1000ft the aircraft satisfies the criteria for a stable approach but from 500ft, the airspeed has increased rapidly and the pitch angle is negative. The impact of these parameters is visible on all DAPs.

Table 5.9: A Sample of Points of Interest Flight 619605.

Height	Parameter	Parameter Value	Parameter Percentile	Average Value	Parameter
500	V-Vref	30.16	100	8.336	
500	RODDIFF	-139.9	5	4.87	
500	Pitch	-2.1	0	1.871	
400	V-Vref	27.16	99	8.239	
400	Pitch	-2.5	0	2.002	
300	V-Vref	27.16	100	7.914	
300	RODDIFF	-229.2	1	2.87	
300	Pitch	-0.7	1	2.073	

Table 5.10: Event List Flight 619605.

Event Name	Severity Level	Height
Pitch Low 1000-100ft	1	568
High Speed 500-50ft	3	284
Low Pitch at Touchdown	3	20
G Landing	1	0

Figure 5.14: Flight 619605 DAP using SVM.

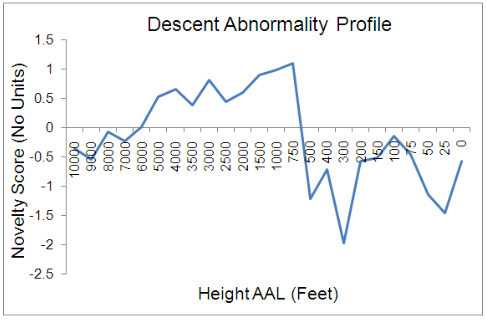

5.2.1.6 Flight 312013 - Normal descent

This descent is smooth with airspeed and rate of descent typical for this approach. Landing gear and flaps are deployed at typical heights and by 1500ft, the aircraft is established on the ILS with good speed. By 1000ft, the aircraft's airspeed is around vref + 8 kts with a rate of descent appropriate for its groundspeed. The approach power is set and flap 30 (landing flap) has been chosen.

Table 5.11 shows some of the heights of interest for this flight. The SVM and the K-means DAP (see figures 5.17 and 5.18) present a roughly similar profile.

Figure 5.15: Flight 619605 DAP using K-means.

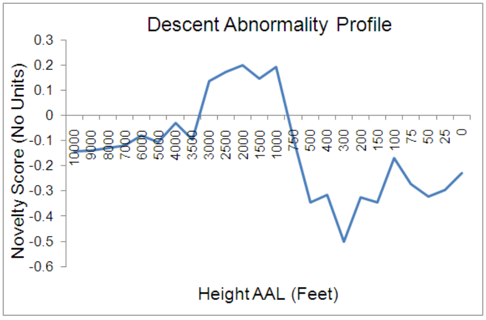

Figure 5.16: Flight 619605 DAP using MoG.

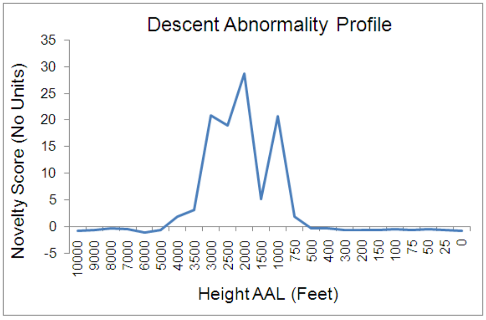

Figure 5.17: Flight 312013 DAP using SVM.

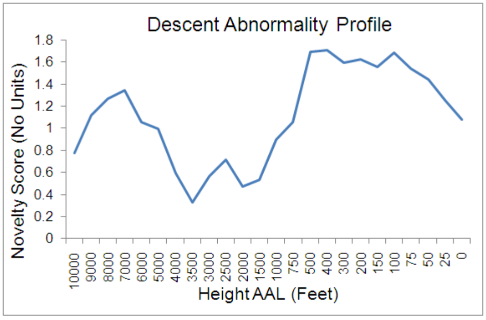

All data points are positive. The MoG DAP (see figure 5.19) however appears to regard some heights as negative, for example at 2000ft and 1500ft where there are some abnormal parameter values (see table 5.11). These are not enough to regard the descent as abnormal.

Table 5.11: A Sample of Points of Interest Flight 312013.

Height	Parameter	Parameter Value	Parameter Percentile	Average Value	Parameter
2000	IAS	145	1	172	
2000	Flap	25	98	8.52	
1500	IAS	130	2	156	

Figure 5.18: Flight 312013 DAP using K-means.

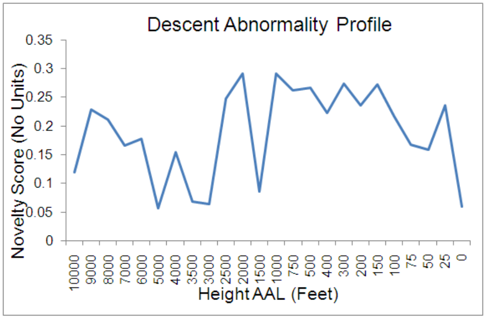

Figure 5.19: Flight 312013 DAP using MoG.

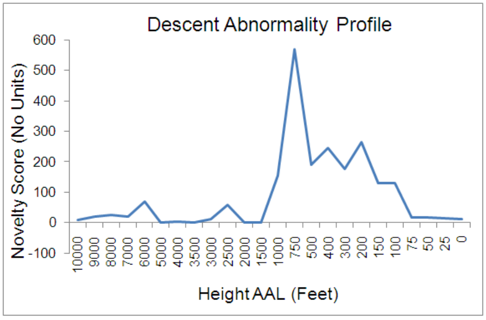

5.3 2nd Phase Results

5.3.1 Ranking Decents

The DAPs provide a clear visual method for identifying abnormalities on a descent and the heights at which they occur at. In section 1.3, it was stated that it would be a highly valuable feature to be able to compare flights and identify those descents with the most abnormalities and those with the largest abnormalities. To reiterate the task, the system needs to compare the abnormality scores at each of the heights for individual descents and somehow rank them so that the descents with large regions of abnormalities are ranked at the top and descents with mostly positive regions are ranked near the bottom. It should not be assumed however that a descent with only positive novelty scores has a lower ranking than a descent with a few abnormalities. For example, a descent whose snapshot data took the values at the centroid of each hypersphere for each height could be described as "perfect" and hence rather unusual in the sense that there is no such thing as the perfect descent. Therefore it would be ranked higher than a descent with a few small abnormalities as this is more common. Two methods are compared here to create a set of ranked descents.

5.3.1.1 Raw-Value

Each descent can now be represented by a feature vector of the 24 novelty values (one from each of the 24 heights). The training and testing sets for this method consists of those descents that formed the training and testing sets respectively in the first phase. The output is the distance of each data point from the classifier threshold. These are then sorted in ascending order so that the descents with the most significant abnormalities are ranked at the top.

5.3.1.2 Combination Rule

The number of heights for which snapshot data could be taken from is quite large. For example, if snapshot data was taken at 50ft intervals from 10000ft to 100ft and also taken from 100ft to 0ft in 25ft intervals, there would be a total of 203 heights. Using the raw value method could result in noise from heights where there is little abnormality. The combination rule method seeks to alleviate this pitfall by extracting information about the shape and content of the DAPs. The following set of statistics are generated:

For novelty values $(x_1, x_2, ..., x_{24})$, we compute

1. StDev $\sigma = \sqrt{\frac{1}{24}\sum_{i=1}^{24}(x_i - \mu)^2}$,

2. Max $Ma = \max_{i=1}^{24}(x_i)$,

3. Min $Mi = \min_{i=1}^{24}(x_i)$,
4. NumNeg $= \left(\sum_{i=1}^{24} i\right)$ where$x_i < 0$,
5. SumNeg $\sum^- = \left(\sum_{i=1}^{24} x_i\right)$ where$x_i < 0$,
6. SumPos $\sum^+ = \left(\sum_{i=1}^{24} x_i\right)$ where$x_i \geq 0$,
7. Ratio Pos/Neg $= \ln\left|\frac{\sum^+ +1}{\sum^- -1}\right|$.

The standard deviation of the abnormality values was selected because an abnormal descent could alternate between positive and negative abnormality values, whereas a normal descent would have mostly positive values, suggesting that for an abnormal descent, the standard deviation might be larger.

The maximum abnormality value was chosen because if an abnormal descent has mostly negative values, it might well have a low maximum. However, it is also possible that an abnormal descent could have regions of heights where the descent is largely normal and thus also have a large maximum. It is anticipated that this feature may not be as useful as some of the others.

The minimum abnormality value was chosen because highly negative abnormality values should indicate regions of flight where the aircraft data has deviated from the norm. A very high negative value could indicate a level 3 event or an unseen serious event.

The number of negative values was chosen because a large number could indicate significant regions of abnormality which a flight safety officer would like to know about. In contrast, for a normal descent, the value should be very low or perhaps zero.

The sum of the negative values should have a large absolute value if the descent has many negative abnormality values. For a normal descent, the absolute value of this sum should be small or zero.

The sum of the positive values was chosen because a large value should indicate a normal descent, though conversely a small value may not indicate an abnormal descent as they can also have normal regions.

Rather than a simple ratio of positive and negative sums, plus one is added to the numerator and plus one is subtracted from the denominator (to ensure neither becomes zero), and the natural log of the absolute value is taken. It is anticipated that ratios less than one (giving negative natural logs) should be a strong indicator of an abnormal descent.

5.4 Performance Metrics and F-score

5.4.1 Performance Metrics

To assess the performance of the classifiers in this paper, the standard confusion matrix will be utilised, where True Positive (FN) denotes the percentage of correctly identified normal descents, True Negative (FN) denotes the percentage of correctly identified abnormal descents, False Positive (FP) denotes the percentage of incorrectly identified normal descents and False Negative (FN) denotes the percentage of incorrectly identified abnormal descents.

The Balanced Error Rate (BER) is given by BER = (FP + FN)/2. It is a very useful error metric in one class classification problems where there is an imbalance between positive and negative examples. Consider an example with 90 positive examples and 10 negative examples and a classifier that predicts all examples are positive. The accuracy is 90% and the error is only 10%, which appears high. The BER however is 50%, highlighting the fact that the classifier is very poor at detecting negative examples.

The other metric used is the number of abnormal descents appearing in the top 63 ranked descents. Given that these descents have been analysed by hand as the most abnormal, they should appear at the top so this metric should be a good indicator of classifier performance. Note that the top 63 ranked positions are considered because there are 63 descents in the abnormal test set

5.4.2 A Basic Analysis of the Performance of the 2nd Phase Classifiers

With flights numbering in the tens of thousands, it is not practical in terms of time and man power to analyse each flight by hand and check that all 'abnormal' descents are detected. A quick way of analysing this is by considering the average number of standard deviations a datapoint is from the mean vector of all the features in the training set and then taking the average over all heights used. This simple approach provides a basic measure of detecting the level of abnormality and may help to identify possible descents that have not been included in the abnormal test set.

Let the training sets be given by $\{X_k | 1 \leq k \leq 24\}$ and an individual training set be represented by $X_k = \{\mathbf{x}_{ij} | 1 \leq i \leq 1215, 1 \leq j \leq a_k\}$ where a_k is the number of columns in X_k

Let the vector of column-wise averages of parameters for height training set X_k be given by $\overline{\mathbf{x}_k}$.

Then the matrix of novelty scores for X_k is given by

$$S_k = \left[\sqrt{\sum_{k=1}^{24} (\mathbf{x}_{jk} - \overline{\mathbf{x}_k})^2} | 1 \leq k \leq 24 \right] \tag{5.1}$$

The overall novelty score for an individual descent y_j is $s_j = \sqrt{\sum_{k=1}^{24} S_k^2(j)}$.

A novelty score of 0 for a descent is such that all parameters at all heights are equal to their relevant averages. It implies the descent is, by this definition, 'perfect'. The higher the value, the larger the absolute distance between the parameters and their averages and thus the greater the overall abnormality. Sorting these values in descending order provides a list of descents that are comparable to the ranking systems already introduced.

Table 5.12 shows the average ranking positions of level 3 flights for all classifiers and all methods are presented and it is seen that the Norm method is 5th out of 7 and outperforms the MoG classifier. Furthermore, in the top 63 ranked positions, there are 44 abnormal descents which is comparable to the performances of the SVM and K-means classifiers.

Table 5.12: Average ranking position for descents with level 3 events for all methods.

Classifier	Highest Event Level	Average Ranking Position	Method
SVM	3	49	Combination Rule
K-means	3	53	Combination Rule
SVM	3	55	Raw Value
K-means	3	62	Raw Value
Norm	3	79	N/A
MoG	3	88	Combination Rule
MoG	3	194	Raw Value

Table 5.13: Average Best BER using raw value method.

Method	Best Parameters	Best Average BER (Standard Deviation)
SVM	$\sigma_P 1$=1, $\nu_P 1$=0.05, $\sigma_P 2$=0.1, $\nu_P 2$=0.05	0.029 (0.005)
K-means	$\nu_P 1$=0.3, $C_P 1$=3, $\nu_P 2$=0.05, $C_P 2$=1	0.034 (0.007)
MoG	$\nu_P 1$=0.1, $T_P 1$=1, $O_P 1$=1, $\nu_P 2$=0.05, $T_P 2$=1, $O_P 2$=1	0.296 (0.055)

The norm method is included as an added check to illustrate the validity of the proposed method since abnormalities in general are defined as a larger than usual distance from the average.

5.4.3 Ranking Analysis of the Performance of the 2nd Phase Classifiers

Table 5.13 shows the average best BER using the raw-value method. Whilst the SVM and the K-means classifier are very similar, the MoG classifier is much worse. Table 5.14 shows the corresponding averages for the false positives and false negatives. False positives of nearly 5% and 6% for the K-means and SVM classifiers may be seen as a little high. However, given the nature of the problem and the lack of defined abnormalities, it may well be that some of these apparent false positives are also of interest. Table 5.15 shows the AUC values for the best BER values and whilst the SVM AUC and the K-means AUC are very similar, the MoG AUC is very poor in comparison.

Tables 5.16 and 5.17 show the average best BERs and accompanying false positives and negatives. The best average BER is a little higher than the best

Table 5.14: Average Best BER using raw value method.

Method	Average FP for Best BER (SD)	Average FN for Best BER (SD)	Best Average BER (SD)
SVM	0.058 (3.929)	0.000 (0.000)	0.029 (0.005)
K-means	0.048 (3.778)	0.019 (1.135)	0.034 (0.007)
MoG	0.363 (3.400)	0.229 (2.591)	0.296 (0.055)

Table 5.15: Average Best BER using raw value method.

Method	AUC for Best Average BER	Best Average BER (Standard Deviation)
SVM	0.9896	0.029 (0.005)
K-means	0.9893	0.034 (0.007)
MoG	0.6802	0.296 (0.055)

BER for the raw-value method but only marginally. What is of interest is the far better performance of the MoG classifier with a average best BER of 0.084, although it is still higher than the other classifiers. Table 5.18 compares the AUC values for each of the best BERs. The MoG AUC is much higher for the method compared to the raw-value method but it is still a little way behind the AUCs of the SVM and the K-means classifiers.

Tables 5.19 and 5.20 show the average number of abnormal descents in the top positions of the second phase ranking for the raw-value and the combination rule methods. For the top 63 positions, for all classifiers, the combination rule method does better with on average 5 more abnormal descents (for the SVM classifier) in the top 63 than the raw-value method.

Tables 5.21 and 5.22 show the average ranked position of a descent with at least one level 3 event. The SVM and K-means classifiers give similar performances with the MoG classifier giving a worse performance, particularly using the raw-value method.

In producing the data found in tables 5.21 and 5.22, two descents with level 3 events were excluded. One of these descents (see figure 5.20) triggered a Ground Proximity Warning System (GPWS) event and the other triggered a Go Around. Both of these descents had a very low novelty ranking and on further inspection, it was found that the go around was spurious and whilst the GPWS alert appeared valid, there was no appreciable effect on the flight data, hence the low novelty

Table 5.16: Average Best BER using combination rule method.

Method	Best Parameters	Best Average BER (Standard Deviation)
SVM	σ_{P1}=1, ν_P1=0.01, σ_P2=0.1, ν_P2=0.05	0.044 (0.005)
K-means	ν_P1=0.05, C_P1=6, ν_P2=0.05, C_P2=1	0.035 (0.005)
MoG	ν_P1=0.05, T_P1=1, O_P1=1, ν_P2=0.1, T_P2=3, O_P2=2	0.084 (0.010)

Table 5.17: Average Best BER using combination rule method.

Method	Average FP for Best BER (SD)	Average FN for Best BER (SD)	Best Average BER (SD)
SVM	0.055 (4.248)	0.037 (0.675)	0.044 (0.005)
K-means	0.048 (2.367)	0.022 (0.516)	0.035 (0.005)
MoG	0.108 (5.238)	0.060 (1.135)	0.084 (0.010)

Table 5.18: Average Best BER using combination rule method.

Method	AUC for Best Average BER	Best Average BER (Standard Deviation)
SVM	0.9865	0.044 (0.005)
K-means	0.9878	0.035 (0.005)
MoG	0.9154	0.084 (0.010)

Table 5.19: Average Position of Abnormal descents for best BER using raw value method.

Method	Top 63 (Standard Deviation)	Top 100 (Standard Deviation)	Top Outlier (Standard Deviation)
SVM	48.2 (0.95)	60.1 (1.49)	63.0 (0.79)
K-means	46.3 (1.34)	58.2 (0.63)	61.8 (1.14)
MoG	23.5 (7.38)	31.6 (7.34)	48.6 (3.34)

Table 5.20: Average Position of Abnormal descents for best BER using combination rule method.

Method	Top 63 (Standard Deviation)	Top 100 (Standard Deviation)	Top Outlier (Standard Deviation)
SVM	53.2 (4.60)	60.0 (0.00)	60.7 (4.28)
K-means	47.3 (1.06)	57.6 (1.17)	61.6 (0.52)
MoG	41.9 (1.29)	49.6 (0.97)	59.2 (1.14)

Table 5.21: Average ranking and overall novelty score for descents with level 3 events using raw value method.

Method	Highest Event Level	Average Ranking Position
SVM	3	55
K-means	3	62
MoG	3	194

Table 5.22: Average ranking and overall novelty score for descents with level 3 events using combination rule method.

Method	Highest Event Level	Average Ranking Position
SVM	3	49
K-means	3	53
MoG	3	88

Figure 5.20: Testing Flight DAP with a spurious level 3 Go Around event using SVM.

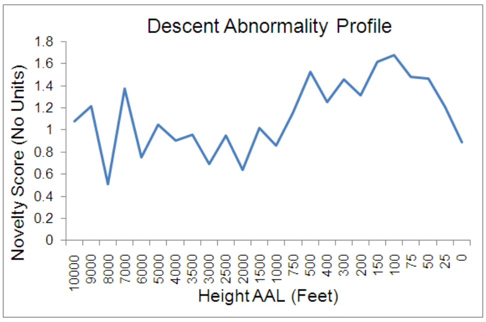

ranking. It is possible that the GPWS system on this aircraft has developed a fault.

5.4.4 An Analysis of False Positives

There will always be a degree of opinion in ranking the descents as different airlines will have differing opinions as to what constitutes an unsafe or an unusual descent. Hence some of these false positives, in the opinions of some flight safety officers, could be regarded as true negatives. This section analyses the false positives for the SVM raw-value and combination rule methods.

5.4.4.1 False Positives Analysis for SVM

Table 5.23 shows the ranking positions of the false positives in the top 63 ranked descents for both methods. Of immediate interest are the top 3 descents ranked 2, 3 and 4 for the raw-value method and 3, 6 and 5 for the combination rule method respectively. In all three descents, the speedbrake is deployed somewhere between 4000ft and 2000ft and left open all the way to the ground. This is prohibited by the airline's SOP because it could lead much higher rates of descent that are very hard to control. These descents were not included in the abnormal test set because it was known that the speedbrake parameter for those flights developed a fault and the data from it was incorrect. However, the algorithm only uses the parameters as listed in table 4.2 and so based on this information, it was correct to flag these descents as having a high degree of abnormality. The majority of the other false positives are descents where the flaps and/or the landing gear were deployed earlier than usual. These descents are more unusual than unsafe so it depends on the airline whether they might be interested.

Whilst the rankings from the two methods are largely similar, there are a few descents which show a large difference. Flight 420301 is ranked in the top 63 by the raw-value method (see figure 5.22) whereas the combination rule method (see figure 5.21) ranks it nearly bottom. The main region of abnormality (see figure 5.22 is between 3500ft and 2500ft. By 3500ft, the aircraft has deployed the landing gear, which is highly unusual given only 8 of the 1455 descents have deployed it by this height. Furthermore the Distance Ratio value is in the 97% percentile and the IVV is in the 13% percentile. There was only one negative height on the combination rule DAP and so this abnormality had very little impact in the ranking. However, for the raw-value method, the large negative value at this height (3500ft) had a much greater impact, leading it to be ranked in the top 63 positions. Similar reasons explain the difference in rankings for flight 418817.

5.4.4.2 An Analysis of the SVM Performance on the Abnormal Test Set

In this subsection the performance of the glsSVM (Raw-Value and Combination Rule) on the abnormal test set is analysed. Table 5.25 shows how many descents

Table 5.23: Details of False Positives for the SVM Raw-Value and Combination Rule Methods

RV Ranking	CR Ranking	Identifier	Event(s) of Significance
2	3	571049	Deployment of speedbrake from 2000ft to 0ft
3	6	388151	Deployment of speedbrake from 4000ft to 0ft
4	5	262228	Deployment of speedbrake from 4000ft to 0ft
17	20	390195	Early flap deployment
32	32	620240	Very early descent
35	80	419162	Early deployment of landing gear and flap 15 with speedbrake open
38	78	380257	Flap 5 and landing gear deployed early
39	79	420378	Flap 1 at high speeds and high altitudes
41	81	420157	Flap 1 at high speeds and high altitudes
48	69	394803	Flap 5 at 6000ft and 5000ft
55	1504	420301	Landing gear deployed early
60	70	510140	Low on glideslope on final approach with high descent rates
61	1272	418817	Flap 15 and landing gear deployed at 3500ft
62	227	559258	Low pitch and high rates of descent after 1000ft
63	62	591773	Late final flap choice and lower power after 1000ft
71	60	503351	Flap 1 at 9000ft with 276kts airspeed and then at 7000ft with 243kts airspeed
76	53	586293	High on GS from 400ft and vref+20 from 100ft-50ft
88	51	563111	Low power from 100ft-25ft and high pitch at landing
102	63	525252	Distance out from 10000ft to 6000ft goes from 86.5NM to 70NM

Table 5.24: Details of False Negatives for the SVM Raw-Value and Combination Rule Methods

RV Ranking	CR Ranking	Identifier	Event(s) of Significance
42	70	391496	At 3000ft and 2500ft, flap 20 and speedbrakes deployed. High IVV at 500ft.
47	71	522692	At 3000ft, the distance-height ratio is 405. At 2500ft and 2000ft, flap 15 and speedbrakes open. From 150ft to 50ft, low power and high IVV.
64	50	619615	High speeds and low power at 500ft and 400ft. Very high rate of descent at 25ft.
66	57	421096	From 750ft, high rates of descent and some low power.
68	84	348979	Maintains high speeds to 2000ft but has the distance to slow down. High rates of descent after 1000ft.
70	66	545063	Large localiser deviation at 200ft.
74	64	306479	At 750ft, high speed, low IVV, flap 20 and slightly off on the ILS.
77	87	617014	High speeds and low pitches from 1000ft to 0ft.
79	43	398831	High speeds from 1000ft to 0ft and low pitch.
80	55	418007	Very high speeds from 1500ft to 750ft with low power.
86	54	269542	At 1000ft, high speeds, high rates of descent, flap 20 and speedbrake deployed.
91	49	282311	At 50ft, 80% power and pitch angle is 6.3 degrees.
93	76	497945	High speeds after 1000ft and low pitch angles. Low pitch at touchdown.
95	34	345603	High rates of descent and high speeds from 150ft to 75ft.
99	85	414736	High speeds from 400ft to 200ft. High rates of descent from 75ft.
114	203	377538	High speed descent to 2000ft.
126	343	603345	Low pitch at touchdown.

Figure 5.21: Flight 420301 DAP using SVM Optimised for CR.

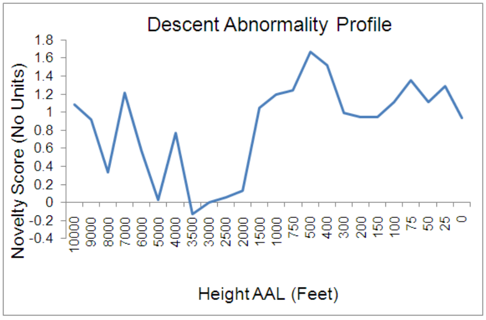

Figure 5.22: Flight 420301 DAP using SVM Optimised for RV

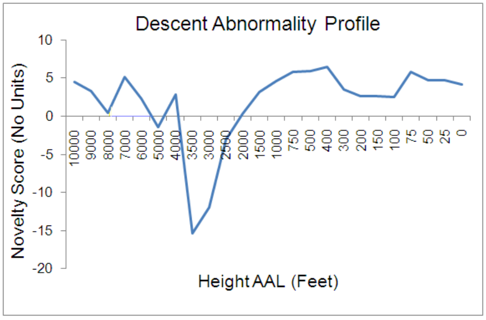

were detected by both methods, either method or neither. Nearly 3 in 4 descents are detected by both methods which is very satisfying. However, 8 of the 63 descents are detected by neither method and in this subsection, these descents are analysed to identify why neither method ranked them in the top 63.

Of the 8 such descents, 6 of these descents have a ranking by both methods of less than 100 and both methods give them negative novelty scores, so abnormalities present in these descents have been identified. The remaining two are ranked 114 (flight 377538) and 126 (flight 603345) by the raw-value method and 203 and 343 respectively by the combination rule method.

Figures 5.23 and 5.24 show the DAPs for flight 377538, where the first is the DAP optimised for the combination rule method and the second is optimised for the raw-value method. Both DAPs are similar, though the raw-value method regards the troughs at 3000ft and 300ft as more severe than the combination rule method, hence its higher ranking by this method. This descent was chosen as part of the abnormal test set because of its unusual descent. The aircraft descends

Figure 5.23: Flight 377538 DAP using SVM Optimised for CR.

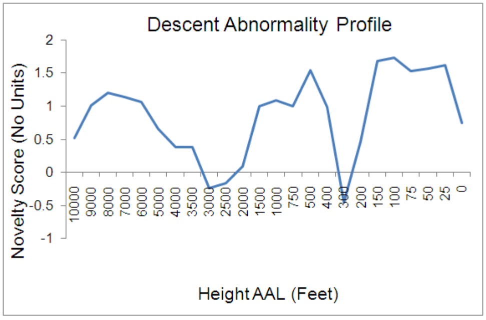

Figure 5.24: Flight 377538 DAP using SVM Optimised for RV

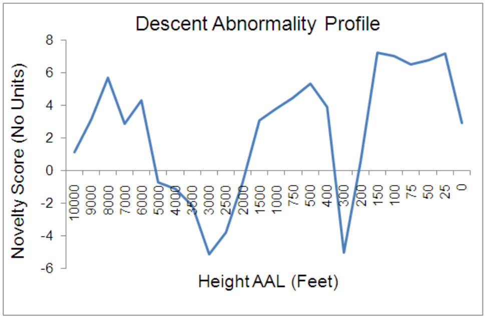

Figure 5.25: Flight 603345 DAP using SVM Optimised for CR.

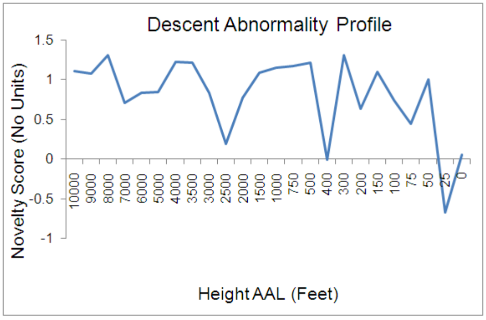

quickly from 7000ft to 3000ft and maintains at least 250kts to 2000ft. It has the distance to lose this speed and does so which satisfies the stable approach criteria by 1000ft. The trough at 300ft results from the airspeed falling below Vref and the pitch rising to 5.4 degrees. This descent has a valid GPWS warning on it, occurring at 363ft. Whilst the descent has some abnormality, the DAP is mostly positive for both methods during the final approach (from 1000ft to 0ft).

Figures 5.25 and 5.26 show the DAPs produced for flight 603345 optimised for

Figure 5.26: Flight 603345 DAP using SVM Optimised for RV

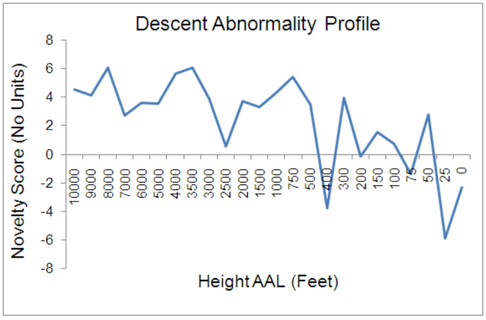

Table 5.25: Details of False Negatives for the SVM Combination Rule Method

Method	Ranked Results in the Top 63 (%)
Both	46 (73%)
None	8 (13%)
CR Only	7 (11%)
RV Only	2 (3%)

the combination rule and the raw-value methods respectively. The main abnormality on this descent is a very low pitch angle at touchdown. This can be serious if the aircraft's nosewheel, rather than the back wheels, touched down first, as the nosewheel was not designed to support such weight and can therefore buckle. The DAPs for both methods are very similar, both identifying this abnormality at 25ft and at 0ft. However the DAP for the raw-value method regards the descent from 400ft to 0ft as more negative than the combination rule method. This is because whilst both methods are using the same kernel width, the raw-value method is set to reject 5% of the training set rather than 1%.

5.4.5 F-score

The classification in Phase 2 provides a method with which to rank descents. Whilst it is very useful to know that a descent has a high ranking, it is also beneficial to a flight safety officer to compare sets of descents to identify any common trends. It would be useful to identify the heights which show the greatest differences in novelty score and the features which cause these differences. F-score [Chen and Lin, 2006] is a method which measures the discrimination between two sets of real numbers. Consider our data set $(x_i)_{i=1}^{n_+ + n_-}$ where n_+ and n_- denote the number of positive and negative examples respectively. The F-score of the ith feature is denoted by

$$F(i) \equiv \frac{\left(\bar{x}_i^{(+)} - \bar{x}_i\right)^2 + \left(\bar{x}_i^{(-)} - \bar{x}_i\right)^2}{\frac{1}{n_+ - 1}\sum_{k=1}^{n_+}\left(x_{k,i}^{(+)} - \bar{x}_i^{(+)}\right)^2 + \frac{1}{n_- - 1}\sum_{k=1}^{n_-}\left(x_{k,i}^{(-)} - \bar{x}_i^{(-)}\right)^2} \tag{5.2}$$

where $\bar{x}_i$, $\bar{x}_i^{(+)}$, $\bar{x}_i^{(-)}$ are the average of the ith feature of the whole, positive, and negative data sets, respectively; $x_{k,i}^{(+)}$ is the ith feature of the kth positive instance, and $x_{k,i}^{(-)}$ is the ith feature of the kth negative instance. The numerator provides a measure of the discrimination between the positive and negative sets. The denominator provides a measure of the discrimination within each of the two sets. Thus the larger the F-score value, the more likely that feature will be useful in separating the positive from the negative examples. A disadvantage of F-score is its inability to reveal mutual information among features.

5.4.6 Using F-score to Analyse the Data

All the descents can be represented by a feature vector of the 24 novelty values as has already been seen. A flight safety officer might well be interested if there are specific heights that affect the 2nd phase classification the most. Figure 5.27 shows the F-score values for each height. The two sets involved in the F-score generation for this figure is the set of all 1455 normal descents and the set of the 63 abnormal descents (Abnormal Test Set). There are two peaks in this figure. The first is around 6000ft to 4000ft and the second is around 500ft to 25ft. The second peak is expected in that if the descent shows abnormalities and has made an unstable approach, evidence of this will be seen in the final approach, perhaps in the form of high airspeeds or low engine power settings. The first peak is more unusual and suggests that early signs of an unstable approach may be visible at higher altitudes.

For each height, F-score can analyse which features are most discriminative. Figure 5.28 shows the F-scores for a selection of individual features over all the heights. In the previous section, two peaks were noted whilst looking at the

Figure 5.27: F-score values for 1st Phase Novelty Scores.

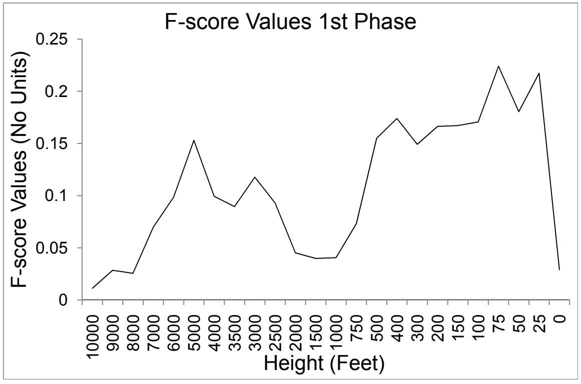

Figure 5.28: F-score values for a selection of 1st Phase Features.

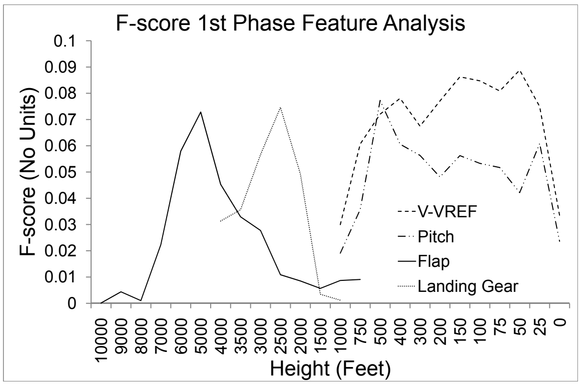

F-score values over all the heights. The second of the two peaks, at the lower altitudes is most influenced by V-Vref and pitch, which is not surprising given the majority of the abnormal descents have higher than average speeds on the final approach. The first peak, at the higher altitudes, is most influenced by flap settings and landing gear deployment. In some descents, the landing gear is deployed in order to make the aircraft descend faster, perhaps because the descent was later than planned. High flap settings at higher altitudes are not usually regarded as unsafe but it is often a sign that the aircraft is making a vectored approach and is thus able to configure the aircraft for landing at a much higher altitude than usual.

5.5 Visualisation

5.5.1 Introduction

With great advances in processing power and ever larger data storage devices, it is becoming increasingly possible to collect extremely large datasets. The dataset in this thesis is a good size (1518 descents) and as such, it is possible to gain a broad familiarity with individual descents. However, when the dataset(s) consists of many millions of data points, it becomes virtually impossible to gain any deep familiarity with the data unless the dataset is of a trivial nature.

Datasets containing particularly high dimensional data can be very hard to interpret and comprehend, especially for those who do not have great experience in data modelling. There are a variety of data visualisation tools such as clustering or dendograms, principle component analysis, the Sammon map, Independent Component Analysis and minimal spanning trees.

Recent innovations in visualisation algorithm development have tried to focus on preserving the structural integrity of the original data. This implies the visualisation space should be topographic in some sense. The very recent methods have tried to extend the Sammon mapping so it is generalisable.

5.5.2 Theory

The Neuroscale algorithm [Lowe and Tipping, 1996] is an example of such a method and is used in this section to visualise the data. The Neuroscale model is a dimensionality reduction algorithm which uses the Sammon mapping [Sammon Jr, 1969] to provide a transformation of data points from N to P dimensions where N is greater than P. It attempts to preserve the structure of the data space (original high-dimensional space) and retain it in the lower dimensional space. It does this by attempting to keep the Euclidean distance between any two data vectors as close as possible in the data space and in the latent space. The transformation is generated by minimising the error function known as the Sammon

Stress Metric, given by

$$E = \sum_{i}^{N} \sum_{j>i}^{N} (d_{*ij} - d_{ij})^2 \tag{5.3}$$

and

$$d_{ij} = \|\mathbf{y}_i - \mathbf{y}_j\|\,, \tag{5.4}$$

$$d_{*ij} = \|\mathbf{x}_i - \mathbf{x}_j\| \tag{5.5}$$

where d_{*ij} and d_{ij} represent the distance between vectors in the high dimensional space the lower dimensional space respectively. A RBF neural network is used to learn the transformation. The number of hidden nodes should be an order of magnitude lower than the number of training vectors [Tarassenko et al., 2008].

Throughout the rest of this thesis, Neuroscale mappings will be trained on the normal descents and tested on the abnormal descents. Given there are 1455 normal descents and that 140 is approximately a tenth of 1455, the number of hidden centres used will be 140.

5.5.3 Results

In this subsection, the results of the visualisation are analysed. Figure 5.29 shows the Neuroscale visualisation of the vectors for each descent produced from the combination rules. There is a good level of separation between the normal and abnormal datasets and if the Euclidean distance between each datapoint and the origin is computed, 54 of the top 63 values are from the abnormal dataset. Furthermore, it illustrates that although there is a good level of separation between the two datasets, there are some descents in the training set that should be regarded as abnormal.

Figure 5.30 shows the Neuroscale visualisation of the vectors for each descent produced from the raw values from Phase 1 classification. The degree of separation is also fairly good, though if the euclidean distance between the datapoints

Figure 5.29: Neuroscale Visualisation for Combination Rule Phase 2 Results.

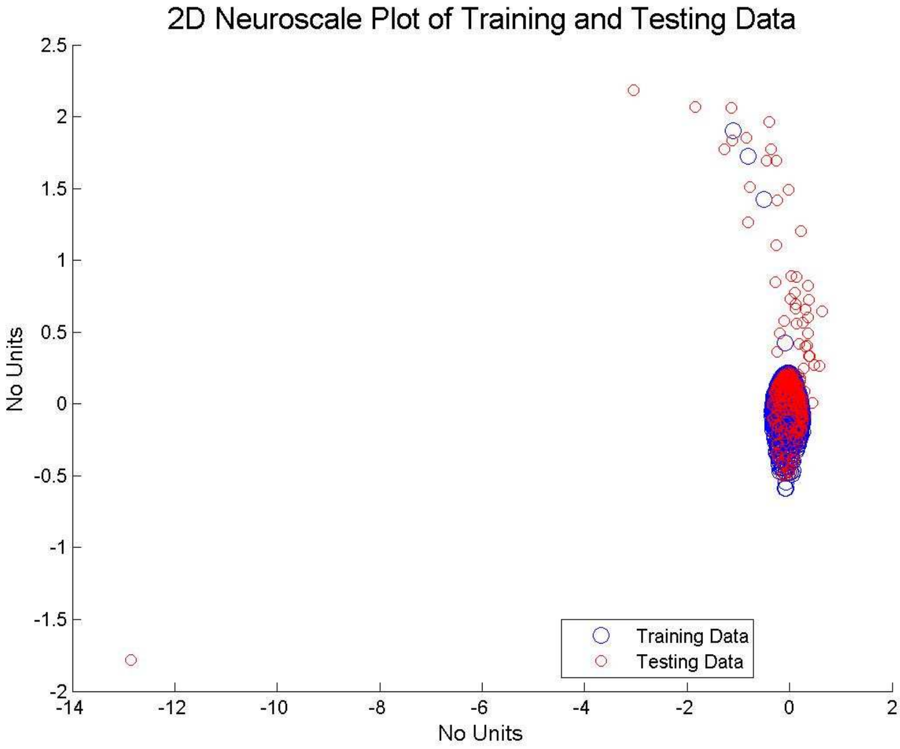

and origin is computed, only 45 of the top 63 values are from the abnormal dataset.

The correlation can be computed between the Euclidean distances of the Neuroscale visualisations and the respective Phase 2 novelty scores. Let the Euclidean distances be denoted by $X = \{x_i | 1 \leq i \leq 1518\}$ and the Phase 2 novelty scores be denoted by $Y = \{y_i | 1 \leq i \leq 1518\}$. Then the linear correlation between the two variables is given by

$$Correl(X,Y) = \frac{\sum\limits_{i=1}^{1518} (x_i - \overline{x})(y_i - \overline{y})}{\sqrt{\sum\limits_{i=1}^{1518} (x_i - \overline{x})^2} \sqrt{\sum\limits_{i=1}^{1518} (y_i - \overline{y})^2}} \tag{5.6}$$

Table 5.26 shows the level of correlation between the Euclidean distances of the Neuroscale visualisation and novelty scores for Phase 2 of the proposed method

Figure 5.30: Neuroscale Visualisation for Raw Value Phase 2 Results.

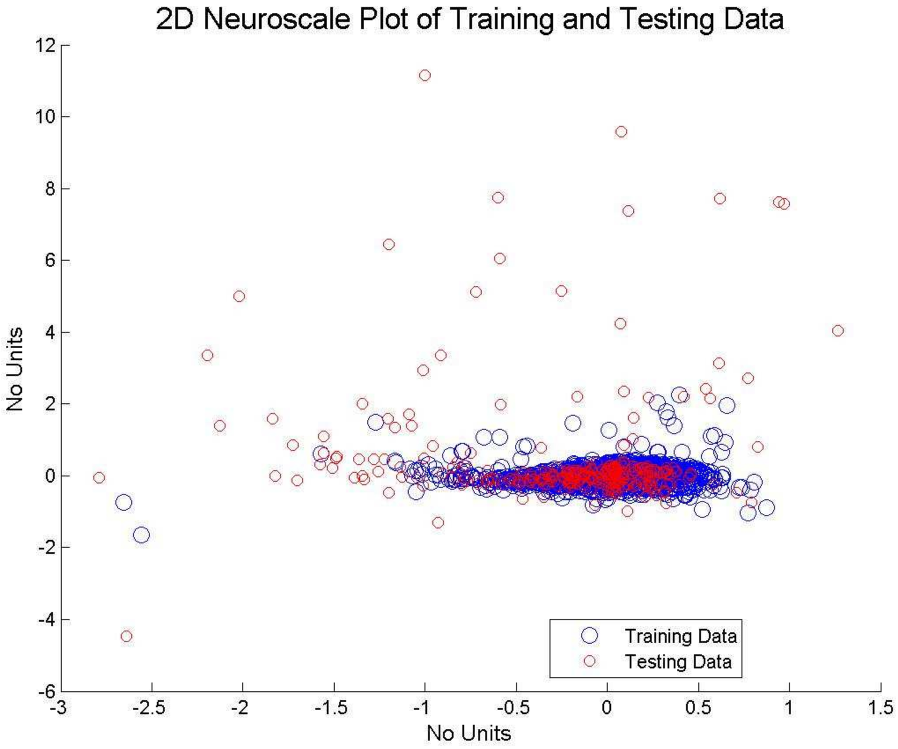

when both use the same SVM parameters optimised for the raw-value method or the combination rule method. It shows there is strong negative correlation in both cases.

Table 5.26: Correlation coefficients between the Visualisation and the Proposed Method

Method	Correlation Coefficients
Optimised for Raw-Value Method	-0.867
Optimised for Combination Rule Method	-0.940

Chapter 6

Conclusions

6.1 Introduction

This thesis has provided a solution to the difficult problem of improving flight safety during the descent for large jet aircraft. The field of flight safety and its existing methods was introduced in Chapter 2. In Chapter 3 novelty detection and one class classification methods were introduced with the aim of identifying which methods were best for the type of data at hand. The proposed method was introduced in Chapter 4 and was described in detail. In Chapter 5 the 1st phase results were presented along with the 2nd phase method, results, F-score analysis and visualisation of the data.

6.2 What has been achieved?

In reviewing current flight safety methods it became clear that there are a number of issues.

There is very little literature concerning flight data analysis and there are a number of reasons why this is so. It could be that it has not received much academic interest, due to the fact that real world data is likely to be confidential and not publicly available. Therefore if research has taken place in this field, it is likely that the vast majority was confidential and undertaken by airlines able to afford researchers or a research department. Statistics show (Board [2010]) that for American airlines between 1990 and 2009, the accident rate per 200,000 departures was less than one for every year bar one. Hence it could be argued that airlines did not feel the need to improve flight data analysis methods when the accident rates were so low. Furthermore, current methods such as Amidan and Ferryman [2005], are almost impossible to assess because there are no details about the numbers of flights used, the detection rates or what they consider to be an abnormal flight.

The event based method appears to be the most common and whilst it has some good advantages, there are a significant number of disadvantages. It is unable to detect exceedances if there are no events created for them. Furthermore, it is difficult to determine if there are any precursors in order to try and explain the event and perhaps reduce its frequency which is part of the guidelines recommended by the CAA (see section 2.3.1).

Given that airlines such as British Airways can analyse as much as 5 Gigabytes a day, it becomes very difficult to provide a thorough analysis of the flights, identifying all abnormalities and their precursors (if they exist). A flight in crude terms can be divided up into 'take off and climb', 'cruise' and 'descent and landing'. The analysis of the event based system shows that over 70% of events occur whilst the aircraft is in the act of descending (see section 2.5). Therefore it was decided to focus on this region of flight as it appears to have a significant number of abnormalities to be identified. Given that for each airport there are a set of approaches that should be followed under normal circumstances and that ALAR recommends that the aircraft satisfy certain conditions at 1000ft 2.6, it was considered that modelling the approach to an airfield and identifying any deviations from the prescribed approach could be very valuable to an airline. A key motivator for this approach was the discovery that the AAIB had already made a similar suggestion (Foundation [2004]).

Having decided on analysing the descent from considerations found in Chapter 2, it was necessary to consider what methods could be used to model an approach to an airport. The overall goal is to detect abnormal descents and the branch of machine learning concerned with this problem is known as 'novelty' detection or one class classification. The target class represents the normal flights and the outlier class represents the abnormal flights. Chapter 3 looks at novelty detection methods and one class classification methods. Perhaps the biggest difficulty in terms of classification was the fact that identifying descents had not been, to the best of the author's knowledge, attempted before. Whilst the analysts at Flight Data Services have over 150 years experience in the field of aviation and are well versed in analysing events, they have not routinely compared individual descents. Therefore, whilst the Abnormal Test Set contains descents with abnormalities, it is possible that the training set (which should contain normal descents only) may contain some abnormal descents. Therefore the classifiers used should not be negatively impaired by the presence of abnormal descents in the training set. Furthermore, given that the parameters occupy different numerical ranges (see table 4.2), scaling becomes necessary so that one feature does not dominate all the others. Therefore the classifiers should not have their performance impaired by scaling. With these attributes in mind, the classifiers chosen were the one class SVM, the MoG that accepts outliers in training and K-means. Furthermore, the number of parameters to be optimised for each method is small, thus reducing the risk of overtraining.

Section 3.4 looks at ranking systems and their applications in modern day problems; for example, ranking bridge players and the most 'harmful' birds to be ingested into aircraft engines. It is clear that ranking systems are often problem specific and rely heavily on domain knowledge. It is felt that none of these systems are applicable to this research but it is noted that such systems can have value. For example, it was considered surprising that blackbirds and starlings were ranked at number 4 in terms of the risk posed to aircraft engines.

Chapter 4 and Chapter 5 introduce the method proposed in this thesis for analysing flight data and the corresponding results. The selection of suitable features was achieved using expert advice as to which parameters the pilots would be monitoring during the descent. In this way it was hoped that deviations from the airline's SOP could be captured. The abnormal test set was also created with advice from the staff at Flight Data Services. The test set is most unusual in its composition (see table 4.5) give that only 32% of the descents have class 3 events. Perhaps the most surprising feature was that it included some flights that had no events at all. It illustrates the fact that the event system is not detecting all abnormalities during the descent.

Classifiers are trained at each of the heights (see table 4.1). The output can be plotted and the corresponding graph is known as a DAP which provides the 1st phase results. This method provides a clear visual aid to the flight safety officer or the flight data analyst as to how the descent was flown. Regions of abnormality are clearly highlighted and open to investigation. Furthermore, the impact of events can usually be seen on the DAP (see figures 5.2, 5.8 and 5.14).

Key influences for phase 2 and to a lesser extent, phase 1, were the recommendation by the AAIB in Foundation [2004] and a paper by Clifton et al. [2006] which details an intriguing method for combining information from several combustion channels in order to determine the first early signs that unstable combustion was taking place. Given the large numbers of flights processed, flight safety officers and flight data analysts are clearly unable to analyse every DAP for abnormalities. Therefore it was considered valuable to attempt to rank the descents in order of severity and details of this approach are found in section 5.3.1. Section 5.4.3 presents the main 2nd phase results and shows that the SVM classifier ranks the most flights from the Abnormal Test Set in the top 63 ranking positions. It also demonstrates that the combination rule method outperforms the raw-value method which is not too surprising given that the combination rule method is less vulnerable to very large or very small abnormality values for a given height.

Section 5.4.6 details the use of the feature selection tool F-score. Firstly, it is able to identify the heights where there are the greatest differences between the training set and the Abnormal Test Set and secondly, it is able to analyse these heights to identify the most significant features that are causing these differences. It was not surprising to see that features pitch and V-Vref are the most significant at altitudes of less than 1000ft given that high speeds are a common feature of an unstable approach. What is more unusual is that flap selection and landing gear deployment are most significant at higher altitudes. This suggest that some aircraft have decelerated early and are flying the approach with lower speeds and a low flap setting in order to maintain lift. The early use of the landing gear for some flights indicates that some aircraft are using it to descend faster because they were a little high, or that some flights were configured ready for landing at higher altitudes than usual.

Section 5.5 introduces the Neuroscale visualisation algorithm which is used to provide a visual representation of the phase 2 results. It is immediately seen that some flights in the training set are plotted away from the main cluster of flights centred on the origin. Section 5.4.4.1 looks at the false positives and shows that 3 flights from the training set are ranked in positions 2, 3 and 4. The data shows that all 3 flights had their speedbrakes deployed at altitudes under 1000ft which is prohibited by the SOP. On further investigation it was found that there was a fault with that parameter and the speedbrake was not deployed this low. However, if the parameter was functioning normally, the ranking system performed as hoped because such an event is a serious deviation from the SOP and should be ranked highly.

6.3 Main Contributions

- The thesis highlights the apparent lack of academic research in the field of flight data analysis and it is hoped that other researchers will be motivated to expand and improve upon these results and conclusions.
- A new method has been introduced that identifies abnormalities and their impact during the descent and furthermore, allows descents to be ranked so that the descents with the most significant abnormalities are ranked in the top positions.
- The DAP is an innovative way of showing an overview of the level of abnormality during the descent. Negative regions can be clearly identified and further studied to gain a greater understanding of that approach.
- The ranking approach has successfully identified up to 84% of the flights in the Abnormal Test Set in the top 63 ranking positions and illustrates the value of the combination rules.
- The proposed method is able to detect abnormalities during descents that the event based system has not. In the Abnormal Test Set, less than a third of the flights have level 3 events. Furthermore, some descents that had class

3 events were ranked very low (see section 5.4.3), indicating that they had no appreciable effect on the main parameters used during the descent.

- Visualisation is a valuable tool to provide a visual analysis of the rankings produced by phase 2 and unusual descents in the training set are easily identifiable.
- The main work of identifying a suitable model and appropriate features has been achieved and this knowledge can be used to create models for different aircraft types at different runways. This will enable an airline to assess how their aircraft handle descents to different runways, take remedial actions where required and identify any improvements in the second phase novelty scores.

6.4 Future Work

To the best of the author's knowledge, this is one of the first times that a large quantity of flight data has been studied in order to improve safety. As a result, there remains many avenues for further study.

- The study can be expanded to see how well the method performs on different airfields.
- The method could also be applied to study the take off and climb phases of flight to look for abnormalities.
- Different airlines flying the same aircraft type into the same airport can be analysed and compared. Furthermore, with the agreement of all parties, deidentified data could be shared to enable one or both airlines to improve their SOP should it be necessary.
- The nature of flying an approach to the same airport is such that the aircraft must fly through the same heights each time. Therefore the method can be applied to any situation where there are a large number of repetitive actions. For example, during a 100 metre sprint in athletics, all runners start at 0m,

then pass through 10m, 20m etc and all pass through 100m. The method could be applied to analyse how the performance of one sprinter or many sprinters change over time. Of course, this assumes that it is possible to extract relevant features.

Appendix A

Published Papers

Smart, E., Liu, H., Jesse, C. and Brown, D. (2009). Qualitative classification of descent phases in commercial flight data. International Journal of Computational Intelligence Studies, 1, 3749. 124

Smart, E. and Brown, D. (2009). Using novelty detection methods to identify abnormalities in aircraft flight data. In: Proceedings of the UK Workshop on Computational Intelligence (UKCI 2009), Nottingham, UK: University of Nottingham.

Smart, E. and Brown, D. (2010). Using One Class Classifiers to Diagnose Abnormalities in Aircraft Flight Data. Intelligent Transportation Systems, IEEE transactions on, Submitted.

References

ACM. Acm kdd cup - acm special interest group on knowledge discovery and data mining, October 2010. URL http://tinyurl.com/356u4m5. Accessed on 13th August 2010. Available at http://tinyurl.com/356u4m5. 44

Aerobytes. Aerobytes fdm, 2010a. URL http://tinyurl.com/2vakxvd. Last Accessed on 10th November 2010. Available at http://tinyurl.com/2vakxvd. 12

Aerobytes. Aerobytes foqa, 2010b. URL http://tinyurl.com/369htay. Last Accessed on 11th November 2010. Available at http://tinyurl.com/369htay. 12

C.C. Aggarwal and P.S. Yu. Outlier detection for high dimensional data. In *Proceedings of the 2001 ACM SIGMOD international conference on Management of data*, page 46. ACM, 2001. 31

Airliners. The tupolev tu-154, 2010. URL http://www.airliners.net/aircraft-data/stats.main?id=376. Last Accessed on 14th November 2010. 8

B.G. Amidan and T.A. Ferryman. Atypical event and typical pattern detection within complex systems. *Aerospace Conference, 2005 IEEE*, pages 3620–3631, March 2005. doi: 10.1109/AERO.2005.1559667. 13, 114

V. Barnett and T. Lewis. *Outliers in statistical data*. Wiley, 1994. 36

C. M. Bishop. *Neural Networks for Pattern Recognition*. Clarendon Press, Oxford, 1995a. 33, 35

C.M. Bishop. Novelty detection and neural network validation. *IEEE Proceedings-Vision, Image and Signal processing*, 141(4):217–222, 1994. 36

C.M. Bishop. *Neural Networks for Pattern Recognition*. Oxford University Press, USA, 1995b. 41, 42, 55

National Transportation Safety Board. Aviation, 2010. URL http://www.ntsb.gov/aviation/Table5.htm. Last Accessed on 12th August 2010. Available from http://www.ntsb.gov/aviation/Table5.htm. 113

Boeing. 787 dreamliner, 2010. URL http://tinyurl.com/kouly. Last Accessed on 16th November 2010. 8

D. Bradley and A. Tyrrell. Immunotronics: Hardware fault tolerance inspired by the immune system. *Evolvable Systems: From Biology to Hardware*, pages 11–20, 2000. 30

C. Bregler and S.M. Omohundro. Surface learning with applications to lipreading. *Advances in neural information processing systems*, pages 43–43, 1994. ISSN 1049-5258. 56

CAA. Cap 739 flight data monitoring, August 2003. URL http://tinyurl.com/3zxtp7w. Last Accessed on 15th November 2010. 8, 9

G.A. Carpenter, S. Grossberg, and D.B. Rosen. Art 2-a: An adaptive resonance algorithm for rapid category learning and recognition. *Neural Networks*, 4(4): 493–504, 1991. 55

Chambers. Abnormality. Hodder Educational Group, August 2010. URL http://tinyurl.com/36psds4. Accessed on 12th August 2010. Available at http://tinyurl.com/36psds4. 28

P.H. Chen, C.J. Lin, and B. Sch
"olkopf. A tutorial on ν-support vector machines. *Applied Stochastic Models in Business and Industry*, 21(2):111–136, 2005. ISSN 1526-4025. 48

Y.W. Chen and C.J. Lin. Combining svms with various feature selection strategies. *Studies in Fuzziness and Soft Computing*, 207:315, 2006. 68, 105

L.A. Clifton, H. Yin, and Y. Zhang. Support vector machine in novelty detection for multi-channel combustion data. *Lecture Notes in Computer Science*, 3973: 836, 2006. 48, 64, 116

G. Cohen, M. Hilario, H. Sax, S. Hugonnet, C. Pellegrini, and A. Geissbuhler. An application of one-class support vector machine to nosocomial infection detection. *Studies in health technology and informatics*, 107(Pt 1):716, 2004. 49

D. Dasgupta. Advances in artificial immune systems. *Computational Intelligence Magazine, IEEE*, 1(4):40–49, 2007. ISSN 1556-603X. 30

D. Dasgupta, K. KrishnaKumar, D. Wong, and M. Berry. Negative selection algorithm for aircraft fault detection. *Artificial Immune Systems*, pages 1–13, 2004. 30

M. Davy, F. Desobry, A. Gretton, and C. Doncarli. An online support vector machine for abnormal events detection. *Signal processing*, 86(8):2009–2025, 2006. 31

R.O. Duda and P.E. Hart. *Pattern classification and scene analysis*. Wiley, New York, 1973. 29, 32, 33, 73

T.V. Duong, H.H. Bui, D.Q. Phung, and S. Venkatesh. Activity recognition and abnormality detection with the switching hidden semi-markov model. In *Computer Vision and Pattern Recognition, 2005. CVPR 2005. IEEE Computer Society Conference on*, volume 1, pages 838–845. IEEE, 2005. 31

J.C. Fayer. *Vols d'essais: le Centre d'essais en vol de 1945 à 1960*. E-T-A-I, 2001. ISBN 9782726885345. 7

FDS. A guide to flight data monitoring. Flight Data Services Ltd, 2010. Accessed on 26/01/2010. Available at http://www.flightdataservices.com. 11

Flight Safety Foundation. Stabilized approach and flare are key to avoiding hard landings. Flight Safety Digest, August 2004. URL http://flightsafety.org/fsd/fsd_aug04.pdf. Accessed on 4th April 2008. Available at http://flightsafety.org/fsd/fsd_aug04.pdf. 24, 27, 114, 116

FSF. Alar - approach and landing accident reduction. Flight Safety Digest, August-November 2000. URL http://flightsafety.org/fsd/fsd_aug-nov00.pdf. 24, 27

K. Fukunaga. *Introduction to Statistical Pattern Recognition.* Academic Press, 1990. 28

A.B. Gardner, A.M. Krieger, G. Vachtsevanos, and B. Litt. One-class novelty detection for seizure analysis from intracranial eeg. *The Journal of Machine Learning Research*, 7:1025–1044, 2006. 50

S. Geman, E. Bienenstock, and R. Doursat. Neural networks and the bias/variance dilemma. *Neural computation*, 4(1):1–58, 1992. 33

F. Girosi, M. Jones, and T. Poggio. Regularization theory and neural networks architectures. *Neural computation*, 7(2):219–269, 1995. 34

A.V. Gomes, R. Voorakaranam, and A. Chatterjee. Modular fault simulation of mixed signal circuits with fault ranking by severity. In *Defect and Fault Tolerance in VLSI Systems, 1998. Proceedings., 1998 IEEE International Symposium on*, pages 341–348. IEEE, 2002. ISBN 0818688327. 62

T. Gyimothy, R. Ferenc, and I. Siket. Empirical validation of object-oriented metrics on open source software for fault prediction. *Software Engineering, IEEE Transactions on*, 31(10):897–910, 2005. ISSN 0098-5589. 62

L.K. Hansen, S. Sigurdsson, T. Kolenda, F.A. Nielsen, U. Kjems, and J. Larsen. Modeling text with generalizable gaussian mixtures. In *Acoustics, Speech, and Signal Processing, 2000. ICASSP'00. Proceedings. 2000 IEEE International Conference on*, volume 6, pages 3494–3497. IEEE, 2002. 41

Paul Hayton, Bernhard Sch Olkopf, Lionel Tarassenko, and Paul Anuzis. Support vector novelty detection applied to jet engine vibration spectra. In *Advances in Neural Information Processing Systems 13*, pages 946–952. MIT Press, 2000. 50

V. Hodge and J. Austin. A survey of outlier detection methodologies. *Artificial Intelligence Review*, 22(2):85–126, 2004. 31

Mike Holtom. Foqa - flight data analysis of aircraft for flight safety. The Airline Pilots, January 2006. URL http://tinyurl.com/3n97vy8. Accessed on 13th March 2010. Available at http://www.theairlinepilots.com/flight/foqaflightdataanalysis.htm. 10, 12, 26

F. Howard. *Wilbur and Orville: A Biography of the Wright Brothers*. Dover Pubns, 1998. ISBN 0486402975. 6

T.K. Huang, C.J. Lin, and R.C. Weng. Ranking individuals by group comparisons. In *Proceedings of the 23rd international conference on Machine learning*, pages 425–432. ACM, 2006. ISBN 1595933832. 62

ICAO. Flight safety section (fls), 2010. URL http://www.icao.int/anb/FLS/flsannex.html. Accessed on 15th November 2010. 7

N. Japkowicz, C. Myers, and M. Gluck. A novelty detection approach to classification. In *International Joint Conference on Artificial Intelligence*, volume 14, pages 518–523. Lawrence Erlbaum Associates LTD, 1995. 31

P-. Juszczak. *Learning to recognise. A study on one-class classification and active learning*. PhD thesis, Delft University of Technology, 2006. URL http://tinyurl.com/3bfgonm. 31

S.S. Keerthi and C.J. Lin. Asymptotic behaviors of support vector machines with Gaussian kernel. *Neural computation*, 15(7):1667–1689, 2003. ISSN 0899-7667. 47, 48

L.I. Kuncheva and L.C. Jain. Designing classifier fusion systems by genetic algorithms. *IEEE Transactions on Evolutionary Computation*, 4(4):327–336, 2000. 54

C. Lai, D.M.J. Tax, R.P.W. Duin, E. Pekalska, and P. Paclík. On combining one-class classifiers for image database retrieval. In *Proceedings of the Third International Workshop on Multiple Classifier Systems*, pages 212–221. Springer-Verlag, 2002. 53

H. T. Lin and C. J. Lin. A study on sigmoid kernels for svm and the training of non-psd kernels by smo-type methods. Technical report, Department of Computer Science and Information Engineering, National Taiwan University, 2003. Available at: http://www.csie.ntu.edu.tw/ cjlin/papers/tanh.pdf. 47

D. Lowe and M. Tipping. Feed-forward neural networks and topographic mappings for exploratory data analysis. *Neural Computing & Applications*, 4(2): 83–95, 1996. ISSN 0941-0643. 108

J. Ma and S. Perkins. Time-series novelty detection using one-class support vector machines. In *Proceedings of the International Joint Conference on Neural Networks, 2003*, volume 3, 2003. 31

L.M. Manevitz and M. Yousef. One-class svms for document classification. *The Journal of Machine Learning Research*, 2:154, 2002. 50

M. Markou and S. Singh. Novelty detection: a reviewpart 1: statistical approaches. *Signal Processing*, 83(12):2481–2497, 2003a. 29, 31

M. Markou and S. Singh. Novelty detection: a reviewpart 2: neural network based approaches. *Signal Processing*, 83(12):2499–2521, 2003b. 29, 31

I. Morgan, H. Liu, B. Tormos, and A. Sala. Detection and Diagnosis of Incipient Faults in Heavy-Duty Diesel Engines. *Industrial Electronics, IEEE Transactions on*, 57(10):3522–3532, 2010. 42

MM Moya, MW Koch, and LD Hostetler. One-class classifier networks for target recognition applications. *NASA STI/Recon Technical Report N*, 93:24043, 1993. 31

S. Nandi and H.A. Toliyat. Condition monitoring and fault diagnosis of electrical machines-a review. In *Industry Applications Conference, 1999. Thirty-Fourth IAS Annual Meeting. Conference Record of the 1999 IEEE*, volume 1, pages 197–204. IEEE, 1999. ISBN 078035589X. 61

S. Nandi and H.A. Toliyat. Novel frequency-domain-based technique to detect stator interturn faults in induction machines using stator-induced voltages after switch-off. *Industry Applications, IEEE Transactions on*, 38(1):101–109, 2002. ISSN 0093-9994. 61

NASA. Apms - aviation performance measuring system, March 2007. Accessed on 28/08/2008. Available at http://apms.arc.nasa.gov/. 13

L. Parra, G. Deco, and S. Miesbach. Statistical independence and novelty detection with information preserving nonlinear maps. *Neural Computation*, 8(2): 260–269, 1996. 36, 42

E. Parzen. On estimation of a probability density function and mode. *The Annals of Mathematical Statistics*, 33(3):1065–1076, 1962. 44

K. Polat and S. Guenes. A new feature selection method on classification of medical datasets: Kernel f-score feature selection. *Expert Systems with Applications*, 36(7):10367–10373, 2009. 68

C. Prendergast. *The First Aviators*. The epic of flight. Time-Life, 2004. ISBN 9781844470372. 6

S. Roberts, L. Tarassenko, J. Pardey, and D. Siegwart. A validation index for artificial neural networks. In *In Proceedings of Int. Conference on Neural Networks and Expert Systems in Medicine and Healthcare*, page pages 2330., 1994. 36

S.J. Roberts. Novelty detection using extreme value statistics. In *Vision, Image and Signal Processing, IEE Proceedings-*, volume 146, pages 124–129. IET, 2002. 29

Jennifer Rosenberg. The first airplane crash, 2010. URL http://tinyurl.com/4y9dssv. Last accessed 17th November 2010. 7

P.J. Rousseeuw and K. Van Driessen. A fast algorithm for the minimum covariance determinant estimator. *Technometrics*, 41(3):212–223, 1999. ISSN 0040-1706. 41

SAGEM. Analysis ground station. Sagem Dfense Securit, September 2008. URL http://www.sagem-ds.com/ags/en/site.php?spage=00000000. Accessed on 21/09/08. Available at http://www.sagem-ds.com/ags/en/site.php?spage=00000000. 11

J.W. Sammon Jr. A nonlinear mapping for data structure analysis. *Computers, IEEE Transactions on*, 100(5):401–409, 1969. ISSN 0018-9340. 108

B. Schölkopf, R. C. Williamson, A. J. Smola, J. Shawe-Taylor, and J. C. Platt. Support vector method for novelty detection. In S. A. Solla, T. K. Leen, and K.-R. Müller, editors, *Advances in Neural Information Processing Systems 12*, pages 582–588, Cambridge, MA, 2000. MIT Press. 45

H. Schwenk. The diabolo classifier. *Neural computation*, 10(8):2175–2200, 1998. ISSN 0899-7667. 56

H.J. Shin, D.H. Eom, and S.S. Kim. One-class support vector machines–an application in machine fault detection and classification. *Computers & Industrial Engineering*, 48(2):395–408, 2005. 50

P. Smolensky, M.C. Mozer, and D.E. Rumelhart. *Mathematical perspectives on neural networks*. Lawrence Erlbaum, 1996. 34

E.J. Spinosa and A.C. de Carvalho. Support vector machines for novel class detection in bioinformatics. *Genet. Mol. Res*, 4(3):608–615, 2005. 50

S. Stepney, R.E. Smith, J. Timmis, and A.M. Tyrrell. Towards a conceptual framework for artificial immune systems. *Artificial Immune Systems*, pages 53–64, 2004. 30

T. Stibor, J. Timmis, and C. Eckert. A comparative study of real-valued negative selection to statistical anomaly detection techniques. *Artificial Immune Systems*, pages 262–275, 2005. 45

G. Strang. *Linear algebra and its applications.* New York-San Francisco-London: Academic Press (A Subsidiary of Harcourt Brace Jovanovich, Publishers), 1980. 39

R. Subramanyam and M.S. Krishnan. Empirical analysis of ck metrics for object-oriented design complexity: Implications for software defects. *IEEE Transactions on Software Engineering*, pages 297–310, 2003. ISSN 0098-5589. 62

L. Tarassenko, P. Hayton, N. Cerneaz, and M. Brady. Novelty detection for the identification of masses in mammograms. In *Artificial Neural Networks, 1995., Fourth International Conference on*, pages 442–447, 1995. 38, 45

L. Tarassenko, D.A. Clifton, P.R. Bannister, S. King, and D. King. *Novelty Detection.* John Wiley and Sons, New York, 2008. 109

D.M.J. Tax. *One-class classification.* PhD thesis, Delft University of Technology, http://ict.ewi.tudelft.nl/ davidt/thesis.pdf, June 2001. 29, 30, 31, 58

D.M.J. Tax. Ddtools, the data description toolbox for matlab, Dec 2009. version 1.7.3. 42

D.M.J. Tax and R.P.W Duin. Data domain description using support vectors. In M. Verleysen, editor, *Proceedings of the European Symposium on Artificial Neural Networks 1999*, pages 251–256. D.Facto, Brussel, April 1999a. 47

D.M.J. Tax and R.P.W Duin. Support vector domain description. *Pattern Recognition Letters*, 20(11-13):1191–1199, December 1999b. 51

M.M.T. Thwin and T.S. Quah. Application of neural networks for software quality prediction using object-oriented metrics. *Journal of Systems and Software*, 76 (2):147–156, 2005. ISSN 0164-1212. 62

N.R. Ullman. *Elementary Statistics: An Applied Approach.* Wiley, 1978. 38

GWH van Es. *Advanced Flight Data Analysis.* National Aerospace Laboratory NLR, 2002. 13

V.N. Vapnik. *The Nature of Statistical Learning Theory.* Springer Verlag, 2000. 45, 51

Q.H. Wang and J.R. Li. A rough set-based fault ranking prototype system for fault diagnosis. *Engineering applications of artificial intelligence*, 17(8):909–917, 2004. ISSN 0952-1976. 63

Y. Wang, J. Wong, and A. Miner. Anomaly intrusion detection using one class svm. In *Information Assurance Workshop, 2004. Proceedings from the Fifth Annual IEEE SMC*, pages 358–364. IEEE, 2005. 50

J. Weston, S. Mukherjee, O. Chapelle, M. Pontil, T. Poggio, and V. Vapnik. Feature selection for svms. *Advances in neural information processing systems*, pages 668–674, 2001. 68

Marcus Williamson. David warren: Inventor and developer of the 'black box' flight data recorder, 2010. URL `Availableathttp://tinyurl.com/3gpqake`. Last accessed 15th November 2010. 7

D.Y. Yeung and C. Chow. Parzen-window network intrusion detectors. *Pattern Recognition*, 4:40385, 2002. 44

D.Y. Yeung and Y. Ding. Host-based intrusion detection using dynamic and static behavioral models. *Pattern Recognition*, 36(1):229–243, 2003. ISSN 0031-3203. 30

E.J. Zakrajsek and J.A. Bissonette. Ranking the risk of wildlife species hazardous to military aircraft. *Wildlife Society Bulletin*, 33(1):258–264, 2005. ISSN 0091-7648. 63

Y. Zhou and H. Leung. Empirical analysis of object-oriented design metrics for predicting high and low severity faults. *Software Engineering, IEEE Transactions on*, 32(10):771–789, 2006. ISSN 0098-5589. 62